NMR STUDIES OF PROTEIN HYDRATION AND PROTEIN-LIGAND INTERACTIONS

Yuan Chong

A dissertation submitted to the faculty of the University of North Carolina at Chapel Hill in partial fulfillment of the requirements for the degree of Doctor of Philosophy in the Department of Physics and Astronomy.

Chapel Hill
2017

Approved by:

Yue Wu

Sean Washburn

Laurie E. McNeil

Rosa T. Branca

Y. Jack Ng

ABSTRACT

YUAN CHONG: NMR Studies of Protein Hydration and Protein-Ligand Interactions
(Under the direction of Yue Wu)

Water on the surface of a protein is called hydration water. Hydration water is known to play a crucial role in a variety of biological processes including protein folding, enzymatic activation, and drug binding. Although the significance of hydration water has been recognized, the underlying mechanism remains far from being understood. This dissertation employs a unique *in-situ* nuclear magnetic resonance (NMR) technique to study the mechanism of protein hydration and the role of hydration in alcohol-protein interactions. Water isotherms in proteins are measured at different temperatures via the *in-situ* NMR technique. Water is found to interact differently with hydrophilic and hydrophobic groups on the protein. Water adsorption on hydrophilic groups is hardly affected by the temperature, while water adsorption on hydrophobic groups strongly depends on the temperature around 10 C, below which the adsorption is substantially reduced. This effect is induced by the dramatic decrease in the protein flexibility below 10 C. Furthermore, nanosecond to microsecond protein dynamics and the free energy, enthalpy, and entropy of protein hydration are studied as a function of hydration level and temperature. A crossover at 10 C in protein dynamics and thermodynamics is revealed. The effect of water at hydrophilic groups on protein dynamics and thermodynamics shows little temperature dependence, whereas water at hydrophobic groups has stronger effect above 10 C. In addition, I investigate the role of water in alcohol binding to the protein using the *in-situ* NMR detection. The isotherms of alcohols are first measured on dry proteins, then on proteins with a

series of controlled hydration levels. The free energy, enthalpy, and entropy of alcohol binding are also determined. Two distinct types of alcohol binding are identified. On the one hand, alcohols can directly bind to a few specific sites on the protein. This type of binding is independent of temperature and can be facilitated by hydration. On the other hand, alcohols can bind to many nonspecific sites on the protein. In dry proteins, this type of binding only occurs above a threshold of alcohol vapor pressure. Such a threshold is gradually reduced by increasing the hydration level and can be removed above a critical hydration level. Hydration also shifts the nonspecific alcohol binding from an entropy-driven to an enthalpy-driven process. This dissertation reveals the mechanism of protein hydration and the detailed roles of hydration in ligand binding, with important implications for the understanding of protein functions.

ACKNOWLEDGMENTS

I would like to express my gratitude to my advisor, Dr. Yue Wu, for his guidance and help in my PhD study. He brought me into the fascinating area of NMR. He taught me how to do experiments, how to analyze data and find the physics behind it, how to present my works and write manuscripts, and most importantly, how to think deeply and creatively as a real scientist. The knowledge and skills I learnt from him will benefit me throughout my further work, which I appreciate thoroughly and deeply.

I would like to thank Dr. Alfred Kleinhammes, without the help and advice from him, it would not have been possible to complete my PhD work. I am also grateful to Dr. Horst Kessemeier, a pioneer in NMR who sits next to me in the laboratory. I conducted most of my experiments using his magnet and NMR probes. I really enjoy the time talking with him about research as well as life experience.

I want to express my gratitude to Drs. Songhua Chen, Wei Shao, Magdalena Sandor, Mark Butler, and Lilong Li during my internship at Halliburton. With their help, I gained valuable experience in designing and developing NMR software and hardware.

I would like to thank my committee members, Drs. Yue Wu, Sean Washburn, Laurie E. McNeil, Rosa T. Branca, and Jack Y. Ng., for their good advice on my research and valuable suggestion on my dissertation and presentation. The questions they brought up also made me think deeply about my research topics.

I need to thank the present and former members of Wu's group. They are: Patrick Doyle,

Yan Song, Yanchun Ling, Yao An, Yunzhao Xing, Zhixiang Luo, Haijing Wang, Jacob Forstater, Magdalena Sandor, Shaun Gidcumb, B. J. Anderson, and Courtney Hadsell. I benefit from the discussions and collaborations with them and I enjoy the time working with them.

I also want to thank my parents, for their encouragement and support during my PhD study. They have done too much to raise me, support my education, and give me a warm family. I understand that it was not easy for them. I really want to express my love to them.

I am especially grateful to my beloved girlfriend Shenmeng Xu. It was the happiest time of my life at UNC when I met her. I am so lucky to have her in my life. We have spent all of our time together for years, sharing happiness as well as sorrows. She was always by my side when I was working in the laboratory in the midnight and on weekends, when I was writing and revising my manuscripts in my messy office for countless times, and when I was struggled with job hunting and interviews. I would not have gotten through the difficult times without her support, care, and love. She also gave me good suggestion on my research and career, which I really appreciate. I became a better person because of her. I worked hard and will work even harder, for myself, for her, for our bright future.

TABLE OF CONTENTS

LIST OF TABLES

LIST OF FIGURES

LIST OF ABBREVIATIONS

BET	Brunauer, Emmett, and Teller
BSA	Bovine Serum Albumin
EtOH	Ethanol
FID	Free Induction Decay
FT	Fourier Transformation
FWHM	Full Width at Half Maximum
HEWL	Hen Egg White Lysozyme
NMR	Nuclear Magnetic Resonance
RF	Radio Frequency
TFE	Trifluoroethanol

CHAPTER 1

INTRODUCTION

1.1 Water at Interfaces and in Confinement

1.1.1 Water: Structure and Property

Water is present everywhere. It is well known that 70% of the Earth's surface is covered by liquid water and water vapor is an important constituent of the atmosphere [1-4]. In particular, water is essential to living systems [1, 2, 5-8]: without water, life would not exist and evolve.

The chemical structure of water is simple. As shown in Figure 1.1 (A), a water molecule (H_2O) consists of two hydrogen atoms (H) that are attached to one oxygen atom (O). The mean O-H bond length is 0.957 Å and the mean H-O-H angle is 104.5° [1, 2, 9]. The oxygen atom has a nucleus of eight positive charges while the hydrogen atom nucleus only has one positive charge. Moreover, compared with the hydrogen atom, the electrons of the oxygen atom are much closer to its nucleus [1, 2, 9]. As a consequence, the oxygen atom has a much stronger attraction to electrons than the hydrogen atom, making the oxygen atom negatively charged and the hydrogen atom positively charged. This results in the polarity of a water molecule [1, 2, 9]. Therefore, water molecules can attract each other. The attraction is the strongest when the O-H bond of one water molecule and the O atom of a nearby water molecule are on a line [1]. Such an attractive interaction is the well-known hydrogen bond [1]. As shown in Figure 1.1 (B), one water molecule can form up to four hydrogen bonds with four nearby water molecules; at the same time, it interacts with many other water molecules via dipolar interactions [1, 9-11].

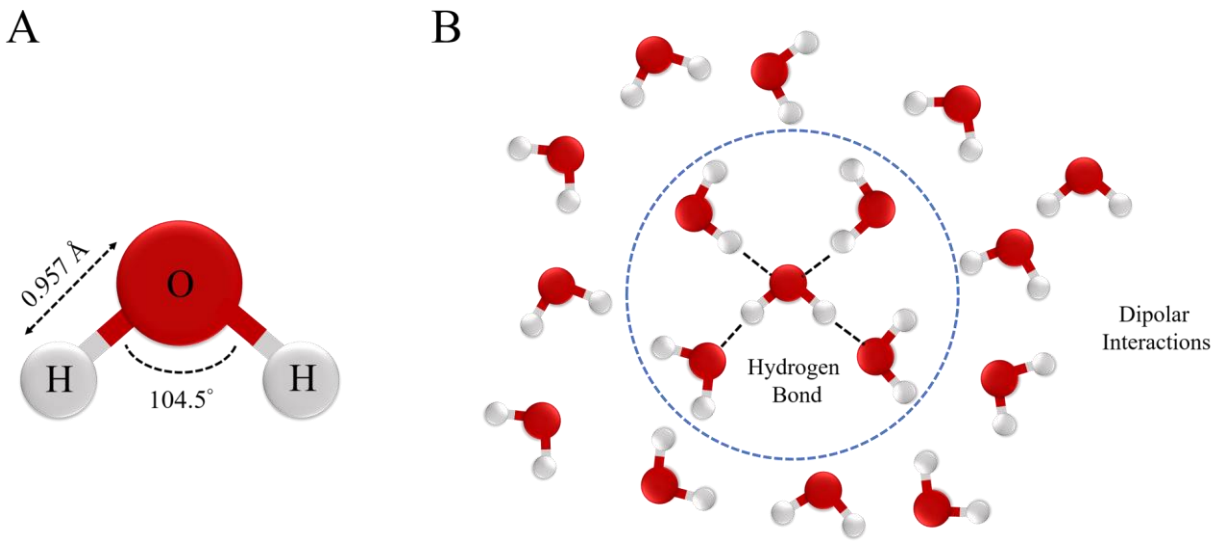

Figure 1.1: (A) Chemical structure of a water molecule (H_2O). The mean O-H bond length is 0.957 Å and the mean H-O-H angle is 104.5°. (B) A water molecule can form up to four hydrogen bonds with nearby water molecules. The hydrogen bonds are illustrated in dotted lines. Meanwhile, the water molecule can interact with many others via dipolar interactions.

Despite its simple chemical structure, the complex and anomalous behaviors of water are still mysterious to us [1, 2, 12, 13]. Just to quote D. H. Lawrence's words: "Water is H_2O, hydrogen two parts, oxygen one, but there is also a third thing, that makes it water and nobody knows what it is." [14] For instance, there exists a maximum in the density of water at 277K (4 C) [1, 2, 12, 15]; the specific heat capacity (C_p) of water has a minimum at 308K (35 C) and a maximum at 228K (-45 C) [1, 2, 12, 15]; the isothermal compressibility (κ_T) of water exhibits a minimum at 319K (46 C) [1, 2, 12]; two macroscopic phases, a low-density phase and a high-density phase, may appear in supercooled water around 180 K (-93 C) [12, 16]. These unique

behaviors of water make it very different from other liquids. Although there exist extensive studies focusing on the properties of water, the mechanism underlying the unique properties of water remains controversial and far from being understood [1, 12]. Therefore, research on water is still one of the most exciting topics in science.

1.1.2 Water on Surfaces: Interfacial Water

When water is in the proximity of a surface, its behavior becomes more intriguing. It has been found that the structure, dynamics (including the diffusion, rotation, and vibration behavior), and thermodynamics (including entropy, enthalpy, and phase transition property) of interfacial water all differ from those of bulk water [13, 17-19]. In general, the influence of an existing surface comes from two aspects [13, 17-19]. First, water can directly interact with the surface via hydrogen bonds, electrostatic forces, and other interactions. Second, water-water interactions can be disturbed and the water network over the surface is then reorganized. Although it has been recognized that these effects can contribute to the unusual properties of interfacial water, there is yet no agreement on the detailed mechanism [17-19].

In general, surfaces can be classified into two types according to their affinity to water [13, 17-19]. One type is the “hydrophilic” surface, such as the surface with charges, ions, or polar groups, which tends to attract water. The other type is the “hydrophobic” surface, such as the surface with non-polar groups, which prefers to repel water. The two types of surfaces are illustrated in Figure 1.2 A and B. These two types of surfaces affect the structure and property of water in distinct ways [13, 17-19]. For instance, water prefers to spread on a hydrophilic surface while it forms clusters on a hydrophobic surface [13, 17-19]. Particularly, as illustrated in Figure 1.2 C, hydrophobic groups in water tend to aggregate and extrude the water molecules [13, 17-

19]. This so-called “hydrophobic effect” results in the well-known oil-water separation [18], and also leads to the cell membrane formation, protein folding, and lipid-protein interaction [17]. Therefore, the interactions of water with hydrophilic and hydrophobic components have been of particular interest to researchers.

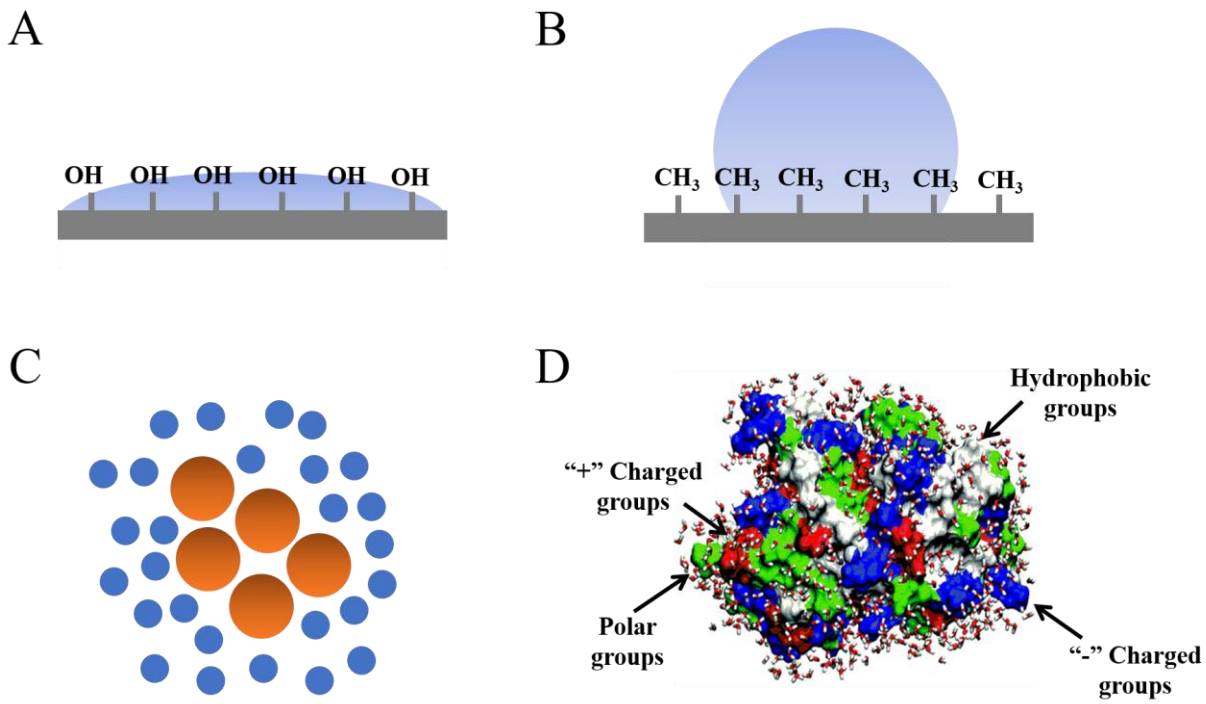

Figure 1.2: (A) A typical hydrophilic surface that is composed of hydroxyl (OH) groups. Water tends to spread on the surface. (B) A typical hydrophobic surface that is composed of methyl (CH_3) groups. The surface tends to repel water molecules. (C) Hydrophobic solutes are illustrated by brown dots, and water molecules are illustrated by blue dots. Hydrophobic solutes tend to aggregate together and repel water molecules out. (D) The surface of a protein is composed of various hydrophilic and hydrophobic groups. The positively (“+”) charged groups (red regions), negatively

charged ("-") groups (blue regions), and polar groups (green regions) are hydrophilic, while nonpolar groups (white regions) are hydrophobic [20].

1.1.3 Water on Biomolecular Surfaces

Water on the surface of a biomolecule is called "hydration water" [6, 7, 21, 22]. Hydration water is an integral part of a biomolecule, because it is of central importance for a biomolecule to maintain its three-dimensional structure and fluctuate between different conformations [6-8, 23]. Moreover, hydration water is actively involved in a variety of essential biological processes, such as protein folding, enzymatic activation, nucleic acid interactions, and drug recognition [6-8, 23]. Due to the importance of hydration water, extensive work has been done to investigate the hydration mechanism of proteins, nucleic acids, and membranes [8].

This dissertation is focused on the hydration of proteins. It has been recognized that without hydration, there is no protein activity [21, 22]. The protein activity is restored only when the amount of hydration water reaches ~0.2 (g water/g protein), and it increases dramatically with hydration till ~0.5 (g water/g protein) [21, 22]. Moreover, it has been suggested that hydration water drives protein folding and denaturation [8, 21-24]. In addition, hydration water mediates the recognition process in proteins [8, 21-23]. It is found that hydration water can help drug molecules target their binding sites [25, 26]. The mechanism underlying protein hydration is the key to understand protein functions; therefore, the effect of hydration on proteins is one of the main topics in this dissertation.

In particular, a protein is composed of a variety of hydrophilic (charged and polar) and hydrophobic (non-polar) groups [8, 20-22]; hence, the surface of a protein is highly heterogeneous. This is illustrated in Figure 1.2 (D). As discussed before, water interacts with

hydrophilic and hydrophobic components in distinct ways [8, 17, 18]. Therefore, this dissertation also aims to investigate how differently water at hydrophilic and hydrophobic groups affect protein properties.

1.1.4 Water in Confinement

When water is confined, it has to interact with the relatively large cavity surface and fit within the available space. Some well-known examples include water in the ion-channels of cell membranes [6, 8] and water in sedimentary rocks in the ground [27]. The configuration, orientation, and motion of confined water are largely restricted [13, 28-30]. The hydrogen-bonding pattern of the confined water network is also altered [13, 28-30]. The property of confined water strongly depends on the degree of confinement and the surface characteristics [13, 28-30].

In general, according to the surface property, there exist two distinct confinement conditions: hydrophilic confinement and hydrophobic confinement [28, 29]. In the hydrophilic confinement, water has strong hydrogen bonding and polar interactions with the cavity surface [28, 29]. A typical example is water in mesoporous silica such as MCM-41 and SBA-15 [29]. In the hydrophobic confinement, water prefers to exclude from the cavity surface and have a denser structure near the center of the cavity [28, 29]. The configuration and coordinates of confined water molecules are affected by weak van der Waals interactions between water and the cavity surface [28, 29]. Carbon nanotubes and activated carbons provide a hydrophobic confinement for water [29]. These two confinement conditions are illustrated in Figure 1.3.

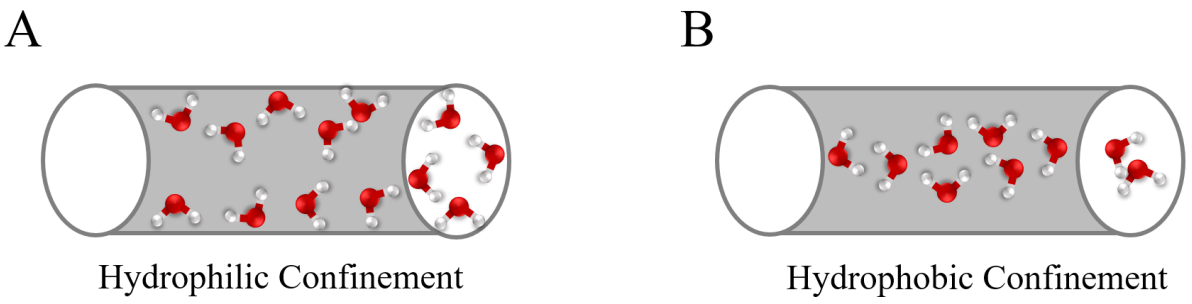

Figure 1.3: (A) In hydrophilic confinement, such as in MCM-41 and SBA-15, water molecules can absorb on the surface. (B) In hydrophobic confinement, such as in carbon nanotubes, water molecules tend to exclude from the surface and stay near the cavity center.

1.2 Nuclear Magnetic Resonance

1.2.1 Nuclei in a Magnetic Field

The atomic nucleus is composed of protons and neutrons, which are known as nucleons. The spins of nucleons give rise to the total spin of the nucleus. In an external magnetic field, the nuclear spin interacts with the field in a way that is analogous to a compass in the Earth's magnetic field. Specifically, the nuclear spin is quantized and the spin quantum number is denoted as I. The spin only has $(2I+1)$ orientations with the magnetic quantum number m equals $-I, -I+1, \ldots I$. Typical spin-1/2 (I=1/2) nuclei include ^{1}H, ^{19}F, ^{31}P, and ^{15}N. Typical spin-1 (I=1) nuclei include ^{2}H and ^{14}N. ^{23}Na is a typical spin-3/2 (I=3/2) nucleus.

When a spin-1/2 nucleus is placed in a static magnetic field B_0, there exist two states for the spin with the magnetic quantum number m equals +1/2 and -1/2, respectively. The magnetic moment μ of the spin is defined as $\mu = \gamma I$, where γ is the gyromagnetic ratio. If we define the direction of the static magnetic field B_0 as z, the z component of the spin $I_z = \frac{h}{2\pi} m$ and the z

component of the magnetic moment $\mu_z = \frac{\gamma h}{2\pi} m$. The energy of the magnetic moment in the magnetic field is $E = -\vec{\mu} \cdot \vec{B_0} = \mu_z \cdot B_0$. Therefore, for the spin-1/2 nucleus, there exist two energy levels with $E_1 = +\frac{1}{2} \cdot \frac{\gamma h B_0}{2\pi}$ and $E_2 = -\frac{1}{2} \cdot \frac{\gamma h B_0}{2\pi}$. The energy difference is $\Delta E = \frac{\gamma h B_0}{2\pi} = \hbar \omega_0$, where $\omega_0 = \gamma B_0$. ω_0 is the well-known Larmor frequency, i.e. the procession rate of a magnetic momentum in a magnetic field [31, 32]. This is illustrated in Figure 1.4. The population of the spins at two energy states can be described by the Boltzmann distribution [31, 32]. The population ratio is $\frac{N_1}{N_2} = \exp(\frac{\Delta E}{k_B T}) = \exp(\frac{\hbar \omega_0}{k_B T})$, where N_1 and N_2 represent the population of spins at the low-energy state and the high-energy state, respectively. Assuming that protons (^{1}H) are in a magnetic field of 1T at room temperature (300K), the population ratio of protons at two states is $(1 + 6.8 \times 10^{-6})$. It is seen that the population of spins on the low-energy state is only slightly higher than that on the high-energy state.

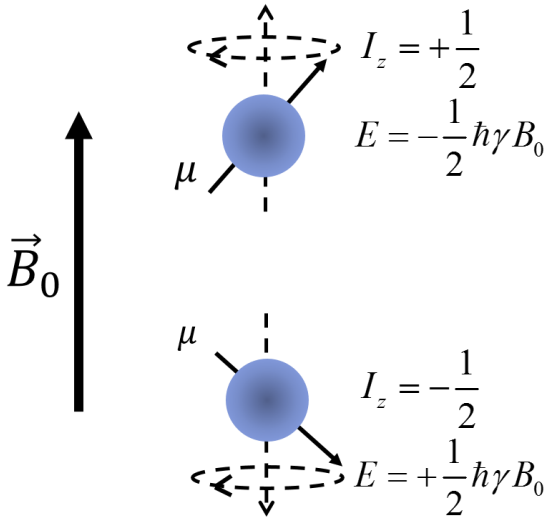

Figure 1.4: A spin-1/2 nucleus in a static magnetic field B_0. The spin processes at Larmor frequency $\omega_0 = \gamma B_0$. The energy of the spin splits into two states and the energy difference is $\Delta E = \hbar \omega_0$.

1.2.2 Resonance and Free Induction Decay (FID)

To transit between two energy levels, the spin must absorb or emit an amount of energy that equals $\Delta E = \hbar \omega_0$. Therefore, if an oscillating RF field (a pulse) with Larmor frequency (ω_0) is applied to the nucleus, the nuclear spin can jump from the low-energy state to the high-energy state. When the RF pulse is removed, the nuclear spin would relax to its low-energy state and re-emit RF waves with the Larmor frequency (ω_0). This process is called magnetic resonance [31, 32].

To describe the behavior of the macroscopic magnetization generated by all spins, it is preferred to switch from the laboratory frame to a rotating frame. The frame is rotating at Larmor frequency with the static magnetic field B_0. The RF field generates a magnetic field B_1 that is perpendicular to the static magnetic field B_0; hence, in the rotating frame, the effect of such RF pulse is to flip the magnetization with a certain angle with respect to the z axis (the direction of B_0). The flip angle θ is determined by the RF pulse width τ and can be described as $\theta = \gamma B_1 \cdot \tau$. When the flip angle θ is 90^o, the magnetization at the z axis (M_z) is flipped to the x-y plane (M_{xy}). When the RF pulse is removed, spins in the x-y plane gradually lose their coherence and re-orient to the z-axis. In other words, the magnetization in the x-y plane (M_{xy}) gradually vanishes and regrows to the z axis (M_z). A receiver coil is placed in the x-y plane to detect the signal that is generated by the change in M_{xy}. Such a signal is called the free induction decay (FID). A typical FID signal is shown in Figure 1.5.

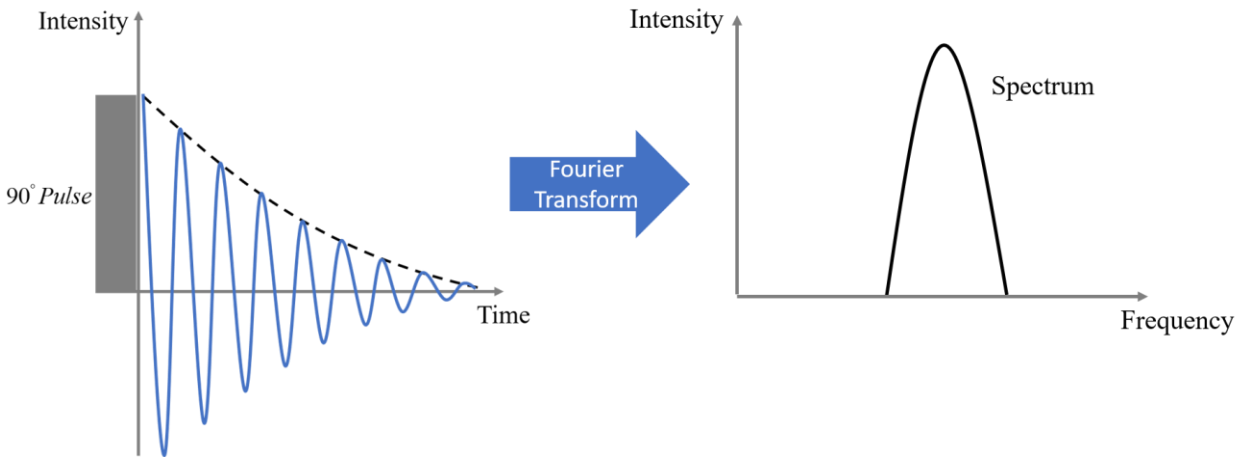

Figure 1.5: Illustration of a typical free induction decay (FID) signal. After Fourier Transform (FT), the spectrum in the frequency domain is obtained.

1.2.3 Relaxation

When the RF pulse is removed, the spin system will return to its equilibrium state. This process is called relaxation. Some common relaxation processes include the spin-lattice relaxation, the spin-spin relaxation, and the spin-lattice relaxation in the rotating frame [31, 32].

The spin-lattice relaxation (or longitudinal relaxation) corresponds to the regrowth of the magnetization in the z direction (M_z) [31, 32]. In this process, the spins in the excited state relax to the equilibrium state and transfer energy to the "lattice". The so-called "lattice" can be rotations and vibrations of the molecule. T_1 is denoted to characterize the spin-lattice relaxation process,

$$\frac{dM_z}{dt} = \frac{M_0 - M_z}{T_1} \tag{1.1}$$

$$M_z = M_0(1 - \exp(\frac{-t}{T_1})) \tag{1.2}$$

where M_0 is the initial macroscopic magnetization. Typical pulse sequences to measure T_1

include the inversion-recovery sequence and the saturation-recovery sequence [31, 32]. The inversion-recovery sequence is illustrated in Figure 1.6. A 180^o pulse is applied to flip the magnetization from M_z to $-M_z$. During a time interval τ, the magnetization regrows to the z direction. After that, a 90^o pulse is applied to flip the magnetization ($M(\tau)$) to the x-y plane. Finally, the FID signal is acquired. The T_1 relaxation time can be obtained by varying the time interval τ and fitting the FID intensity with Equation (1.2).

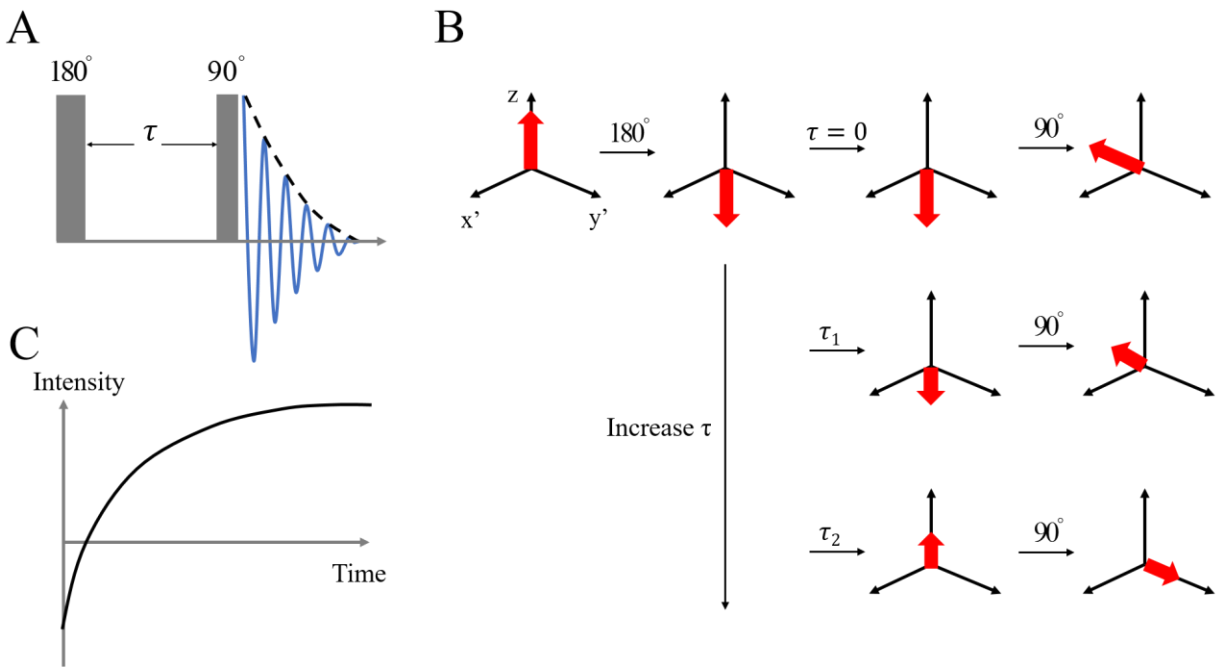

Figure 1.6: (A) Inversion-recovery sequence to measure T_1 relaxation. (B) The change of the magnetization in the rotating frame during the pulse sequence. (C) The regrowth curve of the magnetization in the T_1 measurement.

The spin-spin relaxation (or transverse relaxation) corresponds to the decay of the magnetization in the x-y plane (M_{xy}) [31, 32]. After being flipped to the x-y plane by the RF

pulse, nuclear spins gradually lose their coherence, inducing the decay of M_{xy}. T_2 is denoted to characterize the spin-spin relaxation process,

$$\frac{dM_{xy}}{dt} = -\frac{M_{xy}}{T_2} \tag{1.3}$$

$$M_{xy} = M_0 \exp(-\frac{t}{T_2}) \tag{1.4}$$

A typical pulse sequence to measure T_2 is the spin-echo (Hahn echo) sequence, which is illustrated in Figure 1.7. A 90^o pulse is applied to flip the magnetization from M_z to M_{xy}. During a time interval τ, the magnetization M_{xy} decays. Due to the inhomogeneity in the magnetic field, different spins may process at different rates. A following 180^o pulse is applied to refocus the magnetization a time interval τ, eliminating the inhomogeneous effects [31, 32]. The T_2 relaxation time can be obtained by varying the time interval τ and fitting the echo intensity with Equation (1.4).

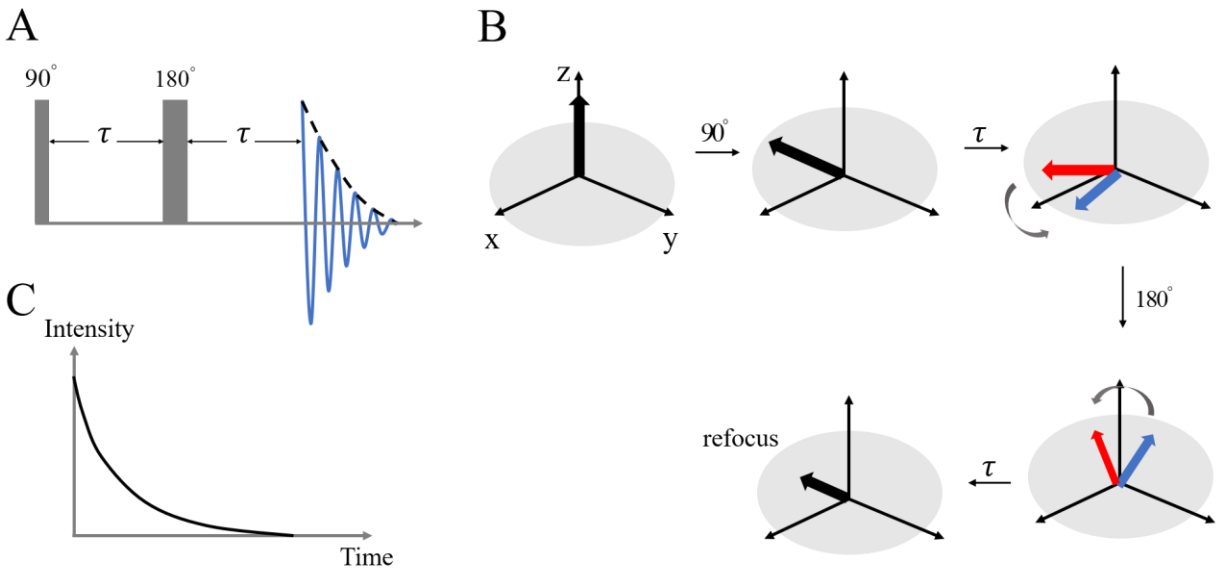

Figure 1.7: (A) Spin echo (Hahn echo) sequence to measure T_2 relaxation. (B) The change of the magnetization during the pulse sequence. After the 90^o pulse, because of the inhomogeneity in the magnetic field, some spins process faster (blue arrows) while some spins process slower (red arrows). A following 180^o pulse is applied to refocus the magnetization, eliminating the inhomogeneous effect. (C) The decay curve of the magnetization in the T_2 measurement.

The spin-lattice relaxation in the rotating frame corresponds to the decay of the magnetization along the RF field (B_1) [31, 32]. $T_{1\rho}$ is the time constant of this decay process. $T_{1\rho}$ is obtained by the spin-locking pulse sequence, which is illustrated in Figure 1.8. A 90^o pulse is applied to flip the magnetization from M_z to M_{xy}. After that, a long-duration and low-power RF pulse is applied in the same direction as the magnetization in the x-y plane. Hence, the magnetization appears to be "locked" in the rotating frame by such an RF pulse, which is also called the "spin-locking" pulse. During the spin-locking time interval τ, the magnetization decays along the RF field (B_1) in the rotating frame. The $T_{1\rho}$ relaxation time can be obtained by varying the time interval τ and fitting the FID intensity with Equation (1.6).

$$\frac{dM_{xy}}{dt} = -\frac{M_{xy}}{T_{1\rho}} \tag{1.5}$$

$$M_{xy} = M_0 \exp(-\frac{\tau_{spin-locking}}{T_{1\rho}}) \tag{1.6}$$

Particularly, $T_{1\rho}$ characterizes the relaxation in the RF field (B_1) which is usually about ~kHz; in contrast, T_1 and T_2 characterize the relaxation under the influence of the static field (B_0) which is usually about ~MHz. Therefore, $T_{1\rho}$ measurement is more sensitive to the slow relaxation

process (~ms), while T_1 and T_2 measurements are usually used to characterize the fast relaxation process (~ns) [31, 32].

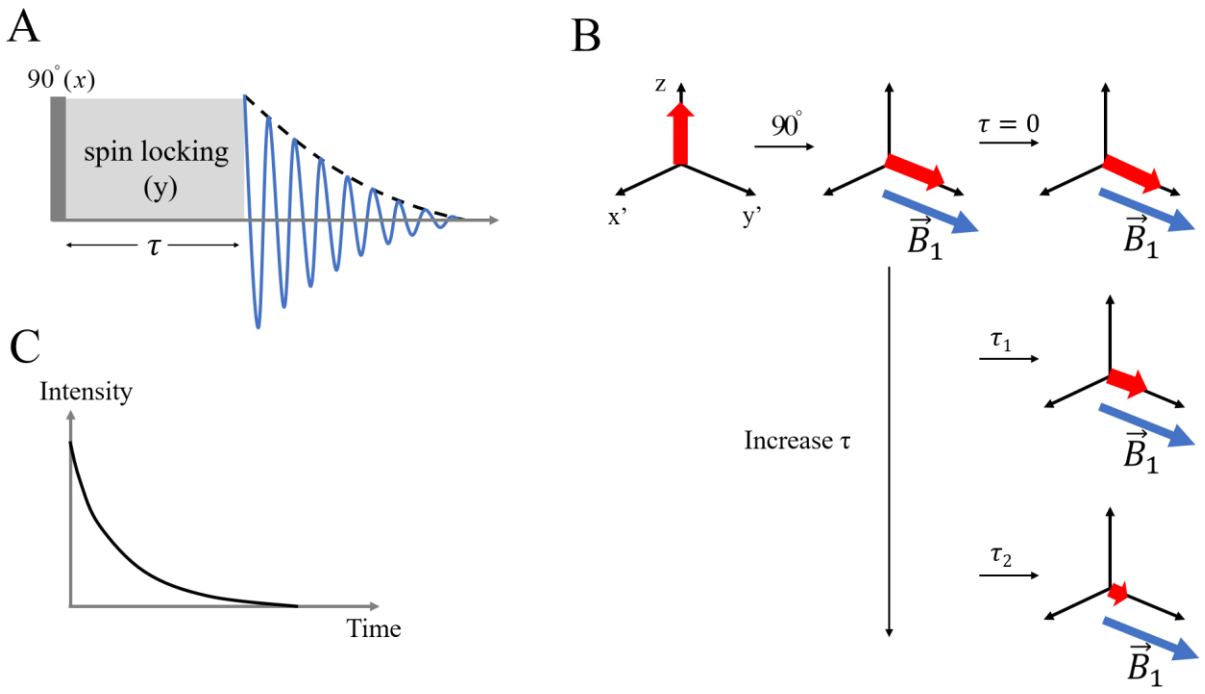

Figure 1.8: (A) Spin-locking sequence to measure $T_{1\rho}$ relaxation. (B) The change of the magnetization in the rotating frame during the pulse sequence. After the 90° pulse, in the rotating frame, the magnetization is on the same direction with the RF field B_1. (C) The decay curve of the magnetization in the $T_{1\rho}$ measurement.

1.3 Outlines of Dissertation

This dissertation is focused on NMR studies of protein hydration and protein-ligand interactions. Specifically, I investigate hydration water on the protein surface, including how hydration water interacts with the protein and the effect of hydration on protein-ligand

interactions. This dissertation is organized as follows:

In CHAPTER 2, I investigate the interaction between hydration water and the protein. I use an *in-situ* NMR technique to measure water isotherms on proteins at different temperatures. The unique NMR technique is introduced in detail. A qualitative change in the water isotherms around 10 C is observed. This phenomenon is explained by the change of protein's elasticity with temperature and is discussed in detail.

In CHAPTER 3, I discuss the thermodynamic and dynamic properties of the protein during its hydration process. The method of determining the changes in the free energy, entropy, and enthalpy of protein hydration is introduced. The dynamics of the protein on the timescales of nanosecond (ns) and microsecond (ms) are measured by NMR. Different roles of hydration at hydrophilic and hydrophobic groups are identified. A crossover in protein dynamics and thermodynamics at 10 C is revealed. This is induced by the qualitative changes in the protein-water interaction at 10 C, which is discussed in Chapter 2.

In CHAPTER 4, I study the interactions between alcohols and proteins. Isotherms of alcohols on dry proteins are obtained by the *in-situ* NMR technique introduced in Chapter 2. The thermodynamics of the alcohol-dry protein interaction are also studied. It is found that alcohol is able to bind to dry proteins and there exist two distinct types of alcohol-protein interactions.

In CHAPTER 5, I study the effect of hydration on the alcohol-protein interaction. Isotherms of alcohols on the protein are measured at different levels of protein hydration. The thermodynamics of the alcohol-protein interaction are studied as a function of hydration level. It is found that hydration facilitates the alcohol binding to nonspecific sites via reducing the binding threshold and shifting the binding from an entropy-driven to an enthalpy-driven process. The different roles of hydration in the binding of alcohols and some common general anesthetics

are also discussed.

In CHAPTER 6, I give a summary of the conclusions I have reached. The mechanism of protein hydration as well as the influence of hydration on protein dynamics and thermodynamics are briefly discussed. Particularly, the effect of hydration on alcohol-protein interactions are discussed.

1.4 REFERENCES

[1] D. Eisenberg, W. Kauzmann, The structure and properties of water, Oxford University Press, 2005.

[2] M. Chaplin, http://www1.lsbu.ac.uk/water/index.html.

[3] L.B. Railsback, An earth scientist's periodic table of the elements and their ions, Geology 31 (2003) 737-740.

[4] S. Mockler, Water vapor in the climate system, Special Report, American, Geophysical Union (1995).

[5] F. Franks, Water: a matrix of life, Royal Society of Chemistry, 2000.

[6] A. Author, Water in biological systems, Royal Society of Chemistry, 2010.

[7] D. Zhong, S.K. Pal, A.H. Zewail, Biological water: A critique, Chem. Phys. Lett. 503 (2011) 1-11.

[8] P. Ball, Water as an active constituent in cell biology, Chem. Rev. 108 (2008) 74-108.

[9] A.G. Császár, G. Czakó, T. Furtenbacher, J. Tennyson, V. Szalay, S.V. Shirin, N.F. Zobov, O.L. Polyansky, On equilibrium structures of the water molecule, The Journal of chemical physics 122 (2005) 214305.

[10] V. Voloshin, Y.I. Naberukhin, Proper and improper hydrogen bonds in liquid water, J. Struct. Chem. 57 (2016) 497-506.

[11] A. Rastogi, A.K. Ghosh, S. Suresh, Hydrogen Bond Interactions Between Water Molecules in Bulk Liquid, Near Electrode Surfaces and Around Ions, INTECH Open Access Publisher, 2011.

[12] A. Nilsson, L.G. Pettersson, The structural origin of anomalous properties of liquid water, Nat. Commun. 6 (2015).

[13] S. Granick, S.C. Bae, A curious antipathy for water, Science 322 (2008) 1477-1478.

[14] D.H. Lawrence, The complete poems of DH Lawrence, Wordsworth Editions, 1994.

[15] H. Tanaka, Simple physical explanation of the unusual thermodynamic behavior of liquid water, Phys. Rev. Lett. 80 (1998) 5750.

[16] O. Mishima, H.E. Stanley, The relationship between liquid, supercooled and glassy water, Nature 396 (1998) 329-335.

[17] L.R. Pratt, A. Pohorille, Hydrophobic effects and modeling of biophysical aqueous solution interfaces, Chem. Rev. 102 (2002) 2671-2692.

[18] D. Chandler, Interfaces and the driving force of hydrophobic assembly, Nature 437 (2005) 640-647.

[19] C. Sendner, D. Horinek, L. Bocquet, R.R. Netz, Interfacial water at hydrophobic and hydrophilic surfaces: Slip, viscosity, and diffusion, Langmuir 25 (2009) 10768-10781.

[20] L. Mitra, N. Smolin, R. Ravindra, C. Royer, R. Winter, Pressure perturbation calorimetric studies of the solvation properties and the thermal unfolding of proteins in solution—experiments and theoretical interpretation, PCCP 8 (2006) 1249-1265.

[21] J.A. Rupley, G. Careri, Protein hydration and function, Adv. Protein Chem. 41 (1991) 37-172.

[22] I.D. Kuntz, W. Kauzmann, Hydration of Proteins and Polypeptides, Adv. Protein Chem. 28 (1974) 239-345.

[23] M. Chaplin, Do we underestimate the importance of water in cell biology?, Nat. Rev. Mol. Cell Biol. 7 (2006) 861-866.

[24] F. Mallamace, C. Corsaro, D. Mallamace, P. Baglioni, H.E. Stanley, S.-H. Chen, A possible role of water in the protein folding process, The Journal of Physical Chemistry B 115 (2011) 14280-14294.

[25] J.E. Ladbury, Just add water! The effect of water on the specificity of protein-ligand binding sites and its potential application to drug design, Chemistry & Biology 3 (1996) 973-980.

[26] R. Baron, J.A. McCammon, Molecular recognition and ligand association, Annual review of physical chemistry 64 (2013) 151-175.

[27] S. Rocks, Petrology of the sedimentary rocks, Cambridge University Press, (1974).

[28] N.E. Levinger, Water in confinement, Science 298 (2002) 1722-1723.

[29] M.F. Chaplin, Structuring and behaviour of water in nanochannels and confined spaces, Adsorption and phase behaviour in nanochannels and nanotubes, Springer, 2010, pp. 241-255.

[30] F. Mallamace, C. Corsaro, D. Mallamace, S. Vasi, C. Vasi, H.E. Stanley, Thermodynamic properties of bulk and confined water, The Journal of chemical physics 141 (2014) 18C504.

[31] A. Abragam, The principles of nuclear magnetism, Oxford university press1961.

[32] M.H. Levitt, Spin dynamics: basics of nuclear magnetic resonance, John Wiley & Sons, 2001.

CHAPTER 2

WATER ADSORPTION ON THE PROTEIN

2.1 Introduction

Hydration water plays a crucial role in protein folding, enzyme catalysis, and protein-ligand interactions [1-3]. For instance, it has been suggested that hydrophobic interactions originating from the disruption and reconstruction of the hydration shell may drive protein folding [1, 2, 4, 5]. Furthermore, it is known that the onset of the enzymatic activity of a protein requires a minimum hydration level h ~0.2 (g water/g protein) [6, 7]. In addition, some researchers have suggested that water molecules at specific groups on the protein surface are critical for ligands to target their binding sites [3, 8, 9]. Therefore, the mechanism governing protein-water interactions has attracted great attention over the past decades.

One way to study protein-water interactions is to measure the adsorption isotherm of water on the protein. Water adsorbs on the protein surface mainly by hydrogen-bonds and Van der Waals interactions [6, 7]. To obtain the isotherm, the amount of adsorbed water on the protein is measured as a function of water vapor pressure at a certain temperature. The water isotherm can give us valuable information on the surface property of the protein as well as the energies of protein-water interactions [6, 7]. In previous work, isotherms are usually obtained by gravimetric and volumetric methods [6, 7, 10]. However, these traditional methods are very inconvenient because they require frequent transfer of adsorbents and the conditions (e.g. the temperature) of the adsorption are hard to control [6, 7, 10-12]. Here, I developed a unique NMR

instrument, which enables me to measure isotherms at *in-situ* sample conditions with precisely controlled vapor pressure and temperature.

By employing this *in-situ* NMR method, I measured water isotherms on proteins over a wide range of water vapor pressure and temperatures. It is found that there is a qualitative change in the water isotherm above the hydration level *h* of ~0.2 (g water/g protein), especially around 10 C. This is induced by the change in the protein elasticity and will be discussed in detail. The work in this chapter shows the significant effect of hydration on protein flexibility and protein function.

2.2 Experiments

2.2.1 Protein Samples

Two typical globular proteins, bovine serum albumin (BSA) and hen egg-white lysozyme (HEWL), are used in the experiments. BSA (lyophilized powder, ≥ 98%, pH ≈ 7, 1% in 0.15 M NaCl) and HEWL (catalog no. L-7561, 3x crystallized, dialyzed, and lyophilized) are purchased from Sigma-Aldrich and used without further purification. These two proteins are very common model proteins because of their well-known protein structure and function [11, 13-15].

2.2.2 NMR Isotherm Measurements

The *in-situ* NMR instrument is illustrated in Figure 2.1.

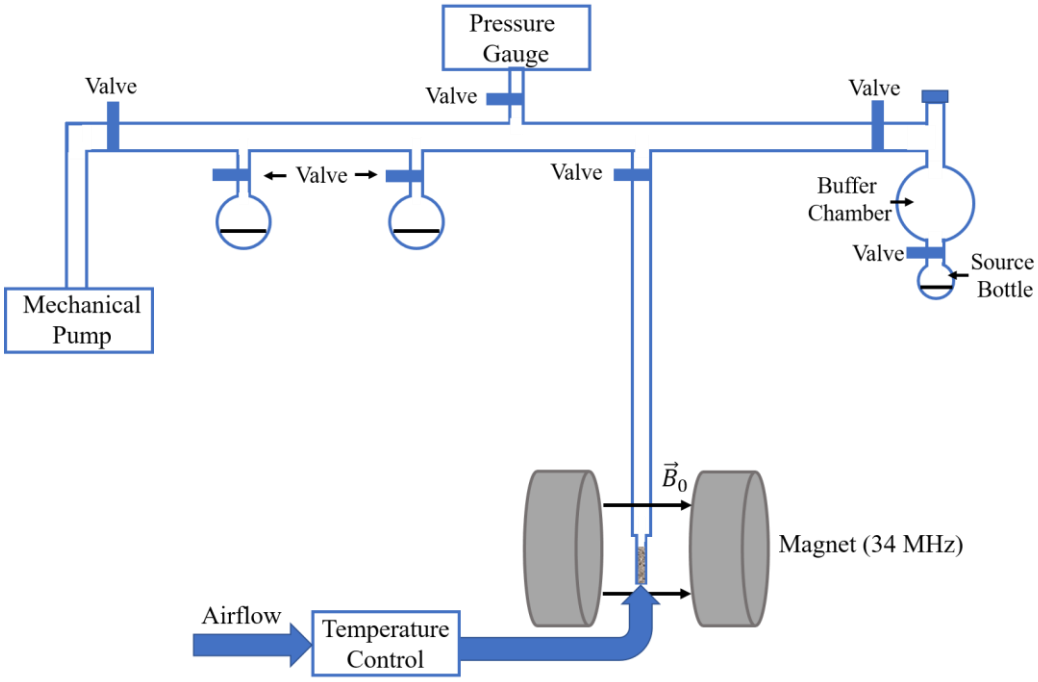

Figure 2.1: Illustration of the *in-situ* NMR instrument (for the 34MHz magnet).

Distilled water (H_2O) is stored in a source bottle with a pressure buffer chamber. The vapor pressure of water is controlled by adjusting the valves close to the buffer chamber. The protein sample is placed at the end of a long quartz NMR tube. The temperature of the protein sample is controlled by regulating the temperature of the airflow surrounding the quartz NMR tube. The protein sample is first pumped at room temperature by a mechanical pump for 1−2 days, to remove preadsorbed water. A single pulse was used to excite the ^{1}H NMR signal of the protein at B_0~0.8 T magnet (~34 MHz ^{1}H NMR frequency) and the ^{1}H free-induction-decay (FID) signal was detected. As seen in Figure 2.2 (A), a broad peak with full width at half maximum (FWHM) of ~30 kHz associated with the dry protein is detected. This spectrum is used as a quantitative reference to evaluate the amount of water sorption in the protein. To measure water isotherms, the dry protein is exposed to water vapor at a given vapor pressure *P*. The ^{1}H FID signal is then detected for the hydrated protein sample. As seen in Figure 2.2 (B), a

sharp peak with FWHM of ~1-2 kHz above the broad peak is now observed. The ^{1}H NMR signal of water vapor in the empty NMR tube without a protein sample is negligible as compared to this sharp peak. Therefore, this sharp peak is associated with water sorption in the protein. The integrated area of the spectrum of the dry protein is subtracted from that of the hydrated protein; hence, such difference in the spectrum intensity is purely attributed to protons from adsorbed water and is used to calculate the protein hydration level *h* (g water/g protein), based on the ratio of proton numbers of the protein and water. Isotherms are obtained by carrying out the measurements as a function of water vapor pressure at 3 C, 5 C, 16 C, and 27 C. Details of the experimental procedure have been reported in the references [11, 12, 16, 17]. The measured isotherms are consistent with those measured by the traditional gravimetric method [6, 7, 10, 11], but this technique is much more convenient to conduct NMR measurement in *in-situ* condition samples over a wide range of hydration level and temperature.

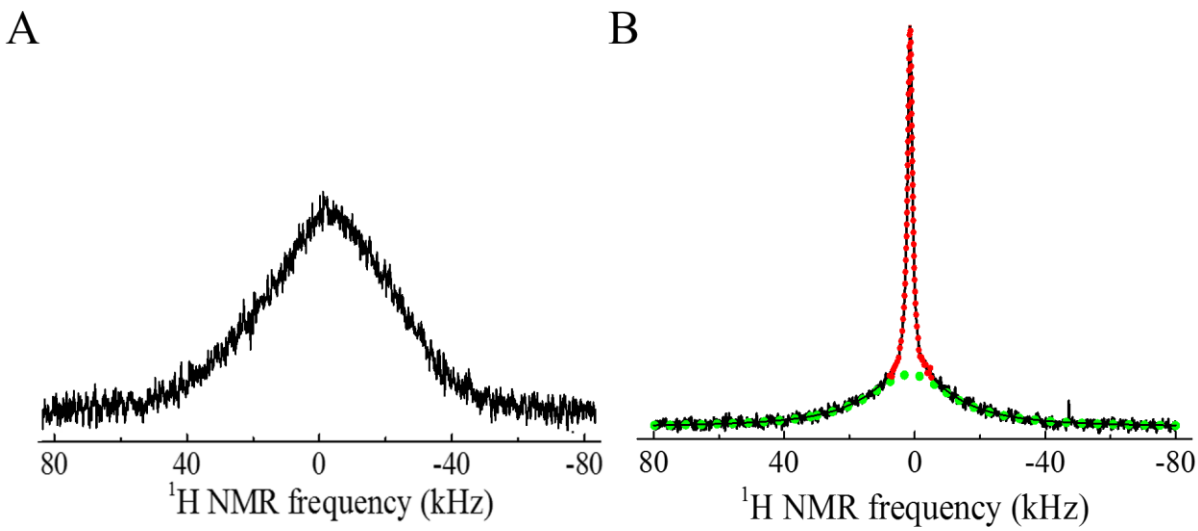

Figure 2.2: (A) ^{1}H NMR spectrum of dry BSA at 16 C. Only a broad peak (FWHM ~40 kHz) is observed. (B) ^{1}H NMR spectrum of BSA at 16 C at hydration level h~0.15 (g water/g BSA). With hydration, the spectrum consists of a broad peak (FWHM ~30 kHz) and a sharp peak (FWHM ~1-2 kHz) above it.

2.3 Results and Discussion

2.3.1 Adsorption Isotherms of Water on Proteins

Water isotherms on BSA and lysozyme were measured at 3 C, 5 C, 16 C, and 27 C and are shown in Figure 2.3 (A) and (B) respectively [17]. In the figure, the amount of adsorbed water, i.e. the protein hydration level h (g water/g protein) is plotted versus P/P_0, where P and P_0 represent the vapor pressure and saturated vapor pressure of water at a certain temperature. It is seen that when $P/P_0 < \sim 0.7$ (i.e. hydration level $h <\sim 0.15$-0.2), water adsorption increases linearly with vapor pressure and water isotherms at different temperatures practically overlap, whereas above $P/P_0 \sim 0.7$ (i.e. hydration level h above ~0.15-0.2), water isotherms show obvious temperature dependence: there is an obvious upswing in the water isotherms at temperatures above 5 C. In addition, when P/P_0 reaches 1, further hydration only causes the condensation of bulk water in the protein with no vapor pressure change.

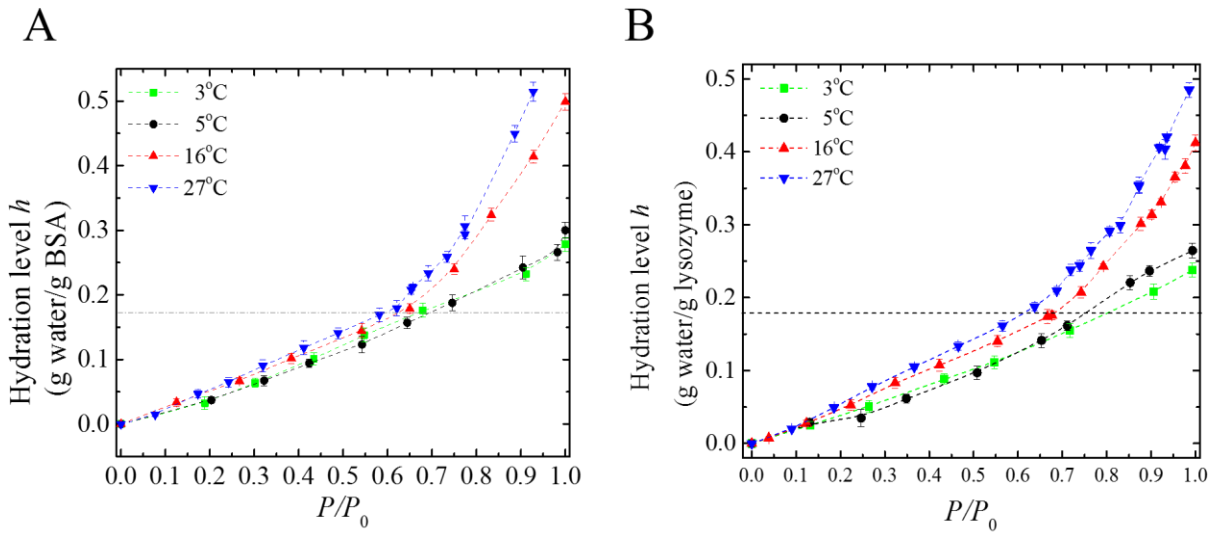

Figure 2.3: Water isotherms on (A) BSA and (B) lysozyme measured *in situ* at 3 C, 5 C, 16 C, and 27 C by NMR.

Similar water isotherms on BSA and lysozyme are observed, indicating that such hydration behavior could be general in globular proteins due to their similar surface chemistry [6, 7, 18]. It has been suggested that water adsorption on globular proteins has several stages [6, 7]. Briefly, when the protein hydration level h < ~0.2 (g water/g protein), water only binds to hydrophilic (charged and polar) groups on the protein surface; when h > ~0.2, all the hydrophilic groups are covered and water starts interacting with hydrophobic (nonpolar) groups. The results in Figure 2.3 indicate that water interacts differently with hydrophilic and hydrophobic groups on the protein, where the temperature plays distinct roles.

2.3.2 Upswing of Water Isotherm above *h*~0.2: Surface Adsorption vs Mixing Model

In the surface adsorption theory, the upswing of the isotherm above h~0.2 is attributed to the formation of multilayers of water on the protein surface [6, 7, 19]. One popular theory

describing this multilayer formation process is the Brunauer-Emmett-Teller (BET) theory [19]. In the BET theory, the amount of the adsorbed molecules v can be expressed as:

$$v = \frac{v_m cx}{(1-x)[(c-1)x+1]} \tag{2.1}$$

or,

$$\frac{v}{v_m} = \frac{x}{1-x} + \frac{(c-1)x}{(c-1)x+1} \tag{2.2}$$

where v_m is the amount of the monolayer adsorbed molecules, $x = \frac{P}{P_0}$, and c is the BET constant which is related to the heat of adsorption. It is seen in Equation (2.2) that the adsorption dramatically increases with increasing vapor pressure, and the amount of adsorption would reach infinity when P/P_0 approaches 1. In fact, the spatial restriction of the protein surface will set a limitation on the number of adsorbed water layers and prevent the condensation of bulk water [6, 7, 11].

In an alternative theory, the upswing of the isotherm above h~0.2 is explained by the mixing of the protein with water molecules based on the Flory-Huggins solution theory [6, 20, 21]. In the Flory-Huggins theory, the number of adsorbed water molecules is N_1 and the protein is composed of N_2 molecules. The adsorption is treated as a mixing process of N_1 water molecules with N_2 protein molecules in a 3-D lattice. In the lattice, each water molecule occupies one lattice cell and the protein occupies x lattice cells. In the view of thermodynamics, the Gibbs free energy change of the mixing process is:

$$\Delta G_m = \Delta H_m - T\Delta S_m + \Delta H_{el} \tag{2.3}$$

There are there terms in Equation (2.3). The first term ΔH_m is the enthalpy of mixing:

$$\Delta H_m = \frac{\chi k_B T N_1 N_2}{N_1 + xN_2} \tag{2.4}$$

where χ is a constant that is related to the strength of the protein-water interaction. The second term ΔS_m is the entropy of mixing:

$$\Delta S_m = -k_B(N_1 \ln v_1 + N_2 \ln v_2) \tag{2.5}$$

where $v_1 = \frac{N_1}{N_1 + xN_2}$ and $v_2 = \frac{xN_2}{N_1 + xN_2}$ are the volume ratios of water and the protein respectively. The third term ΔH_{el} is the elastic energy of the system due to the volume expansion of the protein in the mixing process.

$$\Delta H_{el} = \frac{1}{2} KV(v_2^{-1/3} - 1)^2 \tag{2.6}$$

where K is a parameter representing the elastic modulus of the protein, and V is the total volume of N_1 water molecules and N_2 protein molecules. Therefore, it is seen that the mixing of water and the protein is driven by the favorable change in the entropy of the mixing ΔS_m. The upswing in the isotherm induces a dramatic increase in the entropy of the mixing, hence it is favored by the change in the Gibbs free energy.

2.3.3 Temperature Dependence of Water Isotherms above $h \sim 0.2$

Although the upswing of the water isotherms in proteins above $h \sim 0.2$ has been previously reported, the temperature dependence of the water isotherms was not observed in these previous studies [6, 7, 10, 22-25]. The reason is that these previous works only measure water isotherms at room temperature or temperatures above that, but the temperature dependence of the water isotherms only appears at low temperatures below 10 C (the reason will be discussed later). This is illustrated in Figure 2.4. The solid line (red triangles) is the water isotherm in lysozyme I measured at 27 C and the two dashed lines are the water isotherms in lysozyme

measured at 35 C (magenta squares) and 50 C (green circles) in the reference [23-25]. It is seen that the water isotherms in Figure 2.4 show little temperature dependence, which is different from the result in Figure 2.3.

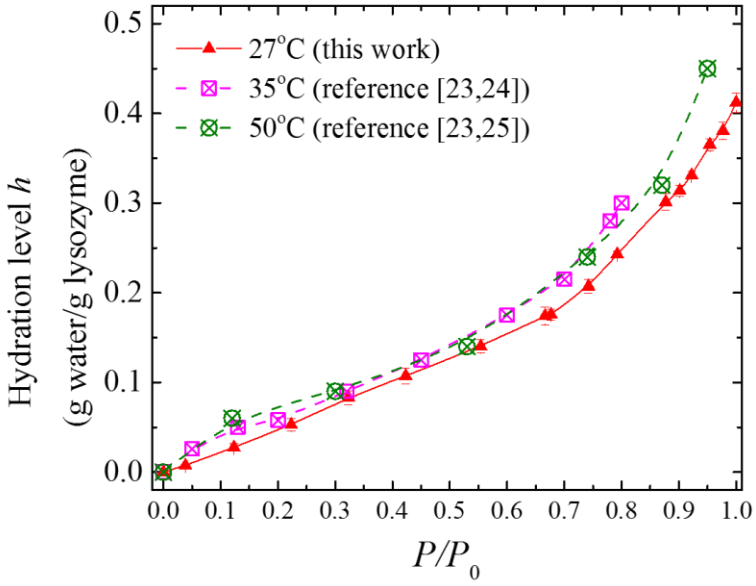

Figure 2.4: Water isotherms on lysozyme measured 27 C (red triangles, this work), 35 C (magenta squares, from reference [23, 24]) , and 50 C (green circles, reference). In contrast to Figure 2.3, these water isotherms only show weak temperature dependence.

There exist two main reasons why there are few previous studies on water isotherms in proteins at low temperatures. One reason is that it was generally believed that water isotherms are temperature independent when it is plotted versus P/P_0 [6, 7]. On the one hand, in the surface adsorption BET theory, the adsorption at high vapor pressure is seen to be dominated by the first term in Equation (2.2), which is obviously independent of the temperature. On the other hand, in the Flory-Huggins solution theory, it was pointed out that the third term in Equation (2.3) is too

small to have any effect on the isotherm [6, 7, 20, 21], so the isotherm was thought to be dominated by the first and second terms in Equation (2.3), which are temperature independent. However, this claim is not correct when the temperature is below 10 C [11] and will be discussed later. Another reason is that it is very inconvenient to measure water isotherms at low temperatures by traditional gravimetric and volumetric methods, especially around 0 C [6, 7, 10-12]. Here, the *in-situ* NMR technique enables me to precisely measure water isotherms below 10 C; hence the unique temperature dependence of water isotherms above $P/P_0 \sim 0.7$ is revealed.

2.3.4 Protein Elasticity and Its Temperature Dependence

In the BET theory, the first term in Equation (2.3) dominates the isotherm at high vapor pressure (above $h \sim 0.2$) and is temperature independent. The second term contains a BET constant c showing weak temperature dependence [6, 7, 19]; however, it has a trivial contribution to the isotherm in such a small temperature variation as in Figure 2.3 (from 27 C to 3 C). Hence, the strong temperature dependence of water adsorption on the protein above $h \sim 0.2$ cannot be explained by the traditional surface adsorption theory.

In the Flory-Huggins theory, the third term ΔH_{el} in Equation (2.3) was generally ignored and the isotherm was believed to be dominated by the other two temperature independent terms [6, 7, 20, 21]; however, our previous work has shown that this is incorrect, especially at temperatures below 10 C [11]. The third term ΔH_{el} actually plays a critical role in water adsorption on the protein, because the elastic modulus K of the protein in Equation (2.6) of ΔH_{el} strongly depends on temperature [11, 26]. As illustrated in Figure 2.5, it has been reported that the elastic modulus K of lysozyme increases dramatically when the temperature decreases [26]; such increase is especially significant when the temperature is below 10 C [11]. This explains the

strong temperature dependence of the water isotherm above h~0.2 around 10 C [11]: when the temperature decreases below 10 C, the elastic modulus of the protein increases dramatically; hence, the elastic energy ΔH_{el} of the system is very large. According to Equation (2.3), this would substantially increase the Gibbs free energy change ΔG_m. In other words, the mixing of water and the protein below 10 C is significantly energy unfavorable. Therefore, water adsorption on the protein below 10 C is substantially suppressed.

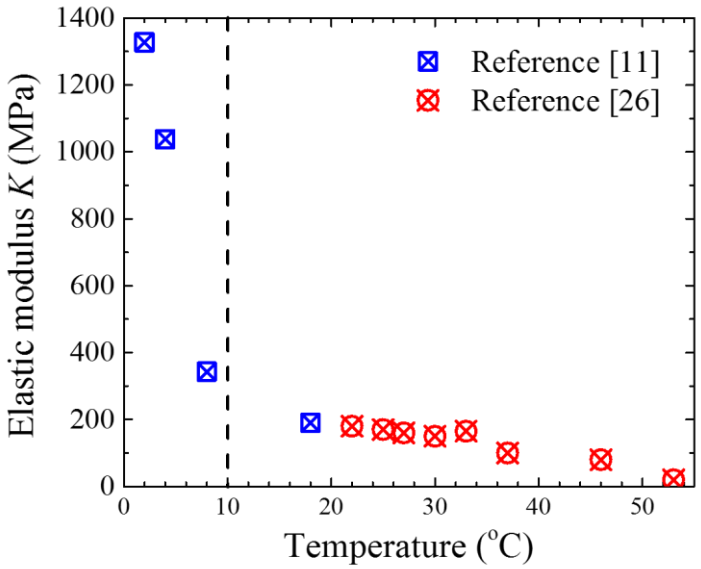

Figure 2.5: Elastic modulus of lysozyme versus temperature. Below 10 C, the elastic modulus of the protein significantly increases with decreasing temperature [11, 26].

2.3.5 Protein Structural Changes with Hydration and Temperature

The elastic modulus K is an averaged macroscopic parameter showing the flexibility of the protein which is microscopically heterogeneous [26, 27]. Hence, the elastic modulus of the protein is closely related to the microscopic structure of the protein, which changes with hydration level and temperature [26, 27].

It has been shown that the elastic modulus of the protein decreases dramatically with increasing hydration level till h~0.2, but it depends weakly on the hydration level above h~0.2 [28]. This indicates that water at hydrophilic groups strongly enhances the protein flexibility, while water at hydrophobic groups weakly affects the protein flexibility. This is because in the dry protein there exist strong hydrogen bonds and electrostatic contacts between hydrophilic groups of the protein, leading to a very compact protein structure [6, 7, 29]. Hydration of hydrophilic groups (h<~0.2) can loosen the compact structure and ease the spatial restriction in the protein, because the strong non-native protein-protein interactions are replaced by water-protein hydrogen bonds [6, 7, 29]. This significantly increases the flexibility of the protein. In addition, it has been recognized that hydration of hydrophilic groups basically removes all non-native interactions in the protein, and the protein structure above h~0.2 is similar to that in solution [6, 7, 29]. Further hydration of the hydrophobic groups (h>~0.2) has a weak effect on the protein structure [6, 7, 29], hence the elastic modulus of the protein hardly changes above h~0.2.

Figure 2.5 shows that the elastic modulus of the protein weakly depends on the temperature above 10 C, while it dramatically increases with decreasing temperature below 10 C. The dramatic change in the protein flexibility around 10 C is strongly related to the microscopic structural change of the protein [27, 30]. Previous work has studied the microscopic structure of proteins such as lysozyme at temperatures below 10 C (around 4 C and 7 C) and above 10 C (around 30 C) [31-33]. It has been found that although the overall protein structure below 10 C is similar to that above 10 C, there exist significant changes in the local structure below 10 C, especially in the flexible regions such as α helices [31-33]. Globular proteins such as BSA and lysozyme have abundant α helix structures, which contribute the most to the flexibility of the

protein [14, 32]. As the temperature decreases below 10 C, the relative angles between α helices significantly change, leading to a more compact packing of helix units [31-33]. Such local structural distortion below 10 C results in a strong spatial restriction of α helices, substantially decreasing the protein flexibility [31-33]. Meanwhile, the cavities between helices are shrunk and water molecules in those cavities are squeezed out [31-33]. These microscopic structural changes in the protein are consistent with the crossover around 10 C in the protein flexibility and water adsorption reported in this chapter.

2.3.6 Implication for Protein Functions

It is worth mentioning that the property of water adsorption on proteins is strongly correlated to protein functions. For instance, the protein has no enzymatic activity without hydration and it requires a minimum hydration level of h~0.2 to restore the enzymatic activity [6, 7]. This agrees with the change in water isotherms around h~0.2. At h~0.2, water starts mixing with the protein, accompanying the activation of the enzyme. In addition, it has been reported that above h~0.2, the enzymatic activity of the protein decreases with decreasing temperature from 50 C to 5 C [34]. This is consistent with the temperature dependence of water isotherms on proteins above h~0.2. As the temperature decreases, the adsorption of water is substantially reduced especially below 10 C, accompanying the decrease in the enzymatic activity. Therefore, the results in this chapter show that hydration water is critical to protein functions.

2.4 Conclusions

By employing an *in-situ* NMR technique, I measure water isotherms on two globular proteins from 3 C to 27 C. The unique NMR technique enables me to study water adsorption on

proteins over a wide range of hydration level and temperature; as a result, some unique properties of protein hydration are revealed. It is found that when the hydration level h is below ~0.15-0.2, water adsorption increases linearly with the water vapor pressure and the isotherms at different temperatures practically overlap. Above h~0.15-0.2, the water isotherms show obvious temperature dependence: there is a dramatic upswing in the isotherms above 10 C, while water adsorption below 10 C is substantially suppressed.

As explained above, at h<~0.15-0.2 water only binds to hydrophilic (charged and polar) groups on the protein surface via electrostatic forces and hydrogen bonding that are hardly affected by the small temperature variation in our experiment. When h>~0.15-0.2, water starts mixing with hydrophobic (nonpolar) protein groups favored by the entropy of mixing. At higher temperatures, the elastic modulus of protein is small and such mixing of the protein with water is energetically less costly in terms of elastic energy. However, at lower temperatures, the protein becomes rigid with much larger elastic modulus and the mixing process becomes energetically unfavorable. The reduction in the protein flexibility with decreasing temperature is particularly significant below 10 C. As a result, adsorption of water at hydrophobic groups is drastically reduced below 10 C.

The changes in the water isotherms are found to be directly related to protein functions. The onset of protein enzymatic activity at h~0.2 is consistent with the upswing of water isotherms at h~0.2. The decrease in protein enzymatic activity below 10 C is consistent with the dramatic reduction of water adsorption below 10 C. Hence, the work in this chapter shows the significance of hydration water in protein functions.

2.5 REFERENCES

[1] P. Ball, Water as an active constituent in cell biology, Chem. Rev. 108 (2008) 74-108.

[2] Y. Levy, J.N. Onuchic, Water mediation in protein folding and molecular recognition, Annu. Rev. Biophys. Biomol. Struct. 35 (2006) 389-415.

[3] Z. Li, T. Lazaridis, Water at biomolecular binding interfaces, PCCP 9 (2007) 573-581.

[4] L.R. Pratt, A. Pohorille, Hydrophobic effects and modeling of biophysical aqueous solution interfaces, Chem. Rev. 102 (2002) 2671-2692.

[5] F. Mallamace, C. Corsaro, D. Mallamace, P. Baglioni, H.E. Stanley, S.-H. Chen, A possible role of water in the protein folding process, The Journal of Physical Chemistry B 115 (2011) 14280-14294.

[6] J.A. Rupley, G. Careri, Protein hydration and function, Adv. Protein Chem. 41 (1991) 37-172.

[7] I.D. Kuntz, W. Kauzmann, Hydration of Proteins and Polypeptides, Adv. Protein Chem. 28 (1974) 239-345.

[8] R. Baron, P. Setny, J. Andrew McCammon, Water in cavity− ligand recognition, J. Am. Chem. Soc. 132 (2010) 12091-12097.

[9] G. Hummer, Molecular binding: Under water's influence, Nat. Chem. 2 (2010) 906-907.

[10] G. Diakova, Y.A. Goddard, J.-P. Korb, R.G. Bryant, Changes in protein structure and dynamics as a function of hydration from 1 H second moments, J. Magn. Reson. 189 (2007) 166-172.

[11] H.-J. Wang, A. Kleinhammes, P. Tang, Y. Xu, Y. Wu, Temperature dependence of lysozyme hydration and the role of elastic energy, Phys. Rev. E 83 (2011) 031924.

[12] H.-J. Wang, A. Kleinhammes, P. Tang, Y. Xu, Y. Wu, Critical Role of Water in the Binding of Volatile Anesthetics to Proteins, The Journal of Physical Chemistry B 117 (2013) 12007-12012.

[13] K.A. Majorek, P.J. Porebski, A. Dayal, M.D. Zimmerman, K. Jablonska, A.J. Stewart, M. Chruszcz, W. Minor, Structural and immunologic characterization of bovine, horse, and rabbit serum albumins, Molecular Immunology 52 (2012) 174-182.

[14] T. Peters Jr, All about albumin: biochemistry, genetics, and medical applications, Academic Press, 1995.

[15] G. Careri, E. Gratton, P.-H. Yang, J. Rupley, Correlation of IR spectroscopic, heat capacity, diamagnetic susceptibility and enzymatic measurements on lysozyme powder, Nature 284 (1980) 572-573

[16] Y. Chong, A. Kleinhammes, P. Tang, Y. Xu, Y. Wu, Dominant Alcohol–Protein Interaction via Hydration-Enabled Enthalpy-Driven Binding Mechanism, The Journal of Physical Chemistry B 119 (2015) 5367-5375.

[17] Y. Chong, A. Kleinhammes, Y. Wu, Protein dynamics and thermodynamics crossover at 10° C: Different roles of hydration at hydrophilic and hydrophobic groups, Chem. Phys. Lett. 664 (2016) 108-113.

[18] H. Saito, N. Matubayasi, K. Nishikawa, H. Nagao, Hydration property of globular proteins: An analysis of solvation free energy by energy representation method, Chem. Phys. Lett. 497 (2010) 218-222.

[19] J.H. de Boer, The dynamical character of adsorption, 2nd ed., Clarendon Press, Oxford, 1968.

[20] P.J. Flory, Thermodynamics of high polymer solutions, The Journal of chemical physics 10 (1942) 51.

[21] P.J. Flory, Principles of polymer chemistry, Cornell University Press, 1953.

[22] A. McLaren, J.W. Rowen, Sorption of water vapor by proteins and polymers: a review, Journal of Polymer Science 7 (1951) 289-324.

[23] S.L. Shamblin, B.C. Hancock, G. Zografi, Water vapor sorption by peptides, proteins and their formulations, Eur. J. Pharm. Biopharm. 45 (1998) 239-247.

[24] J. Leeder, I. Watt, The stoichiometry of water sorption by proteins, J. Colloid Interface Sci. 48 (1974) 339-344.

[25] H.R. Costantino, R. Langer, A.M. Klibanov, Moisture-induced aggregation of lyophilized insulin, Pharm. Res. 11 (1994) 21-29.

[26] A. Gorelov, V. Morozov, Mechanical denaturation of globular protein in the solid state, Biophys. Chem. 28 (1987) 199-205.

[27] K. Gekko, Y. Hasegawa, Effect of temperature on the compressibility of native globular proteins, The Journal of Physical Chemistry 93 (1989) 426-429.

[28] V. Morozov, T.Y. Morozova, G. Kachalova, E. Myachin, Interpretation of water desorption isotherms of lysozyme, Int. J. Biol. Macromol. 10 (1988) 329-336.

[29] E.A.e. Permi͡akov, V.N. Uversky, Methods in Protein Structure and Stability Analysis: Vibrational Spectroscopy, Nova Publishers, 2007.

[30] R.R. Sotelo-Mundo, A.A. Lopez-Zavala, K.D. Garcia-Orozco, A.A. Arvizu-Flores, E.F. Velazquez-Contreras, E.M. Valenzuela-Soto, A. Rojo-Dominguez, M.R. Kanost, The lysozyme from insect (Manduca sexta) is a cold-adapted enzyme, Protein and peptide letters 14 (2007) 774-778.

[31] S. Tsuda, A. Miura, S.M. Gagné, L. Spyracopoulos, B.D. Sykes, Low-Temperature-Induced Structural Changes in the Apo Regulatory Domain of Skeletal Muscle Troponin C†, Biochemistry 38 (1999) 5693-5700.

[32] H. Kumeta, A. Miura, Y. Kobashigawa, K. Miura, C. Oka, N. Nemoto, K. Nitta, S. Tsuda, Low-temperature-induced structural changes in human lysozyme elucidated by three-dimensional NMR spectroscopy, Biochemistry 42 (2003) 1209-1216.

[33] T.M. Blumenschein, T.E. Gillis, G.F. Tibbits, B.D. Sykes, Effect of temperature on the structure of trout troponin C, Biochemistry 43 (2004) 4955-4963.

[34] R.R. Sotelo-Mundo, A.A. Lopez-Zavala, K.D. Garcia-Orozco, A.A. Arvizu-Flores, E.F. Velazquez-Contreras, E.M. Valenzuela-Soto, A. Rojo-Dominguez, M.R. Kanost, The lysozyme from insect (Manduca sexta) is a cold-adapted enzyme, Protein and peptide letters 14 (2007) 774.

CHAPTER 3

DYNAMICS AND THERMODYNAMICS OF PROTEIN HYDRATION

3.1 Introduction

In CHAPTER 2, I studied the protein-water interaction by measuring water isotherms in proteins at different temperatures. In this chapter, I further investigate the dynamics and thermodynamics of the protein-water interaction. Extensive work has been done to investigate the mechanism of protein hydration in terms of dynamics [1-4] and thermodynamics [5-8]; however, there remain two problems in these previous studies.

First, the majority of previous work considers the protein hydration shell as a whole [2-4, 9, 10]. However, the surface of the protein is highly heterogeneous [11-15]. It is shown in CHAPTER 2 that water interacts differently with hydrophilic groups and hydrophobic groups on the protein [12, 13, 16, 17]. It is also found that water at hydrophilic and hydrophobic protein groups affect ligand binding in distinct ways [17]. Therefore, a key question is how differently water at hydrophilic and hydrophobic groups affect protein dynamics and thermodynamics.

Second, as shown in CHAPTER 2, temperature is an important factor in the protein-water interaction [12, 13, 16, 17]. This is illustrated in Figure 3.1: water adsorption on hydrophilic groups is hardly affected by temperature, but water adsorption at hydrophobic groups exhibits a qualitative change around 10 C below which the coupling between water and these groups is substantially reduced [16, 17]. Such a temperature-induced crossover in the protein-water interfacial property could have significant consequences in various biological processes such as

enzymatic activation [13] and cold denaturation of proteins [18]. However, in many studies where the temperature of the hydrated proteins varied substantially, investigators only focused on the change of water structure with temperature, but ignored the dramatic change in the protein-water interfacial interaction [9, 10, 19-23]. It is sometimes assumed that the hydration effect on protein properties at low temperatures (≤150K) could persist up to room temperature [10, 24, 25]. So far, very few studies have explored the effect of hydration on the changes of protein dynamics and thermodynamics through the crossover region around 10 C.

It has been recognized in CHAPTER 2 that water adsorbs on hydrophilic and hydrophobic groups at different hydration stages [12, 13], hence it is possible to distinguish the effects of water at distinct groups via controlling the protein hydration level. A general procedure of controlling the hydration level in previous work is by weighing the protein with a certain amount of water around room temperature [9, 19-23]. However, although the total amount of hydration remains the same, the mechanism of the protein-water interaction changes as temperature varies. In contrast, here, the hydration level of the protein is controlled *in-situ* at each individual temperature.

In this chapter, nanosecond-microsecond (ns-μs) protein dynamics and changes in thermodynamic quantities of protein hydration are investigated as a function of hydration level and temperature by the *in-situ* nuclear magnetic resonance (NMR) technique [26]. Distinct effects of hydration at hydrophilic and hydrophobic groups are clearly identified. In particular, the hydration effects on the temperature-induced crossover at 10 C in protein dynamics and thermodynamics are clearly revealed. The work in this chapter provides new insight into the nature of protein-water interactions, with important implications for protein functions.

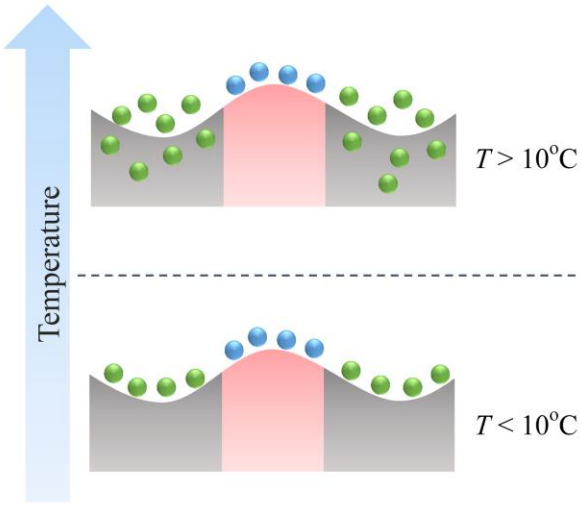

Figure 3.1: Schematic illustration of hydration on the protein surface. Binding of water to hydrophilic groups (convex surface shadowed in red) is insensitive to temperature while water adsorption on hydrophobic groups (concave surface shadowed in gray) depends strongly on temperature. Below 10 C, the coupling between water and hydrophobic groups is greatly suppressed.

3.2 Experiments

3.2.1 *In-situ* NMR Measurement

Two globular proteins, bovine serum albumin (BSA) and hen egg-white lysozyme (HEWL), are used in this chapter. BSA (lyophilized powder, ≥ 98%, pH ≈ 7, 1% in 0.15 M NaCl) and HEWL (catalog no. L-7561, 3x crystallized, dialyzed, and lyophilized) are purchased from Sigma-Aldrich and used without further purification.

The dry protein sample at a given temperature is subjected to controlled water vapor pressure *in situ* in the NMR system as introduced in chapter 2. A typical ^{1}H NMR spectrum of the hydrated protein is shown again in Figure 3.2 (A). A broad peak with full width at half maximum (FWHM) of ~30 kHz and a sharp peak with FWHM of ~1-2 kHz are observed. The

protein hydration level h (g water/g protein) is determined by the spectrum intensity [16, 17, 26] and this method has been reported in CHAPTER 2 SECTION 2.2. Water isotherms are measured at 3 C, 5 C, 16 C, and 27 C in CHAPTER 2. In this chapter, changes in the Gibbs free energy ΔG, enthalpy ΔH, and entropy $T\Delta S$ associated with protein hydration are determined from isotherms at 3 C, 5 C, 16 C, and 27 C. Protein dynamics on ns and μs timescales are investigated by measuring the ^{1}H spin-lattice relaxation time in the laboratory frame (T_1) and the rotating frame ($T_{1\rho}$) respectively [2, 27]. Protein dynamics and thermodynamics are studied as a function of hydration level h and temperature. The detailed procedures are discussed in the following sections [26].

Because the dynamic and thermodynamic properties of BSA and lysozyme are very similar in their hydration process, only partial results of BSA are shown in this chapter. The complete results of BSA and the results of lysozyme are shown in Appendix A.

3.2.2 Determination of ΔG, ΔH, and $T\Delta S$

The thermodynamic quantities, Gibbs free energy change ΔG, enthalpic change ΔH, and entropic change $T\Delta S$ associated with the protein hydration process can be determined from the water isotherms at different temperatures [28-31]. ΔG is calculated from the following integral of the isotherms:

$$\Delta G = -RT\int_0^x \frac{n}{x}dx \tag{3.1}$$

where n (mol water/mol protein) is the amount of sorption as a function of the relative pressure $x = P/P_0$, where P_0 is the saturated vapor pressure. ΔG is expressed in units of kJ/mol. Values of ΔG at different temperatures and vapor pressures can be obtained from the measured isotherm $n(x)$, i.e. the hydration level h (g water/g protein). The enthalpy change is obtained from:

$$\Delta H = -T^2 \frac{\partial}{\partial T}\left(\frac{\Delta G}{T}\right)_x \tag{3.2}$$

which is derived from the Gibbs–Helmholtz equation. If $\Delta G(T, x)$ at two different temperatures T_i and T_f is known, then

$$\frac{\Delta G(\mathrm{T}_f, \mathrm{x})}{T_f} - \frac{\Delta G(\mathrm{T}_i, \mathrm{x})}{T_i} = \Delta H(x)\left(\frac{1}{T_f} - \frac{1}{T_i}\right) \tag{3.3}$$

where $\Delta G(T_i,\ x)$ and $\Delta G(T_f,\ x)$ represent the Gibbs free energy change at a fixed relative pressure x and at temperature T_i and T_f, respectively. Here, $\Delta H(x)$ is the enthalpy change at fixed relative pressure x and at an average temperature T, which is given by

$$\frac{1}{T} = \frac{1}{2}\left(\frac{1}{T_i} + \frac{1}{T_f}\right) \tag{3.4}$$

Hence, water isotherms at 3 C and 16 C can be used to calculate ΔG at ~9 C; water isotherms at 16 C and 27 C can be used to calculate ΔG at ~21 C. Similarly, the entropy change is calculated from

$$\Delta S = -\left(\frac{\partial}{\partial T}\Delta \mathrm{G}\right)_x \tag{3.5}$$

Again, if $\Delta G(T, x)$ at two different temperatures T_i and T_f are known from isotherm measurements, we can calculate $\Delta S(T, x)$ as

$$\Delta S(T, x) = \frac{\Delta G(\mathrm{T}_i, \mathrm{x}) - \Delta G(\mathrm{T}_f, \mathrm{x})}{T_f - T_i} \tag{3.6}$$

This is the estimated entropy change at an average temperature T given by Equation (3.4). For comparison of ΔG with ΔH and $T\Delta S$ at the same temperature, ΔG at the average temperature T can be obtained by

$$\frac{\Delta G(T, x)}{T} = \frac{1}{2}\left(\frac{\Delta G(\mathrm{T}_i, \mathrm{x})}{T_i} + \frac{\Delta G(\mathrm{T}_f, \mathrm{x})}{T_f}\right) \tag{3.7}$$

NMR signals are measured five times at each water vapor pressure and the standard deviations of NMR peak areas are used to calculate the error bars in water isotherms in CHAPTER 2. Here, those errors are further propagated to calculate the error bars in graphs of ΔG, ΔH, and $T\Delta S$. Details of the instrument and the procedure have been reported previously [16, 17, 26].

3.2.3 NMR T_1 Relaxation Measurement

The conventional saturation recovery sequence introduced in CHAPTER 1 is used to measure T_1. Proton T_1 relaxation of a hydrated protein is governed by two mechanisms. One is the intrinsic motions of the protein and water molecules, and the other is the fast proton exchange between the protein and water [32-39]. In order to separate these two mechanisms, we employ the two-pool proton exchange model [34-36, 39, 40]. To be specific, as shown in Figure 3.2 (B), the reduced magnetization of the protein $m_p(t)$ and water $m_w(t)$ are plotted versus the decay time t. $m_p(t)$ and $m_w(t)$ are defined as:

$$m_p(t) = -\frac{M_{op} - M_p(t)}{M_{op}} \tag{3.8}$$

$$m_w(t) = -\frac{M_{ow} - M_w(t)}{M_{ow}} \tag{3.9}$$

where $M_p(t)$ and $M_w(t)$ are the magnetization of the protein and water at time t, which can be represented by the area of the broad peak and the sharp peak in Figure 3.2 (A); $M_{op} = M_p(t \to \infty)$ and $M_{ow} = M_w(t \to \infty)$ are the saturation magnetization of the protein and water. It is seen in Figure 3.2 (B) that, the effect of proton exchange on magnetization decay is very obvious at t<~20 ms, after which $m_p(t)$ and $m_w(t)$ relax at the same rate. Hence, if T_1 relaxation is measured after t>20 ms, the protein and water render the same T_1 value, making it difficult to distinguish different proton pools [39]. Here, proton exchange rates k_p and k_w are

introduced, which represent the rates at which magnetization transfers from the protein to water and from water to the protein, respectively. The Bloch equations are modified as [34, 35, 39, 40]:

$$\frac{dm_w(t)}{dt} = -R_{1w}m_w(t) - k_w m_w(t) + k_w m_p(t) \tag{3.10}$$

$$\frac{dm_p(t)}{dt} = -R_{1p}m_p(t) - k_p m_p(t) + k_p m_w(t) \tag{3.11}$$

where $R_{1w} = 1/T_{1w}$ and $R_{1p} = 1/T_{1p}$; T_{1w} and T_{1p} are spin lattice relaxation times induced by intrinsic motions of water and the protein without any exchange. The solutions to the above equations are [34, 35, 39, 40]:

$$m_i(t) = c_i^+ exp(-R_1^+ t) + c_i^- exp(-R_1^- t) \tag{3.15}$$

$$R_1^{\pm} = \frac{1}{2}(R_{1p} + R_{1w} + k_p + k_w) \pm \frac{1}{2}\sqrt{(R_{1p} - R_{1w} + k_p - k_w)^2 + 4k_p k_w} \tag{3.16}$$

$$k_w = \frac{p_p}{p_w} k_p \tag{3.17}$$

$$R_{1i} = c_i^+ R_1^+ + c_i^- R_1^- \tag{3.18}$$

where i represents p (protein) or w (water). $\frac{p_p}{p_w}$ is the ratio of protein protons to water protons.

Hence, by fitting the magnetization decays of the broad peak and sharp peak with Equation (3.15), the parameters $R_1^{\pm}$, $c_p^{\pm}$, and $c_w^{\pm}$ are obtained. Then R_{1p}, R_{1w}, k_p, and k_w are obtained by solving Equation (3.16)-(3.18). Take the T_1 measurement of BSA at 3 C and hydration level h = 0.354 (g water/g BSA) as an example, Figure 3.2 (B) shows how to distinguish intrinsic motions of the protein and water as well as the protein-water exchange rates base on the above model. When T_1 that is induced by intrinsic motions is obtained, the formula [27]:

$$\frac{1}{T_1} = \frac{3\hbar^2\gamma^4}{10r^6}\left(\frac{\tau}{1+\omega_0^2\tau^2} + \frac{4\tau}{1+4\omega_0^2\tau^2}\right) \tag{3.19}$$

is used to derive the correlation time τ of molecular motions, where r is the distance between two protons; $\hbar$ and γ are reduced Planck's constant and gyromagnetic ratio of the proton; $\omega_0 = \gamma B_0$, and B_0 is the strength of the static magnetic field. Standard deviations of fitting magnetization decay curves are used to calculate the error bars in graphs of T_1. These errors are propagated to calculate the error bars in graphs of correlation times. The detailed procedure has been reported [26].

3.2.4 NMR $T_{1\rho}$ Relaxation Measurement

The conventional spin-locking pulse sequence introduced in CHAPTER 1 is used to measure $T_{1\rho}$. The strength (B_1) of the spin locking field is controlled by the attenuation of the pulse generator. Two attenuations are chosen, corresponding to B_1~50 kHz and B_1~90 kHz, which are calibrated by measuring the 90° pulse width at these attenuations. Measuring $T_{1\rho}$ is very useful to study slow molecular motions on timescales of micro-millisecond [39, 41-44]. The area of the broad peak and the sharp peak of the spectrum in Figure 3.2 (A) are plotted as a function of spin locking time. Because the protein-water exchange rate is slower than $T_{1\rho}$ experimental times (see SECTION 3.3.2), the broad peak in $T_{1\rho}$ measurement mainly stems from protein protons [39, 45]. The decay of the broad peak, i.e. the protein component, is fitted very well with the stretched exponential function:

$$M(t) = M_0 \exp(-(\frac{t}{T_{1\rho}})^{\beta}) \tag{3.20}$$

where $M(t)$ is the magnetization at decay time t and M_0 is saturation magnetization of the protein.

This is illustrated in Figure 3.2 (C). Furthermore, if $m(t)=\frac{M(t)}{M_0}$, it is seen from Equation (3.20) that the plot of $ln(-ln(m))$ as a function of $ln(t)$ should be linear and the slope equals the stretching parameter β. This is proven in the inset of Figure 3.2 (C). These results indicate a broad distribution of the correlation time of protein protons [46-48]. The mean value of $T_{1\rho}$ of the protein is reported, which is calculated as [46-48]:

$$< T_{1\rho} >= \frac{T_{1\rho}}{\beta}\Gamma(\frac{1}{\beta}) \tag{3.21}$$

The formula [27]:

$$\frac{1}{T_{1\rho}} = \frac{3\hbar^2\gamma^4}{20r^6}\left(\frac{3\tau}{1+4\omega_1^2\tau^2}+\frac{5\tau}{1+\omega_0^2\tau^2}+\frac{2\tau}{1+4\omega_0^2\tau^2}\right) \tag{3.22}$$

is then used to derive the correlation time τ of molecular motions, where $\omega_1 = \gamma B_1$ and B_1 is the strength of spin locking field. In addition, assuming that the stretched exponential relaxation is a superposition of single exponential decays with different correlation time u, then

$$exp(-(\frac{t}{\tau})^{\beta}) = \int_0^{\infty} exp(-\frac{t}{u})\rho(u)du \tag{3.23}$$

where $\rho(u)$ represents the distribution function of the correlation time [46-48]. An inverse Laplace transform can be applied to solve the distribution function $\rho(u)$ [46-48]. Standard deviations of fitting magnetization decay curves are used to calculate the error bars in graphs of $T_{1\rho}$. These errors are propagated to calculate the error bars in graphs of correlation times. The detailed procedure has been reported [26].

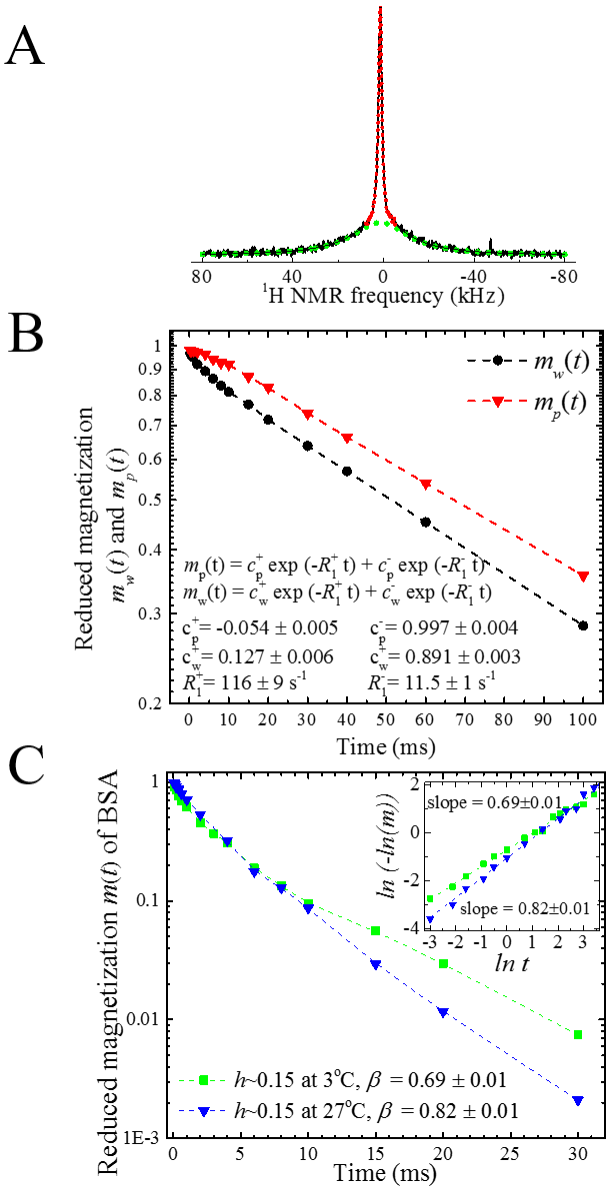

Figure 3.2: (A) ^{1}H NMR spectrum of BSA at 16 C at hydration level h~0.15 (g water/g BSA). It consists of a broad peak (FWHM ~30 kHz) and a sharp peak (FWHM ~1-2 kHz). (B) The decay of $m_P(t)$ and $m_W(t)$ at 3 C at h = 0.354 (g water/g BSA) in T_1 measurement. The decay curves are fitted by Equation (3.15). The fitting parameters $R_1^{\pm}$, $c_p^{\pm}$, and $c_w^{\pm}$ are used in Equation (3.16)-(3.18) to solve the intrinsic T_1 relaxations of the protein and water as well as the proton exchange rate between the

protein and water. (C) The decay of the reduced magnetization $m(t)$ of BSA at 3 C and 27 C at h~0.15 in $T_{1\rho}$ measurement. As shown in the inset, $ln(-ln(m))$ is linear with $ln(t)$, in agree with Eqn (16). The slope of the line equals the stretching parameter β.

3.3 Results and Discussion

3.3.1 Hydration at Distinct Groups: Temperature Effect

As shown in Figure 3.1, water interacts differently with hydrophilic and hydrophobic groups; such a difference is clearly revealed by the temperature effect on the water isotherms of the protein in CHAPTER 2 [16, 17, 26]. As explained previously, when the hydration level h<~0.15-0.2 (g water/g protein), water binds to hydrophilic protein groups by forces that are hardly affected by temperature [12, 13]. When h>~0.15-0.2, water starts mixing with hydrophobic protein groups and the mixing process strongly depends on temperature [16]. At temperatures below 10 C, the protein's elastic constant significantly increases [16]; hence, the mixing is energetically unfavorable, leading to the substantial decrease in water adsorption at hydrophobic groups.

So far, very little attention has been paid to such strong temperature effects on protein hydration at hydrophobic groups. In previous work, the hydration level of a protein is controlled at room temperature, but thereafter the hydrated protein sample is tested at low temperatures (especially < 10 C) [9, 19-23]. Hence, although the hydration level remains the same, those water molecules that intimately mix with hydrophobic groups become inactive and simply condense on the protein surface as the temperature decreases. This makes the interpretation of hydration effects on protein properties ambiguous. Here, the protein dynamics and thermodynamics are

studied *in-situ* as a function of hydration level and temperature, which completely ameliorates this problem.

3.3.2 Nano-Microsecond Protein Dynamics: Crossover at 10 C and Hydration Effect

Many works have probed protein dynamics on the picosecond-nanosecond timescale [9-11, 19, 20]. However, protein dynamics cover a broad range of timescales and the nature of the protein-water dynamic coupling on different timescales may be different [1, 2]. In fact, many biological processes where hydration plays a crucial role take place on the timescale of nanosecond (ns) to microsecond (μs) [2, 42, 43, 49]. Therefore, studies are needed to gain insight into the effects of hydration at distinct groups on protein dynamics at ns-μs timescale.

3.3.2.1 T_1 Relaxation and Nanosecond (ns) Protein Dynamics

Proton T_1 relaxation of a hydrated protein is governed by two mechanisms. One is the intrinsic motions of the protein and water molecules, and the other is the fast proton exchange between the protein and water [32-39]. Here, I separate these two mechanisms (see SECTION 3.2.3) and present the contributions to T_1 of BSA and its hydration water from their intrinsic motions in Figure 3.3 (A) and its inset. It is seen that the intrinsic T_1 of BSA decreases steadily with hydration; above h~0.2, the decrease is stronger at 16 C and 27 C. The intrinsic T_1 of water shows a minimum around h~0.15-0.2, above which it increases noticeably and such increase is more obvious at higher temperatures.

Based on the intrinsic T_1 of BSA, the correlation time of BSA is derived from Equation (3.19). As shown in Figure 3.3 (B), below h~0.2 the correlation time of BSA gradually decreases with hydration, indicating that water at hydrophilic groups effectively enhances ns protein

dynamics. Above h~0.2, the decrease in the correlation time of BSA with hydration remains striking, and such decrease is more remarkable at higher temperatures. This suggests that as the interfacial interaction between water and hydrophobic groups is enhanced at temperatures above 10 C, the effect of water at hydrophobic groups on enhancing ns protein dynamics also becomes stronger.

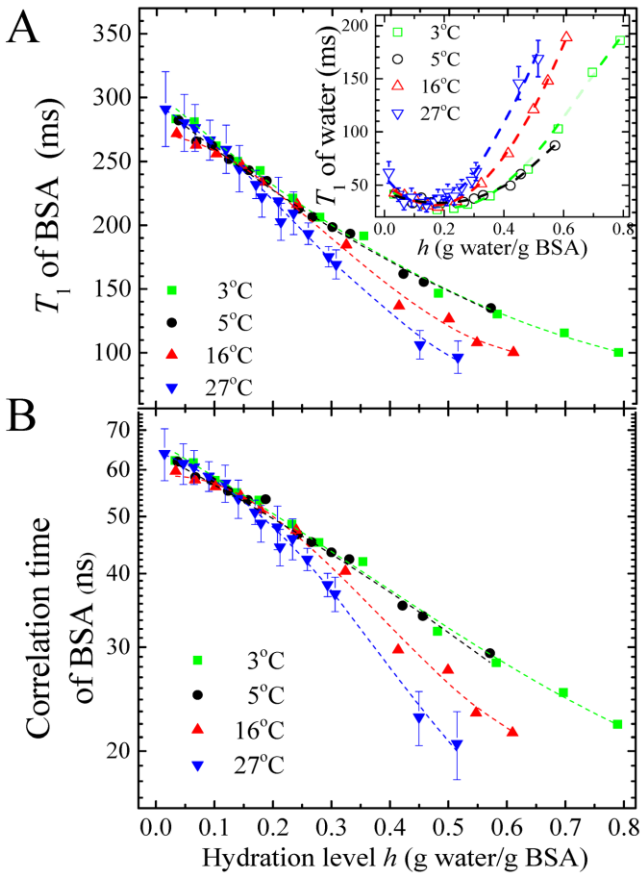

Figure 3.3: (A) Intrinsic T_1 relaxation time of BSA and its hydration water (inset of A) as a function of hydration level at 3 C, 5 C, 16 C, and 27 C. (B) The correlation time of BSA. Relative errors of T_1 relaxations and correlation times at different temperatures are very close. Hence, only error bars at 27 C are shown.

The proton exchange rate from water to the protein (k_w) and from the protein to water (k_p) are calculated (see SECTION 3.2.3) and shown in Figure 3.4 (C) and (D). Two principal observations can be made. First, k_w and k_p exhibit very obvious maxima at h~0.15 above 10 C, which is not observed below 10 C. This is related to the dynamical change in the protein molecule induced by hydration of hydrophilic groups at temperatures higher than 10 C. The mechanism is discussed in the following section. Second, k_w and k_p are hardly affected by hydration and temperature above h~0.3-0.4, which corresponds to the completion of the first hydration shell [12, 13]. This suggests that the protein-water exchange process is dominantly affected by the first hydration layer.

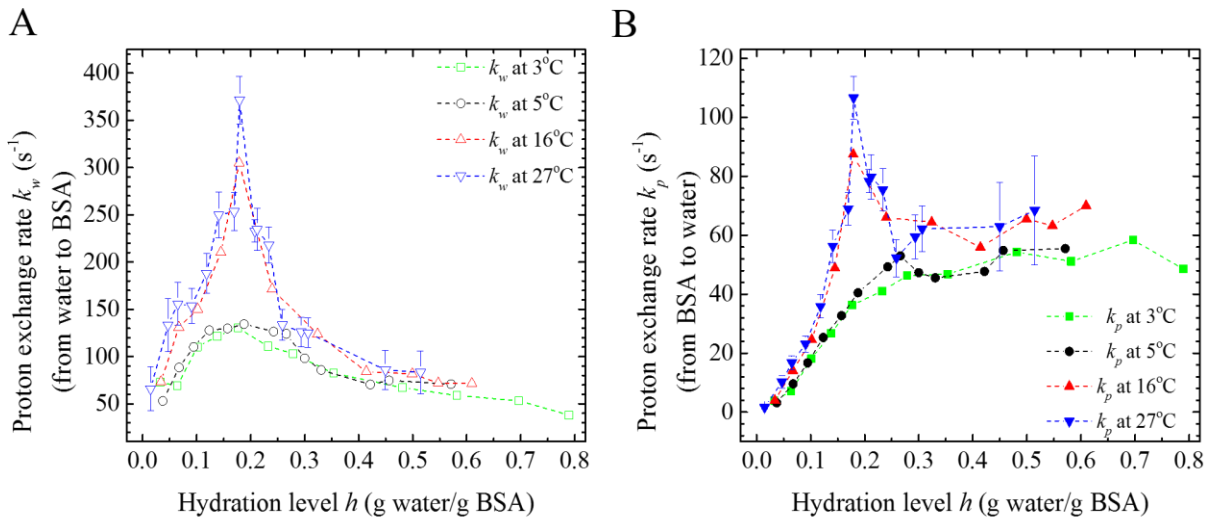

Figure 3.4: Proton exchange rates (A) from hydration water to BSA k_w, and (B) from BSA to hydration water k_p as a function of hydration level at 3 C, 5 C, 16 C, and 27 C. k_w and k_p are calculated from Equation (3.15)-(3.18). Relative errors of exchange rates at different temperatures are very close. Hence, only error bars at 27 C are shown.

3.3.2.2 $T_{1\rho}$ Relaxation and Microsecond (μs) Protein Dynamics

Since the dynamics of the protein cover a wide range of timescales [1, 2, 50], the dynamic coupling between water and the protein may be different on different timescales. Hence, I also measured proton $T_{1\rho}$ relaxation that is sensitive to μs protein dynamics. In $T_{1\rho}$ measurements, a broad peak and a sharp peak are also observed (see Figure 3.2) and they decay at quite different rates. Here, the broad peak is assigned only to the protein component for two reasons. First, according to the results of Figure 3.4, the protein-water exchange time (reciprocal of exchange rate) is >~10ms, which is longer than the $T_{1\rho}$ experimental time. This indicates that the protein-water exchange is insufficient and can be neglected in our $T_{1\rho}$ measurements [39, 45]. Second, although it has been reported that a few water molecules could be so immobile that they may contribute to the broad peak, the number of such water molecules is very limited and their residence time is much shorter than the $T_{1\rho}$ experimental time [36-40, 45]. Hence, $T_{1\rho}$ of the protein can be obtained by directly analyzing the decay of the broad peak.

$T_{1\rho}$ of BSA at the spin locking field B_1~50 kHz is shown in Figure 3.5 (A). Below h~0.15, $T_{1\rho}$ of BSA shows little temperature dependence but decreases dramatically with increasing hydration level, reaching its minimum around h~0.15. Above h~0.15, $T_{1\rho}$ of BSA increases with the level of hydration and such increase is much more obvious at higher temperatures. The correlation time of BSA is derived from Equation (3.22) and presented in Figure 3.5 (B). It is seen that below h~0.2, the correlation time of BSA decreases substantially with hydration level, indicating that water at hydrophilic groups greatly enhances μs protein dynamics. In contrast, above h~0.2, the correlation time of BSA decreases slowly with hydration at 16 C and 27 C, and hardly changes at 3 C and 5 C. This shows that above 10 C, the mixing of water with hydrophobic groups weakly enhances μs protein dynamics; when the coupling

between water and hydrophobic groups is greatly suppressed below 10 C, water adsorbed at these groups has little effect on μs protein dynamics.

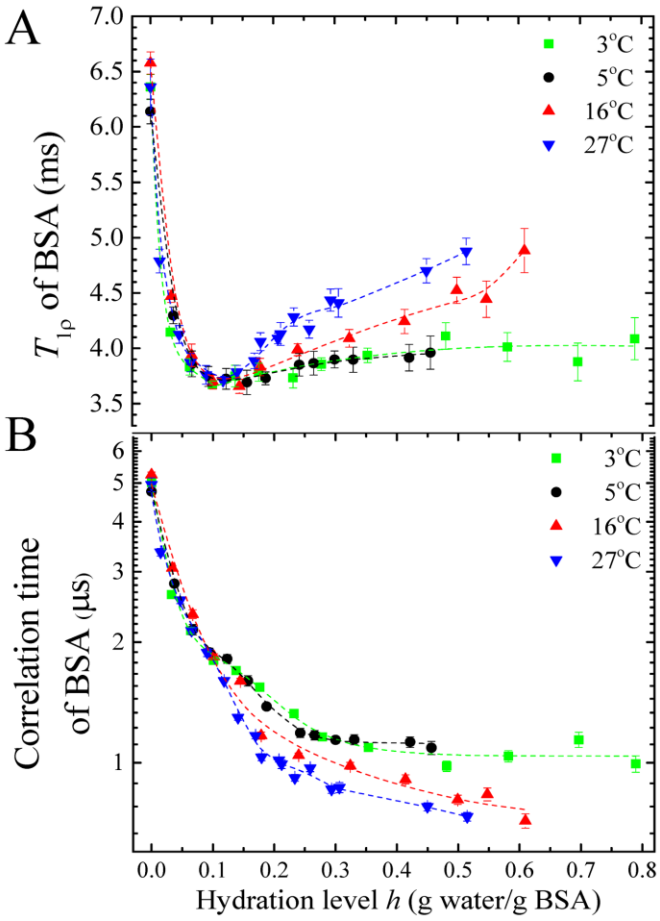

Figure 3.5: (A) $T_{1\rho}$ relaxation of BSA as a function of hydration level at 3 C, 5 C, 16 C, and 27 C. (B) The correlation time of BSA derived from Equation (3.22). Here, $T_{1\rho}$ is measured at the spin locking field B_1 ~50 kHz.

A stretched exponential function is used to analyze the $T_{1\rho}$ relaxation of the protein (see SECTION 3.2.4). The stretching parameter β depends on the temperature and hydration level. As shown in Figure 3.6 (A), β exhibits a maximum around h~0.15 at 16 C and 27 C, while it hardly changes with hydration at 3 C and 5 C. This is similar to the results of Figure 3.4 and is discussed

later. Furthermore, because changes in β are directly related to changes in the distribution of the correlation time [46-48], I calculated the distribution function of the correlation time of BSA at h~0, 0.1, 0.15, 0.2, 0.3, and 0.5 at 3 C and 27 C by Equation (3.23) and present the results in Figure 3.6 (B) and (C). It is seen that: (i) the distribution of the correlation time is very broad with a long tail towards the short (<0.1 μs) timescale regime; (ii) with increasing hydration, the center of the distribution function shifts from ~10 μs to ~1 μs and such shift is much more noticeable below h~0.15; (iii) at 3 C, the width of the distribution is insensitive to the level of hydration; (iv) at 27 C, the width of the distribution gets narrower with increasing hydration level up to h~0.15 and becomes broader again above h~0.15.

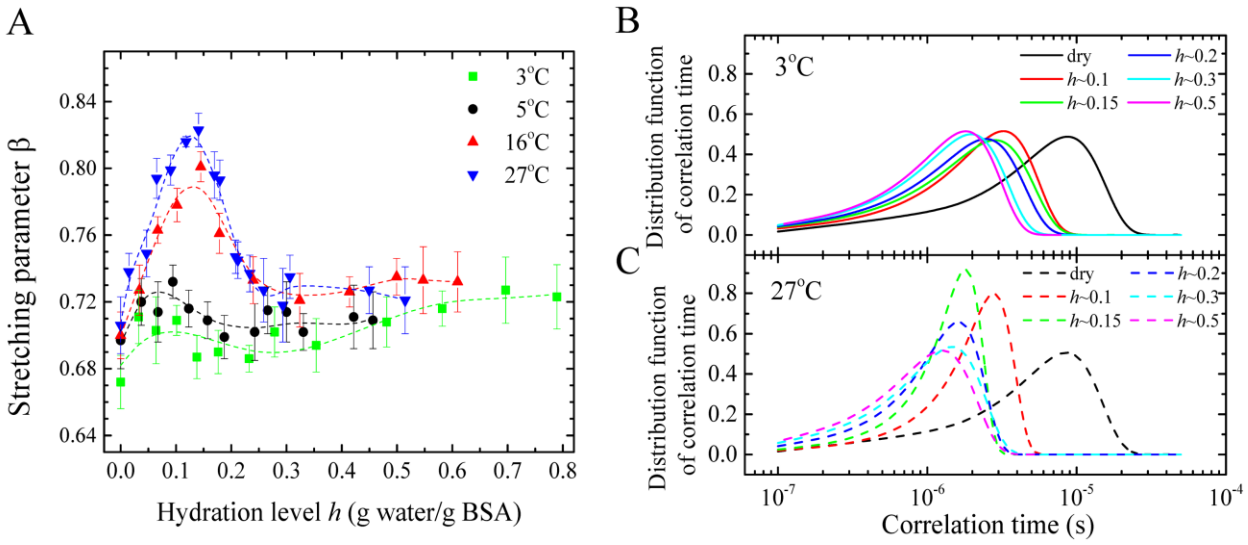

Figure 3.6: (A) stretching parameter β as a function of hydration level at 3 C, 5 C, 16 C, and 27 C. The distribution function of the correlation time at (B) 3 C and (C) 27 C at hydration level h~0 (dry), 0.1, 0.15, 0.2, 0.3, and 0.5, derived from Equation (3.23).

The results of correlation time distribution imply a highly heterogeneous environment of protons in the protein [1, 2]. The spectral density of proton motions at different groups, such as

methyl groups and aromatic groups, have different characteristic frequencies [1, 2]. Moreover, even the same type of group, such as the methyl group, can show a broad distribution of correlation times depending on its chemical environment in the protein [2]. Therefore, our results show that such dynamical heterogeneity is sensitive to hydration at temperatures higher than 10 C. Above 10 C, hydration of hydrophilic protein groups (h<~0.15) makes the proton motion more uniform, narrowing its correlation time distribution; while mixing of water with hydrophobic protein groups (h>~0.15) makes the proton motion more heterogeneous. Below 10 C, such dynamical heterogeneity appears to be "frozen" and the correlation time distribution of the protein hardly changes with hydration.

These results are strongly correlated to the results of Figure 3.4, indicating that the change in the protein-water exchange rate at h~0.15 is very likely to be induced by the dynamic changes in the protein itself. In other words, hydration of hydrophilic groups alters the dynamical heterogeneity in the protein, which in turn modifies the proton exchange between water and the protein.

3.3.2.3 Distinct Effects of Hydration at Hydrophilic and Hydrophobic Groups

The results show that water at hydrophilic and hydrophobic groups have different influences on protein dynamics and the influence depends strongly on the timescale being studied, indicating different mechanisms of protein-water coupling on ns and μs timescales. It has been suggested that protein backbone motion is on the μs timescale, while more localized protein motion such as side chain rotation is on the ns timescale [2, 19]. Water at hydrophilic groups greatly enhances both ns and μs protein dynamics (see Figure 3.3 and Figure 3.5 when h<~0.2), indicating that it is strongly coupled to motions of both the backbone and the side

chains. In contrast, water at hydrophobic groups has a much more pronounced effect on ns protein dynamics than on μs protein dynamics (see Figure 3.3 and Figure 3.5 when h>~0.2), indicating that it has greater influence on localized side chain motions than on backbone motions.

3.3.2.4 Crossover at 10 C in Nano-Microsecond Protein Dynamics

As the temperature increases above 10 C, the interfacial interaction between water and hydrophobic groups is enhanced. Such a temperature-induced enhancement in the protein-water interfacial interaction does have nontrivial influence on both ns and μs protein dynamics (see Figure 3.3 and Figure 3.5 at temperatures higher than 10 C). In contrast, below 10 C the interfacial interaction between water and hydrophobic groups is substantially reduced. This explains why water at hydrophobic groups has a weaker effect on ns and μs protein dynamics below 10 C (see Figure 3.3 and Figure 3.5 at temperatures lower than 10 C).

In addition, at temperatures around 10 C there is an obvious effect on the proton exchange process (see Figure 3.4) and the dynamic heterogeneity (see Figure 3.5) in the protein. Below 10 C, the protein-water proton exchange and the dynamic heterogeneity in the protein are hardly affected by hydration. In contrast, above 10 C, they both show apparent quantitative changes, especially at h~0.15. Such unique temperature dependences of the protein-water exchange process and protein dynamical heterogeneity around 10 C have not been reported previously.

3.3.2.5 Water-Protein Interactions and Protein Dynamics

In dry proteins, there exist strong non-native hydrogen bonding and electrostatic interactions between hydrophilic protein groups [12, 13, 51], hence the protein structure is very compact and the motion of the protein is largely restricted. In the rehydration process, the hydrogen bonds between water and hydrophilic groups replace those unfavorable protein-protein interactions [12, 13, 51]. Hence, hydration at hydrophilic groups eases the spatial restriction of the protein, greatly liberating the motion of the protein backbone as well as the side chains [51, 52].

Moreover, it has been recognized that practically all the non-native contacts in the protein are removed at the hydration level h~0.2; further hydration (h>~0.2) has a weak effect on the overall protein structure [12, 13, 51, 52]. As I discussed, water molecules actively mix with the hydrophobic groups at h>~0.2. Essentially, such a mixing process corresponds to the fluctuation of water molecules into and out of the cavities formed by the side chains on the protein surface [53-55]. Therefore, those mixing water molecules at hydrophobic groups frequently change the arrangement of protein side chains, enhancing their mobility [51, 52]. In contrast, the protein backbone structure is mainly not affected by hydration above h~0.2 [12, 13, 51, 52]. Therefore, the mixing process hardly disturbs the arrangement of the protein backbone. That is why water at hydrophobic groups only weakly affects the protein backbone motion [52].

In addition, the influence of water at hydrophobic groups on protein dynamics is stronger at temperatures above 10 C while it is much weaker below 10 C. As I discussed in CHAPTER 2 SECTION 2.3.5, this is caused by the change in the interaction between water and hydrophobic groups around 10 C. Specifically, when the temperature is below 10 C, the relative orientation between helices in the protein significantly changes, resulting in a more compact packing of the

protein [56-58]. Meanwhile, the cavities in the protein are shrunk due to the spatial distortion and water molecules are squeezed out of the cavities [56-58]. Therefore, below 10 C, the mixing between water and the protein is substantially suppressed and the influence of those mixing water molecules on the protein motion is very weak.

3.3.3 Thermodynamics of Protein Hydration at Crossover Temperature

So far, many works on protein hydration thermodynamics are limited to computational simulations [7, 8, 59, 60]. Some experimental studies are focused on calorimetric measurements of proteins at different hydration levels [5, 6, 21, 22]. However, in addition to the temperature issue discussed before, they have other limitations. First, the equilibrium time of the protein-water interaction depends on the hydration level and could be on the order of hours [16, 17]. This requires the time of the simulation and the calorimetric measurement to be long enough at each hydration level, which is not the case in many works. Second, researchers have focused on proteins with high hydration levels [21-23], but the effect of low hydration on protein thermodynamics remains poorly understood. Here, thermodynamic properties of protein hydration are investigated over a wide range of hydration and at the equilibrium of the protein-water interaction [17].

The change in the Gibbs free energy (ΔG) of the protein-water interaction can be decomposed into enthalpic (ΔH) and entropic ($T\Delta S$) contributions. The enthalpic change (ΔH) may arise from the formation of protein-water interactions and the breakdown of protein-protein interactions; while the entropic ($T\Delta S$) change is related to the reordering of water molecules and protein groups and their degrees of freedom [13, 51, 61, 62]. A detailed study on ΔG, ΔH, and

TΔS of protein hydration provides valuable information of the contribution of different factors to the protein-water interaction, which is still a subject of debate [61, 62].

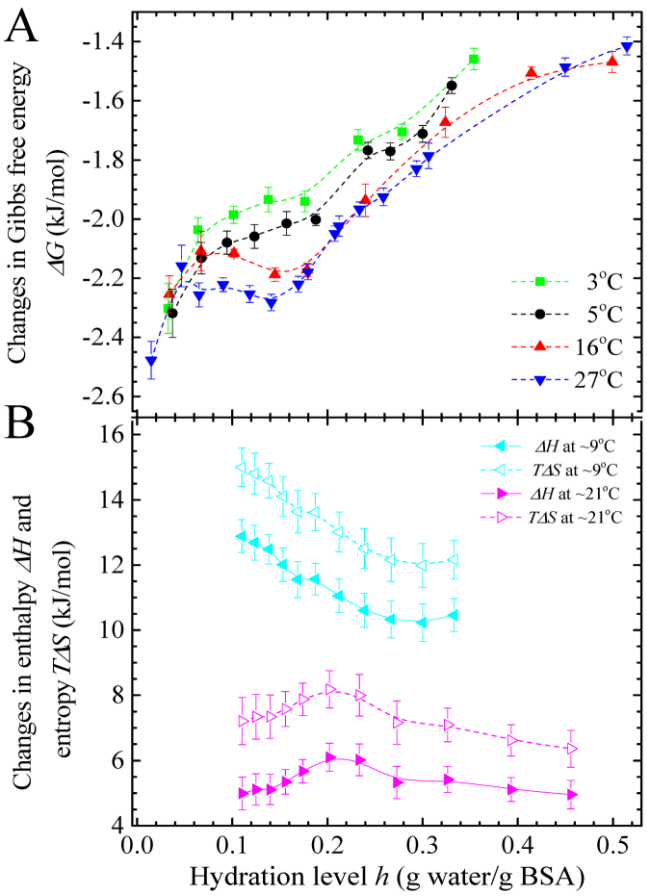

Figure 3.7: (A) Changes in the Gibbs free energy *ΔG* associated with the hydration process of BSA as a function of hydration level at 3 C, 5 C, 16 C, and 27 C. (B) Changes in enthalpy *ΔH* and entropy *TΔS* associated with the hydration process of BSA at ~9 C and ~21 C.

Here, *ΔG*, *ΔH*, and *TΔS* associated with the hydration process of BSA are determined from water isotherms at different temperatures and presented in Figure 3.7. Figure 3.7 (A) shows that at 3 C and 5 C, *ΔG* gradually increases with hydration; however, at 16 C and 27 C, a

minimum in ΔG is observed around h~0.15. The value of ΔG is about -2kJ/mol, in agreement with the average free energy change of -0.5 kcal/mol (i.e. -2.1 kJ/mol) in the protein hydration process [17]. In Figure 3.7 (B), ΔH and $T\Delta S$ are both positive, indicating that the hydration process is driven by the favorable entropic change that compensates for the unfavorable enthalpic change. It has been shown that the protein itself is a large thermodynamic reservoir [17, 61]. Structural and dynamic changes of the protein in the hydration process could significantly affect the changes in free energy, enthalpy and entropy. The dry protein is tight due to strong non-native protein-protein interactions; rehydration is able to "lubricate" the protein [13, 51]. This process accompanies the breakdown of protein-protein interactions [13, 51], while the protein becomes more flexible, proven by the decrease in the correlation times of protein motions (Fig 3.3 (B) and Fig 3.5 (B)). This induces positive ΔH and $T\Delta S$. Such enthalpy-entropy compensation also contributes to a small free energy change in Figure 3.7 (A). Furthermore, Figure 3.7 (B) shows that ΔH and $T\Delta S$ of protein hydration are quite different at temperatures below and above 10 C. At a temperature lower than 10 C, ΔH and $T\Delta S$ decrease with hydration; while at temperatures higher than 10 C, ΔH and $T\Delta S$ increase with hydration till h~0.2 then decrease thereafter.

It is also noticed that the changes in ΔG, ΔH, and $T\Delta S$ around h~0.15-0.2 at ambient temperature are consistent with the changes in protein-water exchange rate and protein dynamical heterogeneity around h~0.15-0.2 at ambient temperature, indicating a strong correlation between thermodynamic and dynamic properties of the protein around the crossover temperature of 10 C.

3.4 Conclusions

By employing an *in-situ* NMR technique, I find the distinct effects of water at hydrophilic and hydrophobic groups [26]. In particular, it is revealed that the change in the protein-water interfacial interaction results in a crossover around 10 C in protein dynamics and thermodynamics. Such an effect could be of significance to biological processes such as the onset of enzymatic activity [13] and protein cold denaturation [18].

To be specific, in terms of dynamics, it is found that on the ns timescale, water at all protein groups effectively enhances protein dynamics; water at hydrophobic groups is important in enhancing ns protein dynamics, especially at temperatures above 10 C. On the μs timescale, water at hydrophilic groups significantly enhances protein dynamics and water at hydrophobic groups weakly enhances protein dynamics above 10 C while having little effect below 10 C. Furthermore, the protein-water exchange rate and the protein dynamic heterogeneity also exhibit a crossover around 10 C at h~0.15. In terms of thermodynamics, it is found that Gibbs free energy, enthalpy, and entropy of protein hydration change with hydration level in different ways at temperatures above and below 10 C. Specifically, these thermodynamic quantities all manifest obvious quantitative changes above 10 C at h~0.15. These results indicate a strong correlation between ns-μs protein dynamics and protein hydration thermodynamics around the crossover temperature of 10 C. The work in this chapter reveals the detailed influence of hydration and temperature on protein dynamics and thermodynamics, providing new insights into the mechanism underlying protein functions.

3.5 REFERENCES

[1] V. Helms, Protein dynamics tightly connected to the dynamics of surrounding and internal water molecules, ChemPhysChem 8 (2007) 23-33.

[2] S. Khodadadi, A.P. Sokolov, Protein dynamics: from rattling in a cage to structural relaxation, Soft Matter 11 (2015) 4984-4998.

[3] H. Frauenfelder, G. Chen, J. Berendzen, P.W. Fenimore, H. Jansson, B.H. McMahon, I.R. Stroe, J. Swenson, R.D. Young, A unified model of protein dynamics, Proceedings of the National Academy of Sciences 106 (2009) 5129-5134.

[4] B.H. McMahon, H. Frauenfelder, P.W. Fenimore, The role of continuous and discrete water structures in protein function, The European Physical Journal Special Topics 223 (2014) 915-926.

[5] V.A. Sirotkin, A.V. Khadiullina, Gibbs energies, enthalpies, and entropies of water and lysozyme at the inner edge of excess hydration, The Journal of chemical physics 139 (2013) 075102.

[6] V.A. Sirotkin, A.V. Khadiullina, Hydration of proteins: excess partial enthalpies of water and proteins, The Journal of Physical Chemistry B 115 (2011) 15110-15118.

[7] H. Saito, N. Matubayasi, K. Nishikawa, H. Nagao, Hydration property of globular proteins: An analysis of solvation free energy by energy representation method, Chem. Phys. Lett. 497 (2010) 218-222.

[8] Y. Maruyama, Y. Harano, Does water drive protein folding?, Chem. Phys. Lett. 581 (2013) 85-90.

[9] S. Khodadadi, J.E. Curtis, A.P. Sokolov, Nanosecond relaxation dynamics of hydrated proteins: Water versus protein contributions, The Journal of Physical Chemistry B 115 (2011) 6222-6226.

[10] V. Conti Nibali, G. D'Angelo, A. Paciaroni, D.J. Tobias, M. Tarek, On the coupling between the collective dynamics of proteins and their hydration water, The Journal of Physical Chemistry Letters 5 (2014) 1181-1186.

[11] D. Zhong, S.K. Pal, A.H. Zewail, Biological water: A critique, Chem. Phys. Lett. 503 (2011) 1-11.

[12] I.D. Kuntz, W. Kauzmann, Hydration of Proteins and Polypeptides, Adv. Protein Chem. 28 (1974) 239-345.

[13] J.A. Rupley, G. Careri, Protein hydration and function, Adv. Protein Chem. 41 (1991) 37-172.

[14] P. Ball, Water as an active constituent in cell biology, Chem. Rev. 108 (2008) 74-108.

[15] Y. Levy, J.N. Onuchic, Water mediation in protein folding and molecular recognition, Annu. Rev. Biophys. Biomol. Struct. 35 (2006) 389-415.

[16] H.-J. Wang, A. Kleinhammes, P. Tang, Y. Xu, Y. Wu, Temperature dependence of lysozyme hydration and the role of elastic energy, Phys. Rev. E 83 (2011) 031924.

[17] Y. Chong, A. Kleinhammes, P. Tang, Y. Xu, Y. Wu, Dominant Alcohol–Protein Interaction via Hydration-Enabled Enthalpy-Driven Binding Mechanism, The Journal of Physical Chemistry B 119 (2015) 5367-5375.

[18] C.-J. Tsai, J.V. Maizel, R. Nussinov, The hydrophobic effect: a new insight from cold denaturation and a two-state water structure, Crit. Rev. Biochem. Mol. Biol. 37 (2002) 55-69.

[19] J.D. Nickels, V. García Sakai, A.P. Sokolov, Dynamics in protein powders on the nanosecond–picosecond time scale are dominated by localized motions, The Journal of Physical Chemistry B 117 (2013) 11548-11555.

[20] F. Mallamace, S.-H. Chen, M. Broccio, C. Corsaro, V. Crupi, D. Majolino, V. Venuti, P. Baglioni, E. Fratini, C. Vannucci, Role of the solvent in the dynamical transitions of proteins: the case of the lysozyme-water system, The Journal of chemical physics 127 (2007) 045104.

[21] F. Mallamace, C. Corsaro, D. Mallamace, S. Vasi, C. Vasi, H.E. Stanley, Thermodynamic properties of bulk and confined water, The Journal of chemical physics 141 (2014) 18C504.

[22] G. Schirò, M. Fomina, A. Cupane, Communication: Protein dynamical transition vs. liquid-liquid phase transition in protein hydration water, The Journal of chemical physics 139 (2013) 121102.

[23] F. Mallamace, C. Corsaro, D. Mallamace, S. Vasi, C. Vasi, H.E. Stanley, S.-H. Chen, Some thermodynamical aspects of protein hydration water, The Journal of chemical physics 142 (2015) 215103.

[24] M. Tarek, D.J. Tobias, The dynamics of protein hydration water: a quantitative comparison of molecular dynamics simulations and neutron-scattering experiments, Biophys. J. 79 (2000) 3244-3257.

[25] B.M. Leu, A. Alatas, H. Sinn, E.E. Alp, A.H. Said, H. Yavaş, J. Zhao, J.T. Sage, W. Sturhahn, Protein elasticity probed with two synchrotron-based techniques, The Journal of chemical physics 132 (2010) 085103.

[26] Y. Chong, A. Kleinhammes, Y. Wu, Protein dynamics and thermodynamics crossover at 10° C: Different roles of hydration at hydrophilic and hydrophobic groups, Chem. Phys. Lett. 664 (2016) 108-113.

[27] A. Abragam, The principles of nuclear magnetism, Oxford university press, 1961.

[28] A. Myers, Thermodynamics of adsorption in porous materials, AlChE J. 48 (2002) 145-160.

[29] T.L. Hill, Statistical mechanics of adsorption. V. Thermodynamics and heat of adsorption, The Journal of chemical physics 17 (1949) 520.

[30] T.L. Hill, Statistical mechanics of adsorption. IX. Adsorption thermodynamics and solution thermodynamics, The Journal of chemical physics 18 (1950) 246.

[31] R. Keren, I. Shainberg, Water vapor isotherms and heat of immersion of Na-and Ca-montmorillonite systems. III. Thermodynamics, Clays Clay Miner. 28 (1980) 204-210.

[32] R.G. Bryant, The dynamics of water-protein interactions, Annual review of biophysics and biomolecular structure 25 (1996) 29-53.

[33] A. Kalk, H. Berendsen, Proton magnetic relaxation and spin diffusion in proteins, Journal of Magnetic Resonance (1969) 24 (1976) 343-366.

[34] H.T. Edzes, E.T. Samulski, Cross relaxation and spin diffusion in the proton NMR of hydrated collagen, Nature 265 (1977) 521-523.

[35] H.T. Edzes, E.T. Samulski, The measurement of cross-relaxation effects in the proton NMR spin-lattice relaxation of water in biological systems: hydrated collagen and muscle, Journal of Magnetic Resonance 31 (1978) 207-229.

[36] P.S. Belton, NMR studies of hydration in low water content biopolymer systems, Magn. Reson. Chem. 49 (2011) S127-S132.

[37] G. Diakova, Y.A. Goddard, J.-P. Korb, R.G. Bryant, Changes in protein structure and dynamics as a function of hydration from 1 H second moments, J. Magn. Reson. 189 (2007) 166-172.

[38] Y.A. Goddard, J.-P. Korb, R.G. Bryant, Water molecule contributions to proton spin–lattice relaxation in rotationally immobilized proteins, J. Magn. Reson. 199 (2009) 68-74.

[39] B. Hills, The proton exchange cross-relaxation model of water relaxation in biopolymer systems, Mol. Phys. 76 (1992) 489-508.

[40] B. Halle, Molecular theory of field-dependent proton spin-lattice relaxation in tissue, Magn. Reson. Med. 56 (2006) 60-72.

[41] A.G. Palmer, F. Massi, Characterization of the dynamics of biomacromolecules using rotating-frame spin relaxation NMR spectroscopy, Chemical reviews 106 (2006) 1700-1719.

[42] A.G. Palmer 3rd, C.D. Kroenke, J.P. Loria, Nuclear magnetic resonance methods for quantifying microsecond-to-millisecond motions in biological macromolecules, Methods in enzymology 339 (2000) 204-238.

[43] D.D. Boehr, H.J. Dyson, P.E. Wright, An NMR perspective on enzyme dynamics, Chemical reviews 106 (2006) 3055-3079.

[44] C. Charlier, S.F. Cousin, F. Ferrage, Protein dynamics from nuclear magnetic relaxation, Chem. Soc. Rev. 45 (2016) 2410-2422.

[45] B. Blicharska, H. Peemoeller, M. Witek, Hydration water dynamics in biopolymers from NMR relaxation in the rotating frame, J. Magn. Reson. 207 (2010) 287-293.

[46] C.P. Lindsey, G.D. Patterson, Detailed comparison of the Williams–Watts and Cole–Davidson functions, The Journal of chemical physics 73 (1980) 3348-3357.

[47] M.N. Berberan-Santos, E.N. Bodunov, B. Valeur, Mathematical functions for the analysis of luminescence decays with underlying distributions 1. Kohlrausch decay function (stretched exponential), Chemical Physics 315 (2005) 171-182.

[48] W. Schnauss, F. Fujara, K. Hartmann, H. Sillescu, Nonexponential 2 H spin-lattice relaxation as a signature of the glassy state, Chemical Physics Letters 166 (1990) 381-384.

[49] A.G. Palmer Iii, NMR characterization of the dynamics of biomacromolecules, Chemical reviews 104 (2004) 3623-3640.

[50] J.R. Lewandowski, M.E. Halse, M. Blackledge, L. Emsley, Direct observation of hierarchical protein dynamics, Science 348 (2015) 578-581.

[51] V.N. Uversky, E.A.e. Permi̇akov, Methods in Protein Structure and Stability Analysis: Vibrational Spectroscopy, Nova Publishers, 2007.

[52] A. Krushelnitsky, T. Zinkevich, N. Mukhametshina, N. Tarasova, Y. Gogolev, O. Gnezdilov, V. Fedotov, P. Belton, D. Reichert, 13C and 15N NMR study of the hydration response of T4 lysozyme and αB-crystallin internal dynamics, The Journal of Physical Chemistry B 113 (2009) 10022-10034.

[53] K. Gekko, Y. Hasegawa, Effect of temperature on the compressibility of native globular proteins, The Journal of Physical Chemistry 93 (1989) 426-429.

[54] P.J. Flory, Thermodynamics of high polymer solutions, The Journal of chemical physics 10 (1942) 51.

[55] E.A.e. Permi̇akov, V.N. Uversky, Methods in Protein Structure and Stability Analysis: Vibrational Spectroscopy, Nova Publishers, 2007.

[56] S. Tsuda, A. Miura, S.M. Gagné, L. Spyracopoulos, B.D. Sykes, Low-Temperature-Induced Structural Changes in the Apo Regulatory Domain of Skeletal Muscle Troponin C†, Biochemistry 38 (1999) 5693-5700.

[57] H. Kumeta, A. Miura, Y. Kobashigawa, K. Miura, C. Oka, N. Nemoto, K. Nitta, S. Tsuda, Low-temperature-induced structural changes in human lysozyme elucidated by three-dimensional NMR spectroscopy, Biochemistry 42 (2003) 1209-1216.

[58] T.M. Blumenschein, T.E. Gillis, G.F. Tibbits, B.D. Sykes, Effect of temperature on the structure of trout troponin C, Biochemistry 43 (2004) 4955-4963.

[59] S.-H. Chong, S. Ham, Component analysis of the protein hydration entropy, Chem. Phys. Lett. 535 (2012) 152-156.

[60] D. Russo, E. Pellegrini, M.A. Gonzalez, S. Perticaroli, J. Teixeira, In situ molecular dynamics analysis of the water hydrogen bond at biomolecular sites: Hydrophobicity enhances dynamics heterogeneity, Chem. Phys. Lett. 517 (2011) 80-85.

[61] A.J. Wand, The dark energy of proteins comes to light: conformational entropy and its role in protein function revealed by NMR relaxation, Current opinion in structural biology 23 (2013) 75-81.

[62] S. Homans, Dynamics and thermodynamics of ligand–protein interactions, Bioactive Conformation I, Springer2006, pp. 51-82.

CHAPTER 4

ALCOHOL-PROTEIN INTERACTIONS: SPECIFIC AND NONSPECIFIC BINDING

4.1 Introduction

Many biological, pharmacological and medical questions are concerned with the core issue of interactions between proteins and ligands. A large number of small-molecule ligands, such as general anesthetics and alcohols, exert their biological functions via binding to target proteins with low affinity [1-4]. Among these drugs, alcohols can affect neurological responses in various ways. For instance, it is well known that small ethanol doses stimulate a pleasurable sensation as well as cause depressant effects such as anxiety reduction; a larger dosage produces anesthetizing effects, including unconsciousness and analgesia [3, 4]. The very low binding affinity of alcohols to proteins makes it difficult to recognize and characterize bound alcohols. Hence, the mechanism governing alcohol binding remains poorly understood [3-8].

Previous works have revealed that general anesthetics such as halothane and isoflurane exert their functions via interacting with a few specific sites on the protein [1, 2, 9]. Importantly, such interaction is “indirect”: without the existence of water at the sites, general anesthetics cannot directly bind to the protein [9]. Because of the similarity in the molecular structure and biological functions of general anesthetics and alcohols, it remains controversial whether they share the same binding mechanism [10-14].

In fact, it has been found that there also exist a small number of specific binding sites for alcohols; such sites are believed to be of crucial importance to physiological processes and have

been the focus of intensive investigations [10, 15-17]. However, it is also suggested that alcohols could bind to some nonspecific sites on proteins; at very high alcohol concentration, such nonspecific binding may even cause protein structural changes [5, 7, 18]. Unfortunately, the property of nonspecifically-bound alcohols remains ambiguous [12-14, 19, 20]. For one reason, in the solution environment, alcohols bind to specific and nonspecific sites concurrently; it is very difficult to distinguish them via traditional methods [4, 5]. For another reason, X-ray crystallography and molecular dynamic simulations are typical ways to study alcohol binding; however, X-ray crystallography requires alcohols to be immobilized at the binding sites during the exposure time [21] and molecular dynamic simulations are usually limited to short time scales [22], hence these methods are effective in studying strongly bound alcohols at a few specific sites but are ineffective in investigating very weakly bound alcohols at a large number of nonspecific sites. Therefore, so far, there is no consensus on nonspecifically-bound alcohols with regards to their binding mechanism [14, 19, 23-25] and relevance to physiological processes [12-14, 19].

Here, I employ the *in-situ* NMR technique to selectively characterize specifically- and nonspecifically-bound alcohols by measuring alcohol isotherms on the dry protein [26]. Furthermore, changes in Gibbs free energy, enthalpy, and entropy associated with alcohol binding are determined. Two alcohols, ethanol (EtOH) and trifluoroethanol (TFE) are investigated. EtOH has a wide range of physiological effects on the human body [3, 4] and TFE is a potent anesthetic [27, 28]. A typical globular protein bovine serum albumin (BSA) is used, because of its well-known crystal structure and function and great binding capacity [29, 30]. It is found that in contrast to other general anesthetics, alcohols can directly bind to the dry protein. There exist three stages in alcohol binding to the protein [26]. At the initial stage, alcohols only

bind to a few specific sites on the protein. Above a threshold of alcohol vapor pressure, alcohols start binding to nonspecific sites and such binding is dependent on temperature. At the final stage, nonspecific alcohol binding denatures the protein. The flexibility of the protein plays a significant role in nonspecific alcohol binding. The work in this chapter reveals the mechanism of alcohol-protein interactions, with implications for the understanding of alcohol's biological effects.

4.2 Experiments

4.2.1 NMR Isotherm Measurements

BSA (lyophilized powder, ≥98%, pH~7, 1% in 0.15M NaCl) is purchased from Sigma Aldrich and used without further purification. Ethanol (EtOH) (99.5%, anhydrous) and 2,2,2-trifluoroethanol (TFE) (99.8%, extra pure) are purchased from Fisher Scientific. BSA is put into a quartz tube which is connected directly to the *in-situ* NMR system introduced in CHAPTER 2 [9, 31]. Liquid alcohols are stored in source bottles in the system. Dry BSA is exposed to alcohols with controlled vapor pressure. The temperature of the system is controlled at 6 C, 15 C, and 25 C. ^{1}H and ^{19}F NMR spectra are used to determine the isotherms of EtOH and TFE on the protein, respectively. The detailed procedure to measure isotherms has been introduced in CHAPTER 2 SECTION 2.2 [26]. At each alcohol vapor pressure, NMR signal is measured five times when the interaction reached equilibrium, and then the standard deviations of NMR peak areas are used to calibrate the error bars in the isotherms.

4.2.2 Determination of ΔG, ΔH, and $T\Delta S$

Changes in the Gibbs free energy ΔG, enthalpy ΔH, and entropy $T\Delta S$ associated with alcohol binding are determined from alcohol isotherms at different temperatures [26]. Briefly, $\Delta G = -RT\int_0^x \frac{n}{x}dx$, where n is the amount of absorbed alcohol molecules and $x = P / P_0$, where P and P_0 are the vapor pressure and saturated vapor pressure of the alcohol. Based on the Gibbs–Helmholtz equation, $\Delta H = -T^2 \frac{\partial}{\partial T}(\frac{\Delta G}{T})_x$, and $\Delta S = -(\frac{\partial}{\partial T}\Delta G)_x$. The method has been reported in CHAPTER 2 SECTION 2.2 [26, 32-35]. Here, alcohol isotherms measured at 6 C and 15 C, 15 C and 25 C can be employed to calculate ΔG, ΔH, and $T\Delta S$ around 10 C and 20 C, respectively. The error bars of alcohol isotherms are propagated to calculate the error bars of ΔG, ΔH, and $T\Delta S$.

4.3 Results and Discussion

4.3.1 Isotherms of Alcohols on the Protein

Figure 4.1(A) and (B) show the adsorption isotherms of EtOH and TFE in dry BSA at 6 C, 15 C, and 25 C, respectively [26]. The insets show isotherms below the relative vapor pressure of P/P_0~0.7 where P is the vapor pressure and P_0 is the saturated vapor pressure of the pure liquid alcohols at the given temperature.

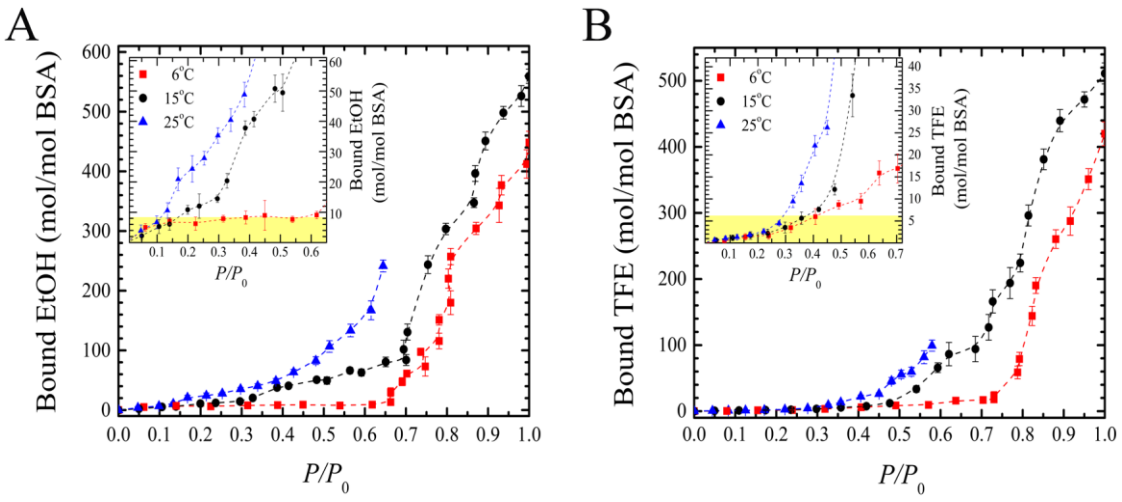

Figure 4.1: Adsorption isotherms of (A) EtOH and (B) TFE in dry BSA at 6 C, 15 C, and 25 C. The insets show isotherms below P/P_0~0.7. Thresholds of relative vapor pressure in the isotherms are recognized. The threshold of relative vapor pressure is P/P_0~0.15 for EtOH (Inset of A) and P/P_0~0.3 for TFE (Inset of B). The sorption of both alcohols shows little temperature dependence below this threshold and is marked with shade in yellow. Above the threshold, alcohol sorption is enhanced by temperature. Sharp alcohol uptake above the relative vapor pressure of P/P_0~0.7 occurs for both alcohols, associated with protein denaturation.

Three stages are clearly recognized in the isotherms. Below the first threshold pressure of P/P_0~0.15 for EtOH and P/P_0~0.3 for TFE, isotherms of both alcohols are independent of the temperature and the number of bound alcohol molecules is relatively small, reaching ~8 EtOH and ~6 TFE per BSA, in agreement with the number of high-affinity binding sites on serum albumin surface for alcohols and other similar amphiphilic molecules [36-38]. Above this first threshold pressure, isotherms of both alcohols increase rapidly and are greatly enhanced by increasing temperature. The number of bound alcohols far exceeds the number of high-affinity

binding sites and increases with alcohol vapor pressure, implying that binding at multiple nonspecific sites takes place [12-14]. In addition, above P/P_0~0.7, a sharp uptake of both alcohols occurs, corresponding to the denaturation of proteins [39-41].

Desorption isotherms of EtOH and TFE in dry BSA are also measured at 6 C. The results are shown in Figure 4.2. For both EtOH and TFE, strong hysteresis is observed at such a low temperature. Also, when the pressure decreases to 0, there are some residual EtOH and TFE molecules that bind permanently to BSA, even after pumping for several days. Figure 4.2 shows that the hysteresis loops of EtOH and TFE are quite large and have a similar shape. There are about 50-60 EtOH molecules/BSA that cannot be removed after pumping. For TFE, there are 40-50 permanently bound TFE/BSA. The irreversibility of desorption isotherms and large hysteresis above P/P_0~0.7 prove that alcohols denature the protein above P/P_0~0.7. The insets of Figure 4.2 show that the alcohol-protein interaction is totally reversible below P/P_0~0.7 and the protein is not denatured.

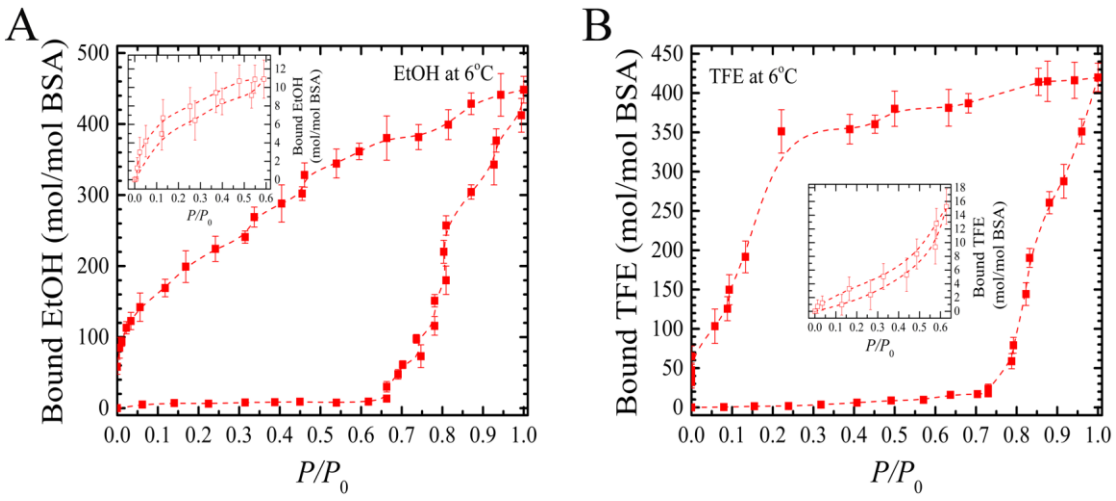

Figure 4.2: Adsorption-desorption isotherms of (A) EtOH and (B) TFE in dry BSA at 6 C. Large hysteresis is observed for both alcohols. In desorption curves, there are

~50 bound EtOH and ~40 bound TFE that cannot be removed from BSA when the vapor pressure reaches 0. Such irreversibility indicates the denaturation of BSA by alcohols. The insets show adsorption-desorption isotherms below P/P_0~0.65, showing that the alcohol-protein interaction is reversible below P/P_0~0.65.

Hence, the results of Figure 4.1 and Figure 4.2 reveal three steps of alcohol binding. At low vapor pressure, alcohols bind to a few pre-existing high-affinity sites; above a threshold vapor pressure, alcohol binding at multiple nonspecific sites is turned on; at very high vapor pressure, a large number of alcohols bind, causing denaturation of the protein.

It is worth mentioning that other anesthetics such as halothane and isoflurane cannot directly bind to dry proteins; hydration water is necessary in the adsorption of halothane and isoflurane on proteins [9]. This is in contrast to the result of alcohols. Alcohols are able to directly adsorb on dry BSA. This result indicates that although alcohols and other anesthetics exert similar functions, the underlying mechanisms are completely different. The effect of hydration on alcohol binding will also be discussed in detail in CHAPTER 5.

4.3.2 Thermodynamics of nonspecific alcohol binding

The method introduced in SECTION 4.2.2 only applies to adsorption that depends on temperature [26, 32-35]. Because only the adsorption of alcohols on nonspecific sites depends on temperature, changes in Gibbs free energy ΔG, enthalpy ΔH, and entropy $T\Delta S$ associated with nonspecific alcohol binding are calculated. Based on SECTION 4.2.2, alcohol isotherms at 6 C and 15 C in Figure 4.1 are used to calculate ΔG, ΔH, and $T\Delta S$ at 10 C; alcohol isotherms at 15 C and 25 C in Figure 4.1 are used to calculate ΔG, ΔH, and $T\Delta S$ at 20 C.

Figure 4.3 (A) and (B) show the energy diagrams of EtOH binding to dry BSA at 10 C and 20 C; Figure 4.3 (C) and (D) show the energy diagrams of TFE binding to dry BSA at 10 C and 20 C. Representative results of nonspecific alcohol binding in dry BSA are summarized in Table 4.1. Inspection of Figure 4.3 and Table 4.1 reveals that the binding of EtOH and TFE to BSA produces similar thermodynamic changes. First, ΔG is negative, suggesting that the binding is spontaneous. Second, ΔH and $T\Delta S$ are both positive, indicating that above the thresholds, the nonspecific alcohol binding is completely driven by the favorable entropy change that compensates for the unfavorable enthalpy change.

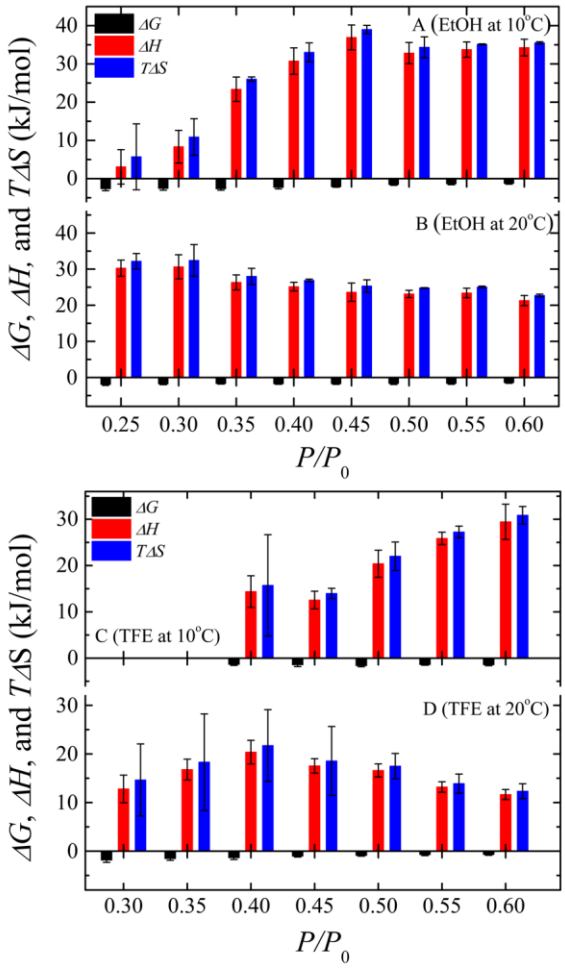

Figure 4.3: Changes in the Gibbs free energy ΔG (black), enthalpy ΔH (red), and entropy $T\Delta S$ (blue) of (*A*) EtOH in dry BSA at 10 C, (*B*) EtOH in dry BSA at 20 C, (*C*) TFE in dry BSA at 10 C and (*D*) TFE in dry BSA at 20 C. The binding of both alcohols in the dry protein is totally driven by favorable entropy changes that compensate for the unfavorable enthalpy changes. The error bars of isotherms in Figure 4.1 are propagated to calibrate the error bars.

Table 4.1: ΔG, ΔH, and $T\Delta S$ of EtOH and TFE binding to dry BSA at 10 C and 20 C. Relative vapor pressures in the region where nonspecific binding dominates the isotherms (after completion of binding to high-affinity sites and before denaturation taking place) are used in the calculation (EtOH at 10 C, P/P_0~0.4; EtOH at 20 C, P/P_0~0.35; TFE at 10 C, P/P_0~0.55; TFE at 20 C, P/P_0~0.4). ΔG, ΔH, and $T\Delta S$ are calculated at such relative vapor pressures and summarized.

		ΔG (kJ/mol)	ΔH (kJ/mol)	$T\Delta S$ (kJ/mol)
EtOH	10 C	-2.4±0.4	30.7±3.5	33.1±2.5
	20 C	-1.7±0.2	26.3±2.1	28.0±2.2
TFE	10 C	-1.4±0.2	25.9±1.4	27.3±1.3
	20 C	-1.3±0.4	20.4±2.4	21.7±3.4

4.3.3 Comparison of Specific and Nonspecific Alcohol Binding

Two types of alcohol binding are revealed by the alcohol isotherms in dry BSA. One corresponds to the binding of alcohols to a few specific sites and the binding energy is around ~4.2 kJ/mol [4, 14]; the other corresponds to adsorption at multiple low-affinity nonspecific sites and the binding energy is around 1~3.5 kJ/mol (see Figure 4.3 and Table 4.1). The adsorption of alcohols to these two types of sites show different temperature dependences, indicating that they are governed by different binding mechanisms.

Approximately 8 EtOH or 6 TFE bind to the specific sites on dry BSA (Figure 4.1) and this type of alcohol binding is independent of temperature. These results imply that there are several pre-existing easily-accessible alcohol binding sites on the protein surface [36-38]. These sites are preserved in the dehydration process. Alcohol binding to these high-affinity sites is mainly through direct protein-alcohol interactions, such as hydrogen bonds or van der Waals forces, which are minimally affected by the temperature in the range examined here [42]. In general, a specific site for alcohols is a pre-existing hydrophobic cavity with hydrophilic residues at the opening of the cavity [5]. The hydrophobic end of the alcohol is inserted into the hydrophobic cavity which is usually formed by methyl or methylene protein groups [5]. The hydrophilic end of the alcohol is usually anchored by the hydroxyl protein groups at the opening of the cavity [5].

In contrast, a large number of alcohols bind to nonspecific protein sites above a certain alcohol vapor pressure threshold (Figure 4.1). The microscopic structure of a nonspecific site is similar to that of a specific site, but nonspecific sites are not accessible to alcohols at low concentrations [5]. Figure 4.1 shows that the nonspecific alcohol binding is very sensitive to

temperature. Such strong temperature dependence is attributed to the active involvement of the protein structure in nonspecific binding and is discussed in detail in the following section.

4.3.4 Active Role of Protein in Nonspecific Binding

I have discussed that alcohols can bind to a few specific sites on the protein surface via direct alcohol-protein interactions. Usually, traditional surface binding theories such as Brunauer-Emmett-Teller (BET) or Langmuir theory are applied to explain surface adsorption isotherms [42-44]. In these theories, the protein is treated as a rigid surface; the corresponding isotherms show little temperature dependence and no thresholds [42]. Therefore, unlike high-affinity alcohol binding, alcohol binding at multiple low-affinity nonspecific sites cannot be interpreted by those traditional surface adsorption theories.

There are certain similarities between the temperature dependence of water isotherms (CHAPTER 2, Figure 2.3) and that of alcohol sorption isotherms in dry proteins (Figure 4.1). Protein hydration above h~0.2 is also strongly enhanced by temperature. In CHAPTER 2, it has been discussed that those water molecules above h~0.2 actually intimately mix with the protein structure rather than sitting on the protein surface. Specifically, the elastic constant of the protein is small at high temperature and the increase in elastic energy due to swelling is small; hence, mixing of the protein with water molecules is energetically not too costly at high temperature. However, at low temperature, the protein is more rigid with a larger elastic constant and mixing with water molecules is more costly in increased elastic energy [31]. The elasticity of the protein is critical to the temperature dependence of water isotherms. Hence, the results in this chapter suggest that nonspecific alcohol binding, which is similar to the hydration process above h~0.2, is also a mixing process, in which the protein structure is actively involved.

Furthermore, this mixing process only occurs above a threshold of alcohol vapor pressure. It is known that dehydration leads to strong protein-protein contacts, hence a rigid structure in the dry protein aggregate [43-46]. Due to the compact protein aggregate structure, a large number of nonspecific sites may not be available to alcohols. However, alcohols are able to change protein structure [3-8, 47] and serum albumin has a great conformational adaptability in ligand binding [29, 30, 38]. Hence, it is likely that the initial alcohol binding at specific sites can disturb intermolecular protein-protein interactions, creating pathways for alcohols to access those nonspecific sites. Subsequently, alcohol molecules start to mix with the protein via adsorption at nonspecific sites.

It is seen that this nonspecific alcohol binding to dry protein accompanies positive changes in enthalpy and entropy (Figure 4.3 and Table 4.1). Such thermodynamic change is consistent with the active involvement of protein structure in alcohol binding. Nonspecific alcohol binding (and hydration above h~0.2), which is essentially a mixing process, can largely disrupt protein-protein interactions and rearrange protein conformations [5, 12-14, 48], resulting in increased enthalpy of the protein. However, the protein could also gain a large number of degrees of freedom upon this alcohol-induced disruption [45] with increased entropy. The results show that the entropy gain in the protein surpasses the unfavorable enthalpy change and drives the nonspecific alcohol binding. In addition, it was suggested that in non-aqueous alcohols or high-concentration aqueous alcohol solutions, a large number of alcohol molecules can penetrate into the hydrophobic interior of the protein and extensively break the native protein structure, resulting in dramatic conformational changes and even unfolding of the protein [5, 6, 40, 49-51]. The denaturation of BSA at higher alcohol pressures (Figure 4.2) further proves that those nonspecifically bound alcohols do mix with the protein, and if the mixing is too extensive, the

intramolecular protein interactions are substantially disrupted causing denaturation.

4.4 Conclusions

In this chapter, I focus on alcohol-protein interactions by studying the isotherms of EtOH and TFE in dry BSA at different temperatures. The changes in the Gibbs free energy, entropy, and enthalpy of alcohol binding are also obtained. It is found that in contrast to other general anesthetics, alcohols can directly bind to the dry protein without the existence of water. Specifically, at low alcohol vapor pressure, only a few alcohol molecules bind to several specific sites on the protein and the binding is independent of temperature. Nonspecific alcohol binding occurs only above a threshold of alcohol vapor pressure and is strongly dependent on temperature. Such nonspecific alcohol binding is driven by the favorable entropy change where the protein's flexibility plays a critical role. At high alcohol vapor pressure, nonspecific alcohol binding causes irreversible changes in protein structure. The work in this chapter elucidates the distinct mechanisms of specific and nonspecific alcohol binding. It also reveals the active role of the protein itself in alcohol binding, shedding light on the mechanism governing alcohol's biological functions.

4.5 REFERENCES

[1] N.P. Franks, General anaesthesia: from molecular targets to neuronal pathways of sleep and arousal, Nat. Rev. Neurosci. 9 (2008) 370-386.

[2] J.A. Campagna, K.W. Miller, S.A. Forman, Mechanisms of actions of inhaled anesthetics, N. Engl. J. Med. 348 (2003) 2110-2124.

[3] R.A. Harris, J.R. Trudell, S.J. Mihic, Ethanol's molecular targets, Sci. Signal. 1 (2008) re7.

[4] R.J. Howard, P.A. Slesinger, D.L. Davies, J. Das, J.R. Trudell, R.A. Harris, Alcohol-Binding Sites in Distinct Brain Proteins: The Quest for Atomic Level Resolution, Alcohol.: Clin. Exp. Res. 35 (2011) 1561-1573.

[5] D. Dwyer, R. Bradley, Chemical properties of alcohols and their protein binding sites, Cellular and Molecular Life Sciences CMLS 57 (2000) 265-275.

[6] J.F. Povey, C.M. Smales, S.J. Hassard, M.J. Howard, Comparison of the effects of 2, 2, 2-trifluoroethanol on peptide and protein structure and function, J Struct Biol 157 (2007) 329-338.

[7] Q. Shao, Y. Fan, L. Yang, Y.Q. Gao, From protein denaturant to protectant: comparative molecular dynamics study of alcohol/protein interactions, The Journal of chemical physics 136 (2012) 115101.

[8] Q. Shao, The addition of 2, 2, 2-trifluoroethanol prevents the aggregation of guanidinium around protein and impairs its denaturation ability: A molecular dynamics simulation study, Proteins 82 (2014) 944-953.

[9] H.-J. Wang, A. Kleinhammes, P. Tang, Y. Xu, Y. Wu, Critical Role of Water in the Binding of Volatile Anesthetics to Proteins, The Journal of Physical Chemistry B 117 (2013) 12007-12012.

[10] L. Sauguet, R.J. Howard, L. Malherbe, U.S. Lee, P.-J. Corringer, R.A. Harris, M. Delarue, Structural basis for potentiation by alcohols and anaesthetics in a ligand-gated ion channel, Nat. Commun. 4 (2013) 1697.

[11] A. Bhattacharji, N. Klett, R.C.V. Go, M. Covarrubias, Inhalational anaesthetics and n-alcohols share a site of action in the neuronal Shaw2 Kv channel, Br. J. Pharmacol. 159 (2010) 1475-1485.

[12] R.G. Eckenhoff, Do specific or nonspecific interactions with proteins underlie inhalational anesthetic action?, Mol. Pharmacol. 54 (1998) 610-615.

[13] B.W. Urban, M. Bleckwenn, M. Barann, Interactions of anesthetics with their targets: Non-specific, specific or both?, Pharmacol. Ther. 111 (2006) 729-770.

[14] R.G. Eckenhoff, J.S. Johansson, Molecular interactions between inhaled anesthetics and proteins, Pharmacological Reviews 49 (1997) 343-368.

[15] S.J. Mihic, Q. Ye, M.J. Wick, V.V. Koltchine, M.D. Krasowski, S.E. Finn, M.P. Mascia, C.F. Valenzuela, K.K. Hanson, E.P. Greenblatt, Sites of alcohol and volatile anaesthetic action on GABAA and glycine receptors, Nature 389 (1997) 385-389.

[16] M.P. Mascia, J.R. Trudell, R.A. Harris, Specific binding sites for alcohols and anesthetics on ligand-gated ion channels, Proceedings of the National Academy of Sciences 97 (2000) 9305-9310.

[17] S.W. Kruse, R. Zhao, D.P. Smith, D.N. Jones, Structure of a specific alcohol-binding site defined by the odorant binding protein LUSH from Drosophila melanogaster, Nat. Struct. Mol. Biol. 10 (2003) 694-700.

[18] H.B. Bull, K. Breese, Interaction of alcohols with proteins, Biopolymers 17 (1978) 2121-2131.

[19] R.W. Olsen, G.D. Li, M. Wallner, J.R. Trudell, E.J. Bertaccini, E. Lindahl, K.W. Miller, R.L. Alkana, D.L. Davies, Structural Models of Ligand-Gated Ion Channels: Sites of Action for Anesthetics and Ethanol, Alcohol.: Clin. Exp. Res. (2013).

[20] M. Wallner, R. Olsen, Physiology and pharmacology of alcohol: the imidazobenzodiazepine alcohol antagonist site on subtypes of GABAA receptors as an opportunity for drug development?, Br. J. Pharmacol. 154 (2008) 288-298.

[21] A.M. Davis, S.J. Teague, G.J. Kleywegt, Application and Limitations of X-ray Crystallographic Data in Structure-Based Ligand and Drug Design, Angew. Chem. Int. Ed. 42 (2003) 2718-2736.

[22] B.J. Alder, T. Wainwright, Studies in molecular dynamics. I. General method, The Journal of Chemical Physics 31 (2004) 459-466.

[23] S. Murail, R.J. Howard, T. Broemstrup, E.J. Bertaccini, R.A. Harris, J.R. Trudell, E. Lindahl, Molecular mechanism for the dual alcohol modulation of Cys-loop receptors, PLoS Comput. Biol. 8 (2012) e1002710.

[24] S. Murail, B. Wallner, J.R. Trudell, E. Bertaccini, E. Lindahl, Microsecond simulations indicate that ethanol binds between subunits and could stabilize an open-state model of a glycine receptor, Biophys. J. 100 (2011) 1642-1650.

[25] R.G. Eckenhoff, J.W. Tanner, J.S. Johansson, Steric hindrance is not required for n-alkanol cutoff in soluble proteins, Mol. Pharmacol. 56 (1999) 414-418.

[26] Y. Chong, A. Kleinhammes, P. Tang, Y. Xu, Y. Wu, Dominant Alcohol–Protein Interaction via Hydration-Enabled Enthalpy-Driven Binding Mechanism, The Journal of Physical Chemistry B 119 (2015) 5367-5375.

[27] M.D. Krasowski, N.L. Harrison, The actions of ether, alcohol and alkane general anaesthetics on GABAA and glycine receptors and the effects of TM2 and TM3 mutations, Br. J. Pharmacol. 129 (2000) 731-743.

[28] L.S. Kaminsky, J.M. Fraser, M. Seaman, D. Dunbar, Rat liver metabolism and toxicity of 2, 2, 2-trifluoroethanol, Biochem. Pharmacol. 44 (1992) 1829-1837.

[29] K.A. Majorek, P.J. Porebski, A. Dayal, M.D. Zimmerman, K. Jablonska, A.J. Stewart, M. Chruszcz, W. Minor, Structural and immunologic characterization of bovine, horse, and rabbit serum albumins, Molecular Immunology 52 (2012) 174-182.

[30] T. Peters Jr, All about albumin: biochemistry, genetics, and medical applications, Academic Press1995.

[31] H.-J. Wang, A. Kleinhammes, P. Tang, Y. Xu, Y. Wu, Temperature dependence of lysozyme hydration and the role of elastic energy, Phys. Rev. E 83 (2011) 031924.

[32] A. Myers, Thermodynamics of adsorption in porous materials, AlChE J. 48 (2002) 145-160.

[33] T.L. Hill, Statistical mechanics of adsorption. V. Thermodynamics and heat of adsorption, The Journal of chemical physics 17 (1949) 520.

[34] T.L. Hill, Statistical mechanics of adsorption. IX. Adsorption thermodynamics and solution thermodynamics, The Journal of chemical physics 18 (1950) 246.

[35] R. Keren, I. Shainberg, Water vapor isotherms and heat of immersion of Na-and Ca-montmorillonite systems. III. Thermodynamics, Clays Clay Miner. 28 (1980) 204-210.

[36] J.A. Reynolds, S. Herbert, J. Steinhardt, Binding of some long-chain fatty acid anions and alcohols by bovine serum albumin, Biochemistry 7 (1968) 1357-1361.

[37] H. Polet, J. Steinhardt, Binding-induced alterations in ultraviolet absorption of native serum albumin, Biochemistry 7 (1968) 1348-1356.

[38] J. Ghuman, P.A. Zunszain, I. Petitpas, A.A. Bhattacharya, M. Otagiri, S. Curry, Structural basis of the drug-binding specificity of human serum albumin, J. Mol. Biol. 353 (2005) 38-52.

[39] R. Liu, P. Qin, L. Wang, X. Zhao, Y. Liu, X. Hao, Toxic effects of ethanol on bovine serum albumin, J. Biochem. Mol. Toxicol. 24 (2010) 66-71.

[40] H. Yoshikawa, A. Hirano, T. Arakawa, K. Shiraki, Effects of alcohol on the solubility and structure of native and disulfide-modified bovine serum albumin, Int. J. Biol. Macromol. 50 (2012) 1286-1291.

[41] N. Hirota, Y. Goto, K. Mizuno, Cooperative α-helix formation of β-lactoglobulin and melittin induced by hexafluoroisopropanol, Protein Sci. 6 (1997) 416-421.

[42] J.H. DEBOER, The Dynamical Character of Adsorption, Soil Sci 76 (1953) 166.

[43] I. Kuntz Jr, W. Kauzmann, Hydration of proteins and polypeptides, Adv Protein Chem 28 (1974) 239-345.

[44] J.A. Rupley, G. Careri, Protein hydration and function, Adv. Protein Chem. 41 (1991) 37-172.

[45] E.A.e. Permi̇akov, V.N. Uversky, Methods in Protein Structure and Stability Analysis: Vibrational Spectroscopy, Nova Publishers, 2007.

[46] A. Fernández, H.A. Scheraga, Insufficiently dehydrated hydrogen bonds as determinants of protein interactions, Proceedings of the National Academy of Sciences 100 (2003) 113-118.

[47] J.R. Trudell, R.A. Harris, Are sobriety and consciousness determined by water in protein cavities?, Alcohol.: Clin. Exp. Res. (2004).

[48] V.A. Sirotkin, I.A. Komissarov, A.V. Khadiullina, Hydration of proteins: excess partial volumes of water and proteins, The Journal of Physical Chemistry B 116 (2012) 4098-4105.

[49] R. Rajan, P. Balaram, A model for the interaction of trifluoroethanol with peptides and proteins, Int. J. Pept. Protein Res. 48 (1996) 328-336.

[50] P.I. Haris, F. Severcan, FTIR spectroscopic characterization of protein structure in aqueous and non-aqueous media, Journal of Molecular Catalysis B: Enzymatic 7 (1999) 207-221.

[51] R. Carrotta, M. Manno, F.M. Giordano, A. Longo, G. Portale, V. Martorana, P.L. San Biagio, Protein stability modulated by a conformational effector: effects of trifluoroethanol on bovine serum albumin, Phys Chem Chem Phys 11 (2009) 4007-4018.

CHAPTER 5

ALCOHOL-PROTEIN INTERACTIONS: THE EFFECT OF HYDRATION

5.1 Introduction

In CHAPTER 2, I discussed the significant effects of water on protein dynamics and thermodynamics. Water is also known to play an important role in a wide range of molecular recognition and association processes, such as protein ligand binding [1-7]. For instance, it has been reported that water can modify the shape and specificity of the binding sites and mediate the binding affinity [3, 4]. Specifically, as discussed in CHAPTER 4, small molecule drugs such as alcohols bind to the protein with very low affinity. These weak association processes are particularly influenced by water, but the details are far from understood [7-10]. Evaluating the role of water in such weak associations is a critical step in understanding the binding mechanisms and biological actions of small molecule drugs such as alcohols, with important implications for drug design.

Specifically, emerging evidence suggests that water exists around alcohol binding sites [11-18]. Although the potential importance of water in alcohol-protein interactions has been recognized, it remains unclear how water contributes to the interaction. In general, it was proposed that water can contribute to alcohol binding via two mechanisms. One proposed mechanism is that water around the binding sites is displaced by alcohols [11-14, 16-19]. The release of ordered water molecules to bulk water is believed to cause a gain in entropy [10-12, 14, 19]; however, this process also reconstructs water-water interactions, providing favorable

enthalpic changes [10, 20-23]. The controversial effects of the displacement of water on binding thermodynamics has attracted great attention [22]. Another proposed mechanism is that water molecules remain at the binding sites and form hydrogen bond bridges linking the protein and alcohols [14, 19]. These two mechanisms are both concerned with the influence of structural modifications in the water network on binding.

In addition to the prevalent mechanisms mentioned above, water may also affect alcohol binding indirectly via altering protein structures and dynamics. Hydration water is known to be an integral part of the protein, as it is tightly coupled to the protein configuration and flexibility [3-5, 24-28]. Ligand binding not only modifies the structure of the water network, but could also cause protein conformation changes enabled by water-protein interactions [29]. Recent works suggest that the protein is actively involved in ligand binding and can act as a potential thermodynamic reservoir: changes in protein configuration may significantly contribute to the enthalpy and entropy of ligand binding [29-33]. This is also proven in CHAPTER 4 SECTION 4.3. In particular, such protein configurational change does not necessarily involve large protein segments; it could be subtle, such as the local structural rearrangement or fluctuation of residues near binding sites [29]. These findings indicate that it might be inappropriate to consider all the binding sites on proteins as rigid cavities and only discuss the contribution of the water network to ligand binding, especially for those proteins with high structural and dynamic adaptability such as serum albumin. The protein's hydration state could greatly influence how the protein responds to alcohol binding, with significant influence on binding free energy. Thus far, however, little is known about the importance of such protein-water interactions in alcohol binding and their functional consequences.

In protein solutions, under the influence of a large amount of bulk solvent, it is difficult to evaluate the influence of hydration on ligand binding. In particular, hydration water molecules bind at different sites on the protein such as hydrophilic and hydrophobic groups [34, 35] and such different hydration water molecules could have very different effects on ligand binding. One way to separate the influence of different hydration water molecules in alcohol binding is to evaluate alcohol binding under controlled protein hydration. As discussed in CHAPTER 2, similar hydration regimes were identified for globular proteins [34, 35]: when the protein hydration level $h<\sim0.2$ (g water/g protein), water only binds to hydrophilic groups on the protein; when $h>\sim0.2$, water interacts with hydrophobic protein regions; when $h>\sim0.5$, bulk water exists around the protein. This suggests that by controlling protein hydration level, we might be able to investigate the distinct roles of hydration water at different protein sites on alcohol binding.

The *in-situ* NMR measurement system introduced in CHAPTER 1 enables me to study low affinity binding with high sensitivity while subjecting the system to a controlled level of hydration. In CHAPTER 4, two types of alcohol binding, specific and nonspecific binding have been found. In this chapter, I focus on the effects of hydration on these two types of alcohol binding [36]. Alcohol isotherms are characterized as a function of protein hydration level. Changes in Gibbs free energy, enthalpy, and entropy associated with alcohol binding are studied under the influence of hydration. It is found that hydration facilitates the saturation of specific alcohol sites. For nonspecific alcohol binding, at low hydration level, it only occurs when the alcohol vapor pressure exceeds a threshold level; however, this threshold is reduced by hydration and becomes negligible at a crossover hydration level of $h\sim0.2$ (g water/g protein). Hydration also gradually changes such nonspecific binding from an entropy-driven to an enthalpy-driven process. Water molecules bound at charged and polar groups on the protein surface are found to

be particularly crucial for such binding. Further hydration of the protein has smaller effects on the enthalpic and entropic changes but still results in significant decrease in Gibbs free energy upon alcohol binding. A significant difference is recognized between the role of water in alcohol binding and its role in the binding of other general anesthetics such as halothane [37]. This work revealed the importance of water-protein interactions in alcohol binding.

5.2 Experiments

BSA (lyophilized powder, ≥98%, pH~7, 1% in 0.15M NaCl) is purchased from Sigma Aldrich and used without further purification. 2,2,2-trifluoroethanol (TFE) (99.8%, extra pure) were purchased from Fisher Scientific. The distilled water (H_2O) and liquid TFE are stored in two source bottles with pressure buffer chambers as illustrated in CHAPTER 1. The vapor pressures of water and TFE are controlled by adjusting the valves close to their buffer chambers. ^{1}H and ^{19}F NMR spectra are used to determine hydration level and the amount of alcohol sorption in the protein respectively. Isotherms of TFE are measured as a function of hydration level at 15 C and 25 C. Specifically, ^{1}H NMR spectra of TFE are used to quantify the amount of sorption and this is then used to quantify the ^{19}F NMR intensity. To measure the isotherms of TFE in partially-hydrated protein, the dry BSA is first exposed to the water vapor, and the hydration level as measured by water sorption is determined by ^{1}H NMR. Thereafter, the partially hydrated BSA is exposed to TFE vapor and ^{19}F NMR is used to measure the adsorption of TFE. At each water/alcohol vapor pressure, the NMR signal was measured five times when the interaction reached equilibrium, and then the standard deviations of NMR peak areas were used to calibrate the error bars in the isotherms. In addition, changes in the Gibbs free energy ΔG, enthalpy ΔH, and entropy $T\Delta S$ of TFE binding are determined from TFE isotherms at

different temperatures [38-41]. Isotherms measured at 15 C and 25 C can be employed to calculate ΔG, ΔH, and $T\Delta S$ around 20 C. The error bars of alcohol isotherms were propagated to calculate the error bars of ΔG, ΔH, and $T\Delta S$. ΔG, ΔH, and $T\Delta S$ are also studied as a function of protein hydration level. The detailed methods of measuring isotherms and determining thermodynamic quantities have been discussed in CHAPTER 2 SECTION 2.2 [36].

5.3 Results and Discussions

5.3.1 Alcohol Isotherms on Hydrated Proteins

Figure 5.1 (A) shows isotherms of TFE at 15 C below P/P_0=0.3 in BSA hydrated at various levels (the complete isotherms can be found in Appendix B). As the level of protein hydration increases, the nonspecific binding of TFE increases dramatically; the shape of the isotherm gradually changes from sigmoidal (h=0.11) to hyperbolic (h=0.32), indicating a change in alcohol binding pattern, which will be discussed later. The threshold level of vapor pressure for nonspecific binding also decreases gradually with increasing hydration level. Figure 5.1 (B) shows that the threshold level decreases linearly with the hydration level and reaches zero around h~0.2. Hydration facilitates TFE to saturate the specific sites and enhances binding at nonspecific sites at lower vapor pressures, showing that hydration promotes alcohol binding at both types of sites. The inset of Figure 5.1 (B) further implies that when h>0.2, nonspecific alcohol binding could take place immediately at very low alcohol vapor pressure and could overwhelm the number of alcohols at specific sites at a high hydration level (h>0.3). The isotherms of TFE in hydrated BSA at 25 C show similar behaviors (See Appendix B). Isotherms of TFE in BSA at h=0.11 and h=0.32 at 15 C and 25 C are shown in Figure 5.1 (C). When h=0.11, nonspecific alcohol binding only takes place above P/P_0~0.25, while no threshold is

observed at h=0.32. It is interesting to note that nonspecific alcohol binding in hydrated BSA is reduced by increasing temperature, showing a temperature dependence opposite to alcohol isotherms in dry BSA (See CHAPTER 4, Figure 4.1).

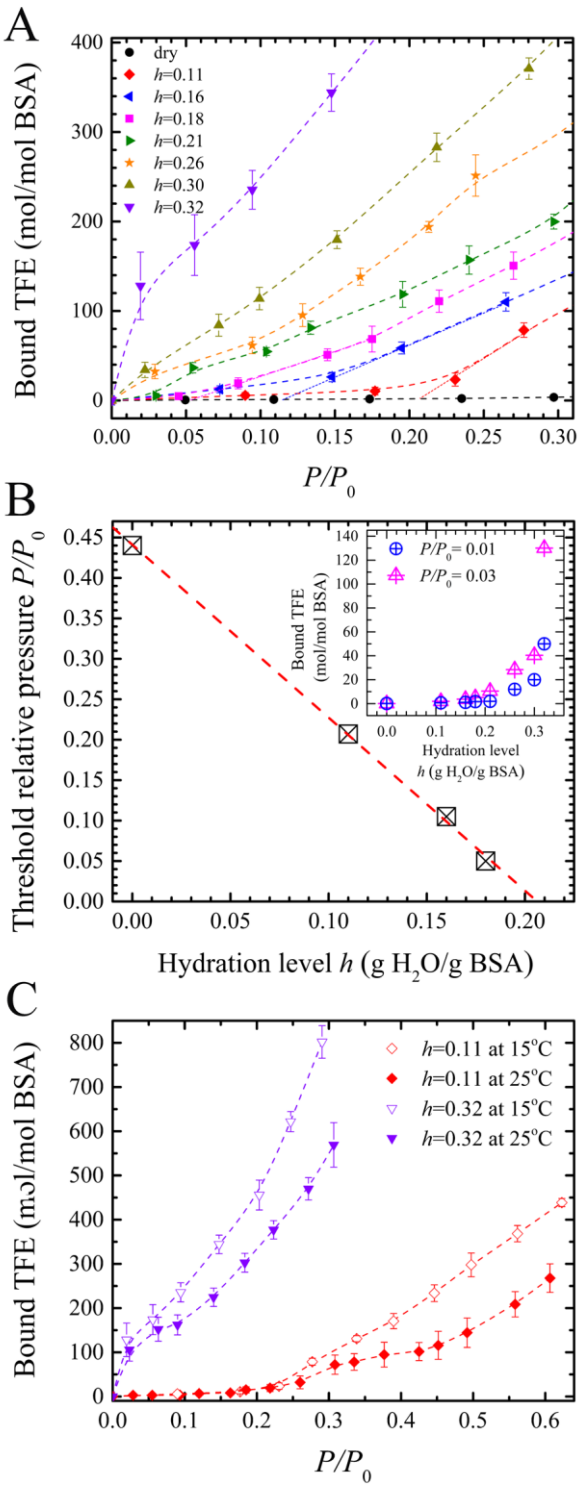

Figure 5.1: (A) Isotherms of TFE in hydrated BSA at 15 C below P/P_0=0.3 at various hydration levels. Dotted straight lines associated with the isotherms of h=0.11, 0.16 and 0.18 illustrate how the threshold (the intercept of the dotted line with the horizontal line of y=0) is determined for a given isotherm associated with nonspecific alcohol binding. (B) The determined alcohol relative vapor pressure threshold is plotted versus h at 15 C. The threshold decreases linearly with h and reaches zero at h~0.2. Inset: the number of bound TFE versus h at 15 C at P/P_0=0.01 and P/P_0=0.03. The value of thresholds and the number of bound TFE were determined from Figure 5.1 (A). (C) Isotherms of TFE in hydrated BSA at h=0.11 and 15 C and 25 C, and at h=0.32 and 15 C and 25 C. The isotherms at h=0.11 show a relative pressure threshold at P/P_0~0.25, while no threshold is seen in isotherms at h=0.32.

5.3.2 Hydration and Protein Flexibility

Water isotherms in BSA have been measured at 6 C, 15 C, and 25 C and are shown in Figure 5.2 (A). Similar to the results in CHAPTER 2 SECTION 2.3.1, below h~0.2 (P/P_0 < ~0.7), isotherms show little temperature dependence; whereas above h~0.2, the sorption of water is enhanced by increasing temperature. It was suggested that below h~0.2, water molecules only bind to charged and polar groups on the protein surface [34, 35]. Such surface-bound water is believed to be able to increase the flexibility of the protein [34, 35, 42]. Figure 5.2 (B) shows the ^{1}H NMR spectra of BSA at different hydration levels. Changes in the linewidth of the spectra are summarized in Figure 5.2 (C). The narrowing in the linewidth of the protein spectra further proves that the protein becomes more flexible with increasing hydration.

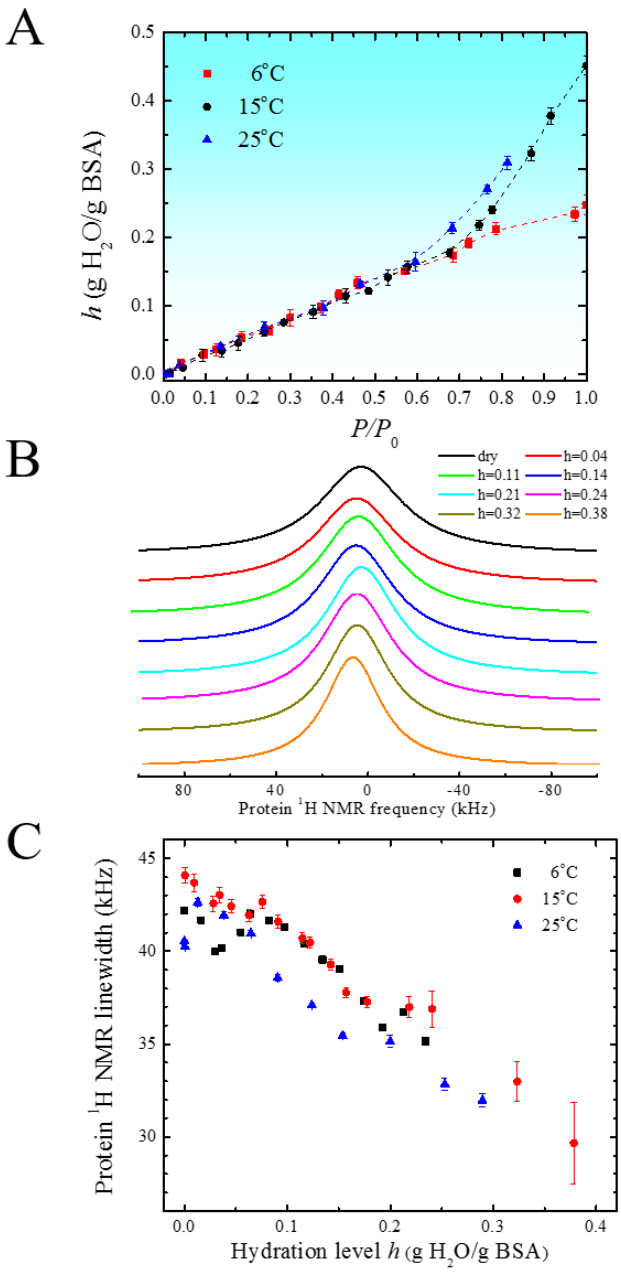

Figure 5.2: (A) Water isotherms on BSA at 6 C, 15 C, and 25 C. (B) ^{1}H spectra of the protein at different hydration levels. (C) Changes of the protein ^{1}H NMR linewidth with hydration level at 6 C, 15 C, and 25 C.

5.3.3 Thermodynamics of Alcohol Adsorption on Hydrated Proteins

The Gibbs free energy ΔG, enthalpy ΔH, and entropy $T\Delta S$ of nonspecific alcohol binding to the dry protein have been discussed in CHAPTER 4 SECTION 4.3.2. In this chapter, I focus on the effect of hydration on these thermodynamic quantities.

The energy diagrams of TFE binding to BSA at h=0.11, h=0.21, and h=0.32 are shown in Figure 5.3 (A), (B) and (C) respectively. As discussed in CHAPTER 4 SECTION 4.3.2, ΔH and $T\Delta S$ of nonspecific alcohol binding to the dry protein are both positive, indicating that such binding in the dry protein environment is completely driven by the favorable entropy change. Interestingly, as shown in Figure 5.3, both ΔH and $T\Delta S$ become negative with hydration, indicating that protein hydration shifts nonspecific alcohol binding from an entropy-driven to an enthalpy-driven process.

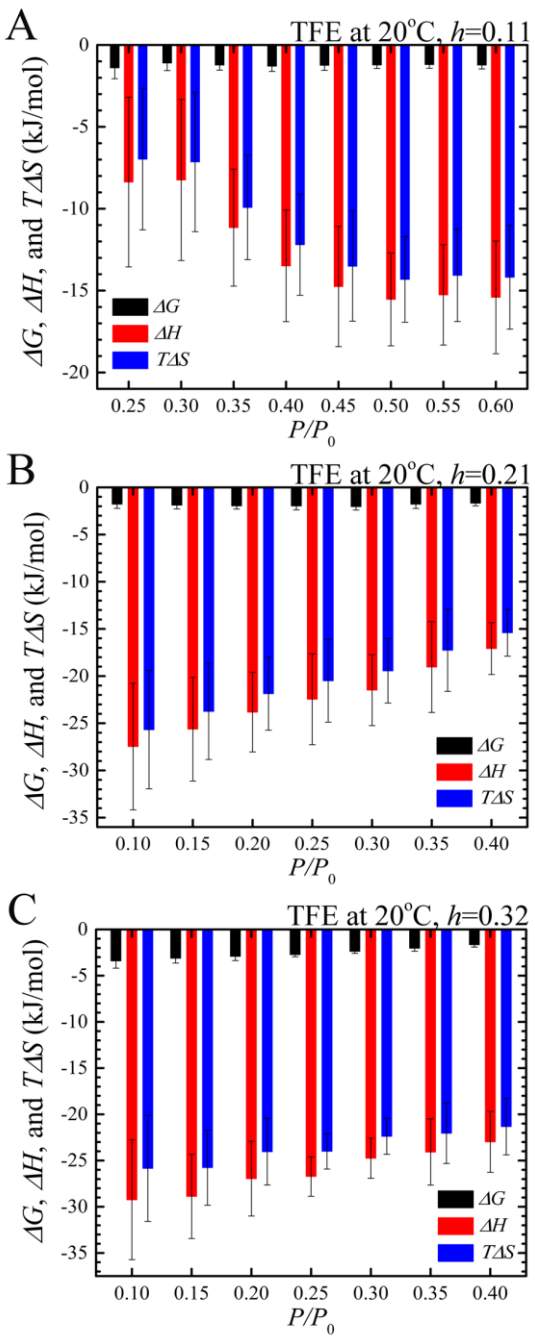

Figure 5.3: Changes in the Gibbs free energy ΔG (black), enthalpy ΔH (red), and entropy $T\Delta S$ (blue) of TFE binding to hydrated BSA at 20 C at (*A*) h=0.11, (*B*) h=0.21, and (*C*) h=0.32. Isotherms at 15 C and 25 C were used to calculate ΔG, ΔH, and $T\Delta S$ at 20 C. In contrast to binding in dry protein, binding of TFE to hydrated

protein is driven by favorable enthalpy changes that compensate for the unfavorable entropy changes.

The thermodynamic changes of nonspecific TFE binding are then plotted versus the protein hydration level *h*. ΔG, ΔH and $T\Delta S$ at h=0.11, h=0.21, and h=0.32 are read from Figure 5.3, while ΔG, ΔH and $T\Delta S$ at h=0 (dry protein) are read from CHAPTER 4 Figure 4.3. The results are shown in Figure 5.4. The increase in $|\Delta G|$ with hydration demonstrates that hydration promotes nonspecific alcohol binding. At high hydration levels (h>0.3), the binding energy ($-\Delta G$) of alcohols at nonspecific regions is slightly smaller than that of alcohols at specific sites, which is around 4.2 kJ/mol [13, 43]. Moreover, ΔH and $T\Delta S$ decrease appreciably at low hydration levels, while ΔG decreases appreciably at high hydration levels. It is interesting to note that ΔH and $T\Delta S$ are close to 0 at h~0.07, which is around the hydration level at which water fully covers charged groups and starts binding to polar groups on protein surfaces [34, 35].

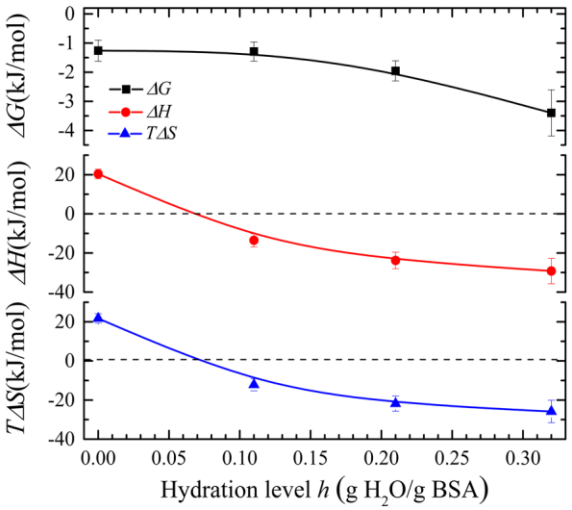

Figure 5.4: ΔG, ΔH, and $T\Delta S$ of TFE binding in hydrated BSA versus hydration level h at 20 C. Relative vapor pressures in the region where nonspecific binding dominates the isotherms (after completion of binding to high-affinity sites and before denaturation taking place) are used in the calculation (dry, P/P_0~0.4; h=0.11, P/P_0~0.4; h=0.21, P/P_0~0.2; h=0.32, P/P_0~0.1). ΔG, ΔH, and $T\Delta S$ are calculated at such relative vapor pressures and plotted in Figure 5.4.

5.3.4 Effects of Hydration on Alcohol Binding

I show that hydration can remove the threshold for nonspecific alcohol binding around h~0.2 and significantly change the shape of the alcohol adsorption isotherms (Figure 5.1). In fact, water adsorption in BSA (Figure 5.2 (A)) also changes appreciably around h~0.2. This implies that a certain amount of hydration (h~0.2) may induce qualitative changes in protein properties, hence affecting alcohol binding. Interestingly, it was also reported that the enzyme activity [34] of proteins is quite different below and above the hydration level h~0.2.

It has been suggested that water only binds to high-affinity regions of hydrophilic groups on the protein surface below h~0.2; above h~0.2, water starts to bind loosely to hydrophobic regions of the protein [34, 35]. I discussed in CHAPTER 2 that those loosely-bound water molecules can actively mix with the protein. Significantly, water adsorption at charged and polar protein groups can activate the protein to a more flexible state with reduced elastic constant [34, 35, 42], enabling the mixing process. This increase in protein flexibility with hydration is proven by the narrowing of the protein ^{1}H NMR linewidth in Figure 5.2 (B) and (C). Moreover, infrared measurements and X-ray studies showed that, like alcohol adsorption, water adsorption also accompanies the disruption of protein-protein contacts in solid serum albumin and other proteins

[35, 44-46]. Specifically, the formation of water interaction with hydrophilic protein groups is likely to cause pronounced protein configuration rearrangements; when the hydration of those groups is complete, the protein structure is basically identical to that in solution [44, 45]. This is consistent with the increase in the protein flexibility with hydration and changes in water isotherms around h~0.2 reported in this work.

The mechanism of water and organic solvents such as alcohols cooperatively changing the protein state was previously suggested [44, 47, 48]. Therefore, a possible explanation of how hydration promotes alcohol binding is: when h< ~0.2, hydration of charged and polar protein sites releases only part of the protein-protein contacts via disturbing the intermolecular protein-protein interactions, and alcohols are needed to further "liberate" the protein-protein contacts, hence the threshold for alcohol binding still exists but decreases with hydration level. When h> ~0.2, the intermolecular protein-protein contacts are largely removed by water; as a consequence, the threshold for alcohol binding disappears. Furthermore, hydration can create new binding space for alcohols [44], thus the number of bound alcohols increases dramatically with hydration.

Alcohol sorption isotherms in hydrated BSA show temperature dependence opposite to those in dry BSA. In dry proteins, the gain in entropy drives alcohol binding, which should be attributed to the increase in the protein's flexibility with alcohol incorporation. In contrast, with increasing hydration level the binding process is gradually changed from an entropy-driven to an enthalpy-driven process at a crossover hydration level of h~0.07, which is the hydration level where water covers all charged groups and starts binding to polar groups on the protein surface [34, 35]. Above that hydration level, it appears that the positive change in the protein's entropy is no longer a dominant factor in driving alcohol binding. With higher hydration, ΔG keeps

decreasing and enthalpic stabilization becomes more significant. Both ΔH and $T\Delta S$ decrease appreciably with increased hydration and exhibit strong enthalpy-entropy compensation, which is usually observed in low-affinity binding ligands [1, 9, 10, 49, 50]. The decrease of ΔH and $T\Delta S$ is more dramatic at low hydration levels, indicating that such enthalpy-driven alcohol binding is mainly enabled by water molecules bound at hydrophilic groups on the protein surface. At high hydration levels, those mixing water molecules induce smaller changes in ΔH and $T\Delta S$, but effectively reduce the enthalpy-entropy compensation, probably due to the expelling of those water molecules by alcohols. Less enthalpy-entropy compensation causes more negative changes of ΔG at high hydration levels, leading to increased alcohol adsorption.

5.3.5 Difference between Alcohols and Anesthetics

Due to the molecular and functional similarities of alcohols and general anesthetics, it was suggested that they might share similar binding mechanisms [15, 43, 51-53]. Recent work elucidated the binding mechanism of halothane and other typical general anesthetics [37]. Halothane cannot directly bind to the protein in the absence of hydration. It only interacts with the protein when $h>0.3$ and the number of bound halothane is limited to a few binding sites, indicating that halothane only binds to a few specific pockets in the protein and the interaction is enabled by hydration above $h=0.3$. It is suggested that water might be displaced by halothane or form a cap above the binding cavity to assist in the halothane binding [37]. CHAPTER 4 shows that a few alcohols can strongly bind to specific sites by direct interactions even in dry proteins. In addition, protein hydration enables low-affinity nonspecific alcohol binding and the number of nonspecifically-bound alcohols is much larger than that of alcohols bound at specific sites. No such nonspecifically-bound halothane molecules were observed. The data here show that the

binding mechanism of alcohols and that of general anesthetics should be examined differently. Water plays a crucial role in the binding of alcohols and general anesthetics such as halothane.

5.4 Conclusions

Great effort has been made to evaluate the effects of structural changes in the water network upon ligand binding. What is little understood is the role of water-protein interaction in ligand binding. Using an NMR-based isotherm measurement approach, I studied the low-affinity alcohol binding to the globular protein BSA under controlled protein hydration [36]. This technique allows me to investigate the effect of water-protein interactions on alcohol binding and the specific roles of different hydration water molecules without being obscured by the presence of bulk solvent. The binding thermodynamics of alcohols are examined as a function of protein hydration level via the temperature dependence of alcohol adsorption isotherms.

It is found that alcohol binding is substantially enhanced by hydration [36]. As discussed in CHAPTER 4, two types of bound alcohols were clearly identified. One type is alcohol binding at pre-existing specific sites that are limited in numbers (less than 10 per BSA). Although hydration enables alcohol adsorption at these sites with lower alcohol vapor pressure, the number remains the same. The second type is alcohol binding at nonspecific sites on the protein. In dry protein, this type of alcohol adsorption only occurs above an alcohol vapor pressure threshold. Hydration at hydrophilic groups on the protein is found to be very effective in reducing the threshold pressure and finally removing it at a hydration level of h~0.2. Such a threshold is probably induced by the strong protein-protein contacts in dry protein aggregates. At the initial stage of hydration, the protein-protein contacts depend strongly on the hydration level until the hydrophilic groups are fully hydrated, which corresponds to h~0.2. Therefore, the threshold for

alcohol adsorption induced by protein-protein contacts is sensitive to the level of hydration. The binding at nonspecific sites was found to be entropy-driven in dry protein but became a fully developed enthalpy-driven process at high hydration levels. These results clearly show that hydration water at hydrophilic groups (h~0.2) plays a crucial role in alcohol binding at nonspecific sites. Although adsorbed water molecules at high hydration levels have smaller effects on alcohol adsorption enthalpy and entropy, they do lead to unmatched enthalpy-entropy compensation, resulting in a more negative Gibbs free energy and enhanced alcohol adsorption. In fact, the number of adsorbed alcohol molecules at nonspecific sites far exceeds those at specific sites in fully hydrated proteins. Hence, this work shows the significance of water-protein interaction in alcohol binding and alcohol's biological actions.

5.5 REFERENCES

[1] B. Breiten, M.R. Lockett, W. Sherman, S. Fujita, M. Al-Sayah, H. Lange, C.M. Bowers, A. Heroux, G. Krilov, G.M. Whitesides, Water networks contribute to enthalpy/entropy compensation in protein–ligand binding, J Am Chem Soc 135 (2013) 15579-15584.

[2] J. Michel, J. Tirado-Rives, W.L. Jorgensen, Energetics of displacing water molecules from protein binding sites: consequences for ligand optimization, J. Am. Chem. Soc. 131 (2009) 15403-15411.

[3] Z. Li, T. Lazaridis, Water at biomolecular binding interfaces, PCCP 9 (2007) 573-581.

[4] Y. Levy, J.N. Onuchic, Water mediation in protein folding and molecular recognition, Annu. Rev. Biophys. Biomol. Struct. 35 (2006) 389-415.

[5] M. Chaplin, Do we underestimate the importance of water in cell biology?, Nat. Rev. Mol. Cell Biol. 7 (2006) 861-866.

[6] C. Barillari, J. Taylor, R. Viner, J.W. Essex, Classification of water molecules in protein binding sites, J Am Chem Soc 129 (2007) 2577-2587.

[7] Y. Shan, E.T. Kim, M.P. Eastwood, R.O. Dror, M.A. Seeliger, D.E. Shaw, How does a drug molecule find its target binding site?, J. Am. Chem. Soc. 133 (2011) 9181-9183.

[8] J.E. Ladbury, Just add water! The effect of water on the specificity of protein-ligand binding sites and its potential application to drug design, Chem Biol 3 (1996) 973-980.

[9] D.L. Mobley, K.A. Dill, Binding of small-molecule ligands to proteins:“what you see” is not always “what you get”, Structure 17 (2009) 489-498.

[10] R. Baron, J.A. McCammon, Molecular recognition and ligand association, Annu Rev Phys Chem 64 (2013) 151-175.

[11] J.R. Trudell, R.A. Harris, Are sobriety and consciousness determined by water in protein cavities?, Alcohol.: Clin. Exp. Res. (2004).

[12] R.A. Harris, J.R. Trudell, S.J. Mihic, Ethanol's molecular targets, Sci. Signal. 1 (2008) re7.

[13] R.J. Howard, P.A. Slesinger, D.L. Davies, J. Das, J.R. Trudell, R.A. Harris, Alcohol-Binding Sites in Distinct Brain Proteins: The Quest for Atomic Level Resolution, Alcohol.: Clin. Exp. Res. 35 (2011) 1561-1573.

[14] D. Dwyer, R. Bradley, Chemical properties of alcohols and their protein binding sites, Cellular and Molecular Life Sciences CMLS 57 (2000) 265-275.

[15] L. Sauguet, R.J. Howard, L. Malherbe, U.S. Lee, P.-J. Corringer, R.A. Harris, M. Delarue, Structural basis for potentiation by alcohols and anaesthetics in a ligand-gated ion channel, Nat. Commun. 4 (2013) 1697.

[16] Q. Shao, Y. Fan, L. Yang, Y.Q. Gao, From protein denaturant to protectant: comparative molecular dynamics study of alcohol/protein interactions, The Journal of chemical physics 136 (2012) 115101.

[17] J.F. Povey, C.M. Smales, S.J. Hassard, M.J. Howard, Comparison of the effects of 2, 2, 2-trifluoroethanol on peptide and protein structure and function, J Struct Biol 157 (2007) 329-338.

[18] Q. Shao, The addition of 2, 2, 2-trifluoroethanol prevents the aggregation of guanidinium around protein and impairs its denaturation ability: A molecular dynamics simulation study, Proteins 82 (2014) 944-953.

[19] R. Rajan, P. Balaram, A model for the interaction of trifluoroethanol with peptides and proteins, Int. J. Pept. Protein Res. 48 (1996) 328-336.

[20] D. Chandler, Interfaces and the driving force of hydrophobic assembly, Nature 437 (2005) 640-647.

[21] R. Baron, P. Setny, J. Andrew McCammon, Water in cavity− ligand recognition, J. Am. Chem. Soc. 132 (2010) 12091-12097.

[22] G. Hummer, Molecular binding: Under water's influence, Nat. Chem. 2 (2010) 906-907.

[23] P. Setny, R. Baron, J. McCammon, How Can Hydrophobic Association Be Enthalpy Driven?, J. Chem. Theory Comput. 6 (2010) 2866.

[24] P. Ball, Water as an active constituent in cell biology, Chem. Rev. 108 (2008) 74-108.

[25] D. Zhong, S.K. Pal, A.H. Zewail, Biological water: A critique, Chem. Phys. Lett. 503 (2011) 1-11.

[26] V. Helms, Protein dynamics tightly connected to the dynamics of surrounding and internal water molecules, ChemPhysChem 8 (2007) 23-33.

[27] H. Frauenfelder, G. Chen, J. Berendzen, P.W. Fenimore, H. Jansson, B.H. McMahon, I.R. Stroe, J. Swenson, R.D. Young, A unified model of protein dynamics, Proceedings of the National Academy of Sciences 106 (2009) 5129-5134.

[28] N.V. Nucci, M.S. Pometun, A.J. Wand, Mapping the hydration dynamics of ubiquitin, J Am Chem Soc 133 (2011) 12326-12329.

[29] A.J. Wand, The dark energy of proteins comes to light: conformational entropy and its role in protein function revealed by NMR relaxation, Curr Opin Struc Biol 23 (2013) 75-81.

[30] K.K. Frederick, M.S. Marlow, K.G. Valentine, A.J. Wand, Conformational entropy in molecular recognition by proteins, Nature 448 (2007) 325-329.

[31] A.C. Chia-en, W. Chen, M.K. Gilson, Ligand configurational entropy and protein binding, Proceedings of the National Academy of Sciences 104 (2007) 1534-1539.

[32] M.S. Marlow, J. Dogan, K.K. Frederick, K.G. Valentine, A.J. Wand, The role of conformational entropy in molecular recognition by calmodulin, Nat. Chem. Biol. 6 (2010) 352-358.

[33] S.-R. Tzeng, C.G. Kalodimos, Protein activity regulation by conformational entropy, Nature 488 (2012) 236-240.

[34] J.A. Rupley, G. Careri, Protein hydration and function, Adv. Protein Chem. 41 (1991) 37-172.

[35] I. Kuntz Jr, W. Kauzmann, Hydration of proteins and polypeptides, Adv Protein Chem 28 (1974) 239-345.

[36] Y. Chong, A. Kleinhammes, P. Tang, Y. Xu, Y. Wu, Dominant Alcohol–Protein Interaction via Hydration-Enabled Enthalpy-Driven Binding Mechanism, The Journal of Physical Chemistry B 119 (2015) 5367-5375.

[37] H.-J. Wang, A. Kleinhammes, P. Tang, Y. Xu, Y. Wu, Critical Role of Water in the Binding of Volatile Anesthetics to Proteins, The Journal of Physical Chemistry B 117 (2013) 12007-12012.

[38] A. Myers, Thermodynamics of adsorption in porous materials, AlChE J. 48 (2002) 145-160.

[39] T.L. Hill, Statistical mechanics of adsorption. V. Thermodynamics and heat of adsorption, The Journal of chemical physics 17 (1949) 520.

[40] T.L. Hill, Statistical mechanics of adsorption. IX. Adsorption thermodynamics and solution thermodynamics, The Journal of chemical physics 18 (1950) 246.

[41] R. Keren, I. Shainberg, Water vapor isotherms and heat of immersion of Na-and Ca-montmorillonite systems. III. Thermodynamics, Clays Clay Miner. 28 (1980) 204-210.

[42] H.-J. Wang, A. Kleinhammes, P. Tang, Y. Xu, Y. Wu, Temperature dependence of lysozyme hydration and the role of elastic energy, Phys. Rev. E 83 (2011) 031924.

[43] R.G. Eckenhoff, J.S. Johansson, Molecular interactions between inhaled anesthetics and proteins, Pharmacological Reviews 49 (1997) 343-368.

[44] E.A.e. Permiakov, V.N. Uversky, Methods in Protein Structure and Stability Analysis: Vibrational Spectroscopy, Nova Publishers2007.

[45] J. Grdadolnik, Y. Marechal, Bovine serum albumin observed by infrared spectrometry. II. Hydration mechanisms and interaction configurations of embedded H2O molecules, Biopolymers 62 (2001) 54-67.

[46] Y. Takayama, M. Nakasako, A few low-frequency normal modes predominantly contribute to conformational responses of hen egg white lysozyme in the tetragonal crystal to variations of molecular packing controlled by environmental humidity, Biophys Chem 159 (2011) 237-246.

[47] W. Klemm, Biological Water and Its Role in the Effects of Alcohol 1, Alcohol 15 (1998) 249-267.

[48] V.A. Sirotkin, D.A. Faizullin, Interaction enthalpies of solid human serum albumin with water–dioxane mixtures: comparison with water and organic solvent vapor sorption, Thermochim Acta 415 (2004) 127-133.

[49] C. Bissantz, B. Kuhn, M. Stahl, A medicinal chemist's guide to molecular interactions, J. Med. Chem. 53 (2010) 5061-5084.

[50] D.H. Williams, E. Stephens, D.P. O'Brien, M. Zhou, Understanding Noncovalent Interactions: Ligand Binding Energy and Catalytic Efficiency from Ligand-Induced Reductions in Motion within Receptors and Enzymes, Angew. Chem. Int. Ed. 43 (2004) 6596-6616.

[51] A. Bhattacharji, N. Klett, R.C.V. Go, M. Covarrubias, Inhalational anaesthetics and n-alcohols share a site of action in the neuronal Shaw2 Kv channel, Br. J. Pharmacol. 159 (2010) 1475-1485.

[52] R.G. Eckenhoff, Do specific or nonspecific interactions with proteins underlie inhalational anesthetic action?, Mol. Pharmacol. 54 (1998) 610-615.

[53] B.W. Urban, M. Bleckwenn, M. Barann, Interactions of anesthetics with their targets: Non-specific, specific or both?, Pharmacol Therapeut 111 (2006) 729-770.

CHAPTER 6

CONCLUSIONS

In this dissertation, I discussed some studies on protein hydration and protein-ligand interactions using the nuclear magnetic resonance (NMR) technique. Specifically, it is known that water on the bimolecular surface, which is the so-called “hydration water”, plays a critical role in a variety of biological processes such as protein folding, drug binding, and enzymatic activation. However, so far, the mechanism underlying protein hydration and the detailed effects of hydration on protein-ligand interactions are far from being understood. Therefore, this dissertation was focused on these questions.

I developed a unique NMR measurement system, which enables me to study protein hydration and protein-ligand interactions at *in-situ* sample conditions with precisely controlled vapor pressure and temperature. In particular, with multiple vapor channels on the system, the concurrent adsorption of different types of vapor can be simultaneously measured. This allows me to characterize ligand binding at controlled protein hydration levels, which is one major advantage over other experimental methods. In this dissertation, this NMR-based technique was employed to measure isotherms, dynamic processes, and thermodynamic quantities associated with protein hydration and protein-alcohol interactions.

Water isotherms in two globular proteins were measured at different temperatures ranging from 3 C to 27 C. It was found that when the hydration level h (g water/g protein) is below 0.2, water only binds to hydrophilic groups on the protein. The binding is mainly driven

by hydrogen bonding between water and these groups and shows little temperature dependence. When the hydration level *h* is above 0.2, water starts interacting with hydrophobic groups on the protein and the interaction strongly depends on the temperature. The adsorption of water on hydrophobic groups is strong above 10 C, but it is substantially reduced below 10 C. Such adsorption is essentially a mixing process of adsorbed water molecules with hydrophobic protein groups, driven by the favorable change in the entropy of mixing. Protein flexibility is critical to the temperature dependence of the mixing process. Above 10 C, the protein is flexible with a very small elastic constant, so the mixing process is not costly in terms of elastic energy; while below 10 C, the protein's elastic constant increases dramatically, so the mixing process becomes energetically unfavorable, leading to the substantial suppression of water adsorption on hydrophobic groups. These results are illustrated in Figure 6.1.

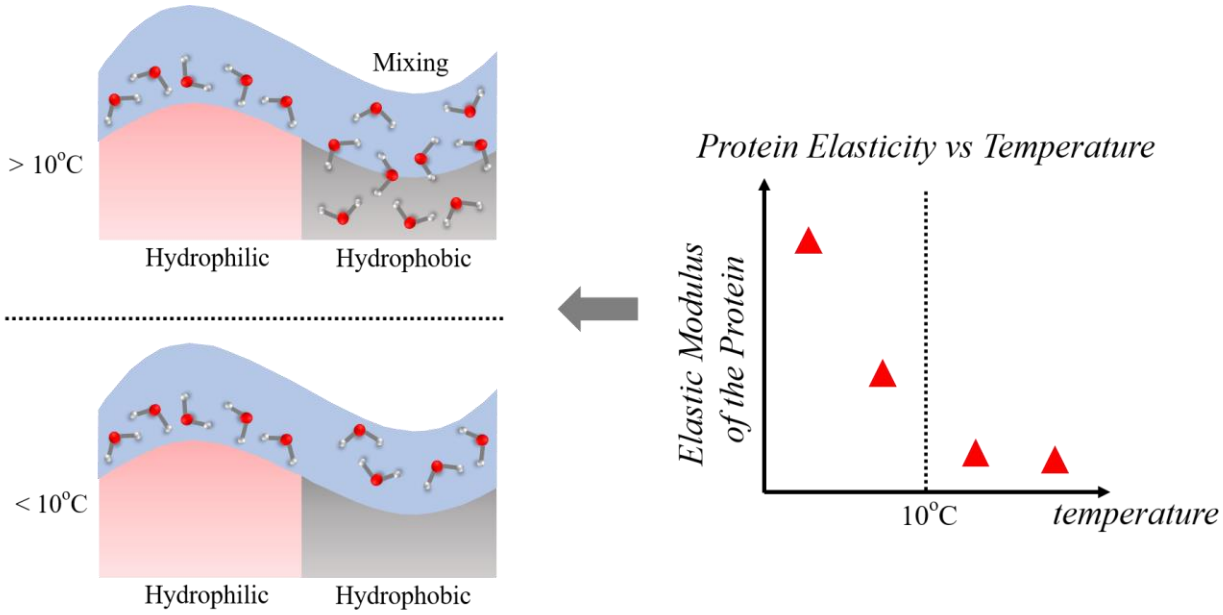

Figure 6.1: Illustration of protein-water interactions. The interaction of water with hydrophilic groups on the protein is temperature independent. In contrast, the

interaction of water with hydrophobic groups strongly depends on the temperature. Above 10 C water intimately mixes with hydrophobic groups, while below 10 C the mixing process is substantially suppressed. Such phenomenon is caused by the change in the protein flexibility with temperature.

As I discussed, water at hydrophilic and hydrophobic groups interacts differently with proteins. Particularly, hydration properties at hydrophobic groups undergo qualitative changes as temperature decreases below 10 C. However, the influence of such interfacial changes on protein dynamics and thermodynamics remains largely unexplored. Therefore, in this dissertation, I investigated nanosecond to microsecond protein dynamics, as well as the Gibbs free energy, enthalpy, and entropy of protein hydration as a function of hydration level and temperature. A crossover at 10 C in protein dynamics and thermodynamics was revealed. In terms of dynamics, on the nanosecond timescale, it was found that water at both hydrophilic and hydrophobic groups has significant effect on enhancing protein dynamics; the effect of water at hydrophobic groups is stronger at temperatures higher than 10 C. On the microsecond timescale, water at hydrophilic groups still greatly enhances protein dynamics whereas water at hydrophobic groups has weak effect on enhancing protein dynamics above 10 C and none below 10 C. In terms of thermodynamics, it was found that the Gibbs free energy, enthalpy, and entropy of protein hydration change with hydration in distinct ways at temperatures above and below 10 C. These results show a close correlation between nanosecond-microsecond protein dynamics and protein hydration thermodynamics at 10 C. These results are illustrated in Figure 6.2.

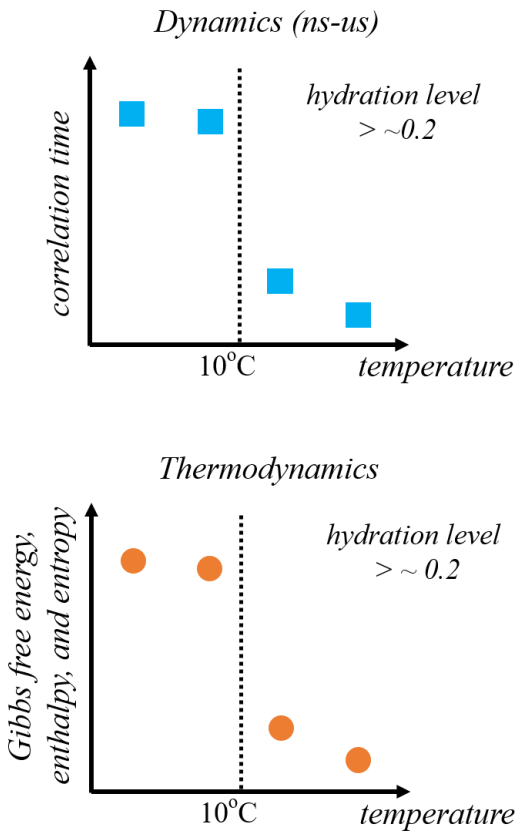

Figure 6.2: Illustration of the crossover at 10 C in protein dynamics and thermodynamics.

Numerous small-molecule ligands such as alcohols and general anesthetics exert their biological functions via binding to target proteins with low affinity. Among these ligands, alcohols such as ethanol can affect the human brain in ways from stimulating a pleasurable sensation to interfering with consciousness. Although the physiological effects of alcohols are well known, the mechanisms at the molecular level are far from being understood. One reason is that it is very challenging to characterize very weak association processes, especially in protein solutions, via traditional methods. In this dissertation, the unique *in-situ* NMR system enables me to selectively characterize different weakly-bound ligands.

Because of the structural and functional similarities between alcohols and general anesthetics, it was suggested that they may share the same binding mechanism. In this dissertation, the mechanism of alcohol-protein interactions was investigated in two steps.

In the first step, I studied the interaction between alcohols and dry proteins. It was found that alcohols can directly bind to dry proteins without the existence of hydration water. Specifically, there exist two distinct types of alcohol binding. One type is specific alcohol binding, where a limited number of alcohols bind to a few specific sites on the protein. This type of binding is shown to be temperature independent. The other type is nonspecific alcohol binding, where a large number of alcohols interact with nonspecific regions on the protein. This type of binding only takes place above a threshold of alcohol vapor pressure and is strongly dependent on the temperature. This dissertation showed that nonspecific alcohol binding is in fact a mixing process of adsorbed alcohols and the protein, driven by the favorable change in the entropy of mixing. This mechanism is similar to that of hydration of hydrophobic groups. The temperature dependence of this type of binding is induced by the change in the protein flexibility with temperature. The threshold of this type of binding is caused by the strong protein-protein interactions in the dehydrated protein state. In addition, at high alcohol vapor pressure, a large degree of nonspecific alcohol binding (i.e. mixing) leads to the denaturation of the protein.

In the second step, I studied the effect of hydration on alcohol binding. Hydration water is known to play an important role in low-affinity ligand binding. Intense focus has been on binding-induced structural changes in the water network surrounding protein binding sites, especially their contributions to binding thermodynamics. However, hydration water is also tightly coupled to protein conformations and dynamics, and so far, little is known about the influence of water-protein interactions on ligand binding. In this dissertation, I measured alcohol

adsorption isotherms under controlled protein hydration using the *in-situ* NMR detection. As functions of hydration level, Gibbs free energy, enthalpy, and entropy of binding were determined from the temperature dependence of isotherms. It was found that hydration water is critical to both types of alcohol binding. On the one hand, hydration is able to facilitate the saturation of specific sites. On the other hand, an increased hydration level effectively reduces the threshold of nonspecific alcohol binding, with it finally disappearing at a hydration level of h~0.2 (g water/g protein), gradually shifting nonspecific alcohol binding from an entropy-driven to an enthalpy-driven process. Water at hydrophilic groups on the protein was found to be particularly important in enabling this binding. Although further increase in hydration has smaller effects on the changes of binding enthalpy and entropy, it results in significant negative change in Gibbs free energy due to unmatched enthalpy-entropy compensation. These results show the crucial role of water-protein interplay in alcohol binding. These results are illustrated in Figure 6.3.

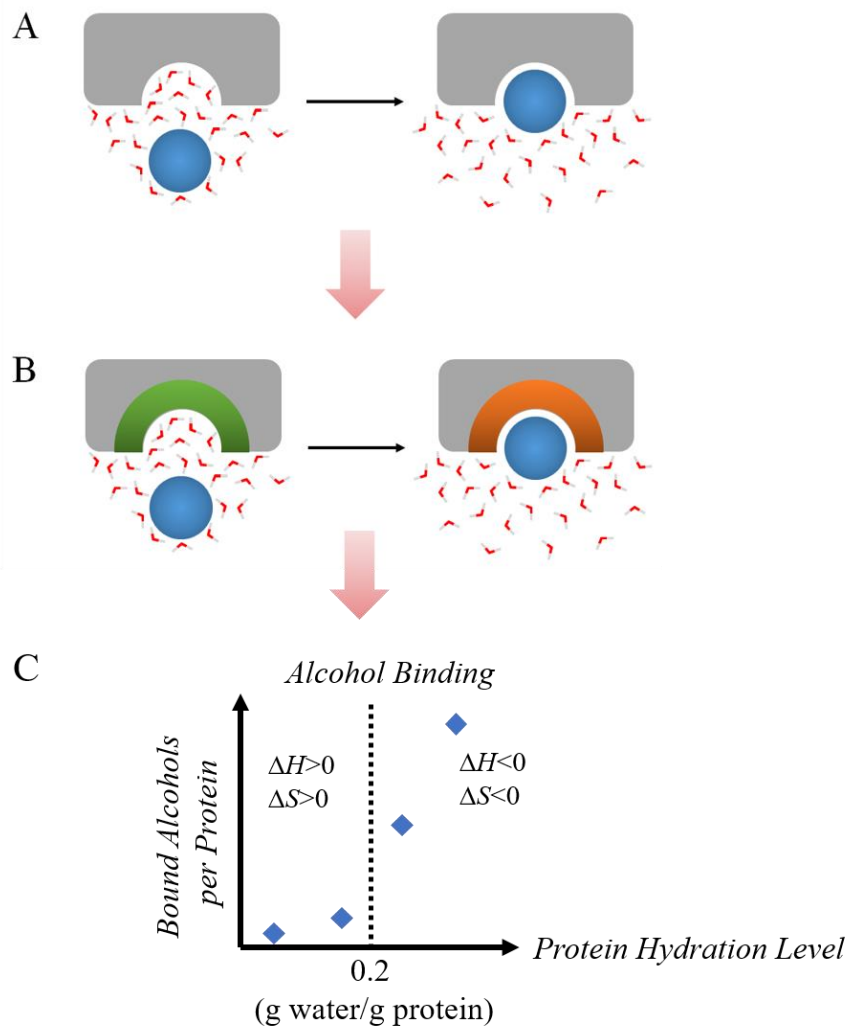

Figure 6.3: Illustration of alcohol (blue ball) binding to the protein (gray block) in water (red-white sticks). When the alcohol molecule approaches the protein, (*A*) in previous works, water around the binding site is displaced and rearranged, resulting in the structural modifications in the water network. In this case, the protein is considered as a rigid cavity. (*B*) in this dissertation, the state of the protein changes before (green) and after (orange) the binding. The change of the protein is enabled by water-protein coupling. Because of this mechanism, alcohol binding increases dramatically with hydration level, especially above the hydration level of 0.2 (g

water/g protein). With increasing hydration, alcohol binding also changes from a entropy-driven process to a enthalpy-driven process.

It is also worth mentioning that this dissertation showed that the binding mechanisms of alcohols and general anesthetics are completely different, although they are similar in molecular structure and physiological function. General anesthetics like halothane and isoflurane only bind to a few specific sites on the protein. They are unable to directly bind to those sites; hydration water is necessary to be present at those sites to drive the binding. In contrast, alcohols can bind to the protein via direct interactions, even if the protein is dry. There also exist a few specific sites for alcohols, but at the same time, alcohols can also bind to a large number of nonspecific sites on the protein. Hydration water is found to be critical to both types of alcohol binding. Therefore, alcohols and general anesthetics should be examined differently.

In conclusion, in this dissertation I focused on the mechanism of protein hydration and the role of hydration in alcohol-protein interactions, by employing a unique *in-situ* NMR technique. Distinct properties of hydration water at hydrophilic and hydrophobic protein groups were identified. Moreover, a crossover at 10 C in protein dynamics and thermodynamics was discovered. In addition, the effects of hydration on different types of alcohol-protein interactions were clearly revealed. This dissertation provides new insights into the nature of protein-water interactions and protein-ligand interactions, with great implications for the understanding of protein functions.

APPENDIX A

A1. $T_{1\rho}$ relaxation of BSA at spin-locking field B_1~90 kHz

^{1}H spin lattice relaxation in the rotating frame ($T_{1\rho}$) of BSA is also measured at the spin locking field B_1 ~90 kHz as functions of hydration level and temperature. $T_{1\rho}$ relaxation times of BSA and its hydration water are presented in Figure A1 (A) and its inset. The corresponding correlation times of BSA proton are presented in Figure A1 (B). A stretched exponential function is used to fit $T_{1\rho}$ decay of BSA. The stretching parameter β at the spin locking field B_1 ~90 kHz is presented in Figure A1 (C). The results of BSA at spin locking field B_1 ~90 kHz are similar to the results at spin locking field B_1 ~50 kHz (see CHAPTER 3 SECTION 3.3).

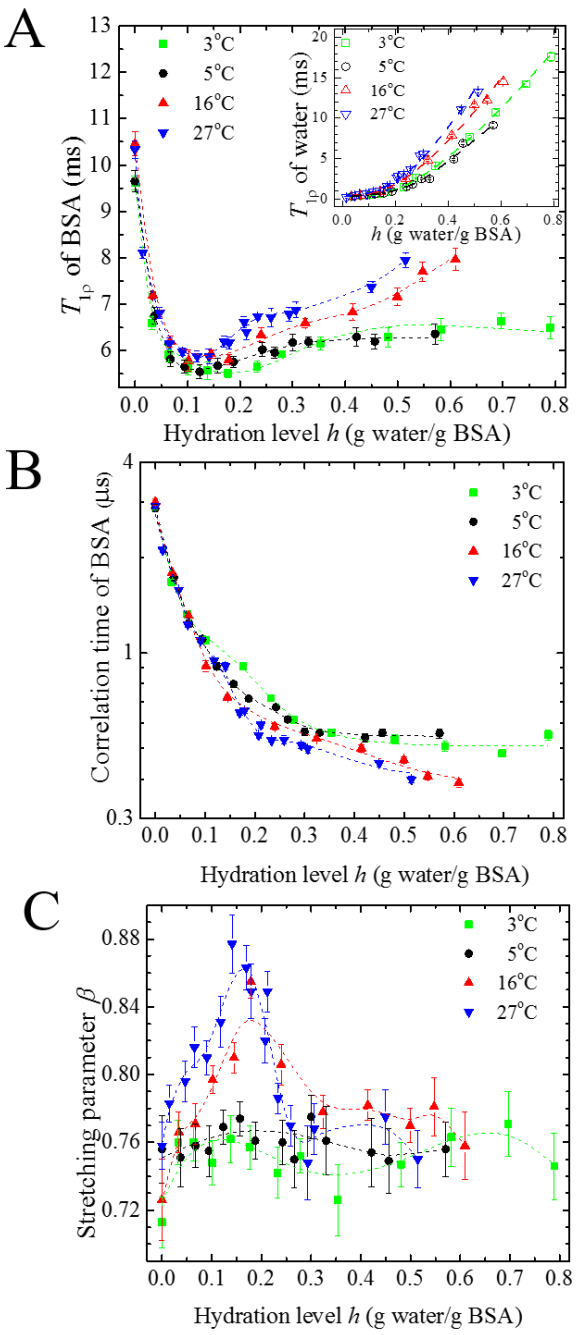

Figure A1: $T_{1\rho}$ measurement on BSA at the spin locking field B_1 ~90 kHz. (A) ^{1}H spin lattice relaxation in the rotating frame ($T_{1\rho}$) of BSA and its hydration water (inset), (B) the correlation times of BSA protons, and (C) stretching parameter β of BSA as a function of hydration level at 3 C, 5 C, 16 C, and 27 C.

A2. Hydration effects on dynamics and thermodynamics of lysozyme around 10 C

To study the dynamics of lysozyme on nanosecond timescale, ^{1}H spin lattice relaxation in the laboratory frame (T_1) of lysozyme and its hydration water are measured. Figure A2 (A) and its inset show the T_1 relaxation times of lysozyme and its hydration water induced by their intrinsic motions. Figure A2 (B) shows the correlation time of lysozyme protons. Figure A3 shows the proton exchange rates between lysozyme and its hydration water.

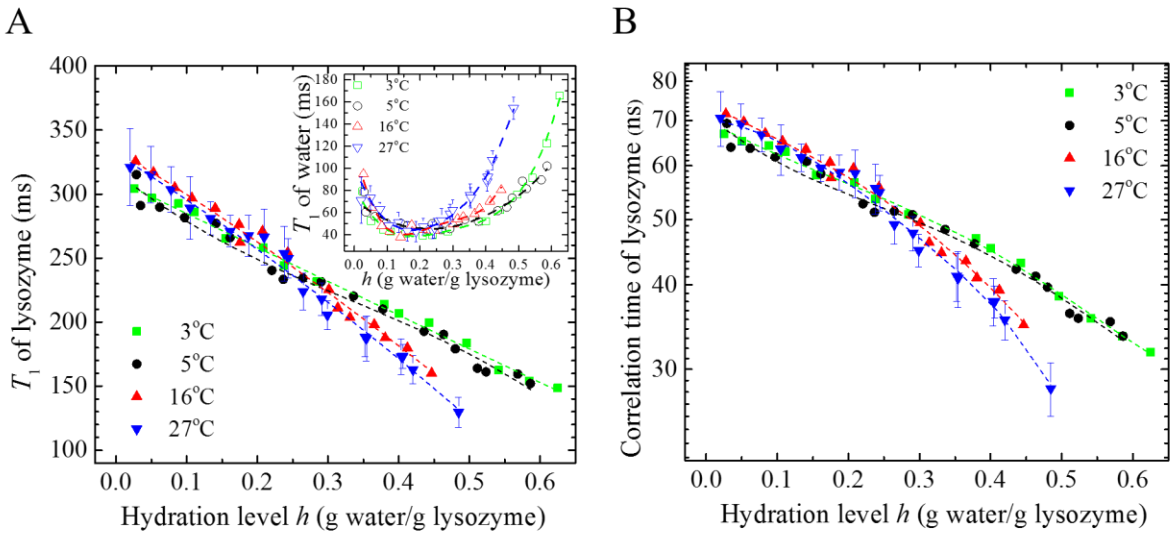

Figure A2: (A) Intrinsic T_1 relaxation time of lysozyme and its hydration water (inset of A) as a function of hydration level at 3 C, 5 C, 16 C, and 27 C. (B) The correlation time of lysozyme. Relative errors of T_1 relaxations and correlation times at different temperatures are very close. Hence, only error bars at 27 C are shown.

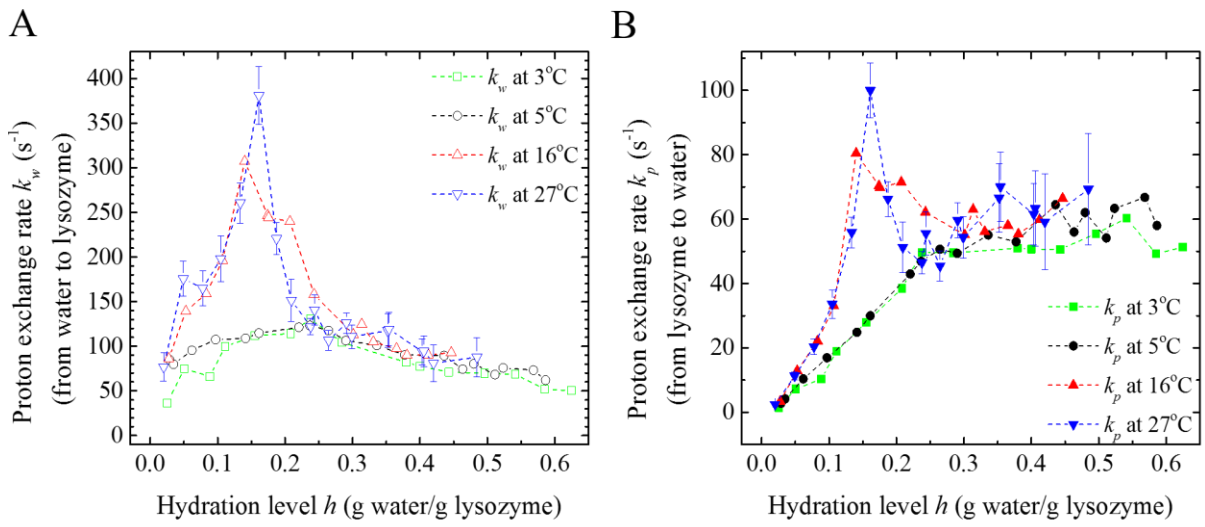

Figure A3: Proton (^{1}H) exchange rates (A) from hydration water to lysozyme k_w, and (B) from lysozyme to hydration water k_p as a function of hydration level at 3 C, 5 C, 16 C, and 27 C. Relative errors of exchange rates at different temperatures are very close. Hence, only error bars at 27 C are shown.

To study the dynamics of lysozyme on microsecond timescale, ^{1}H spin lattice relaxation in the rotating frame ($T_{1\rho}$) of lysozyme and its hydration water at the spin locking B_1 ~50 kHz (Figure A4) and B_1 ~90 kHz (Figure A5) are measured.

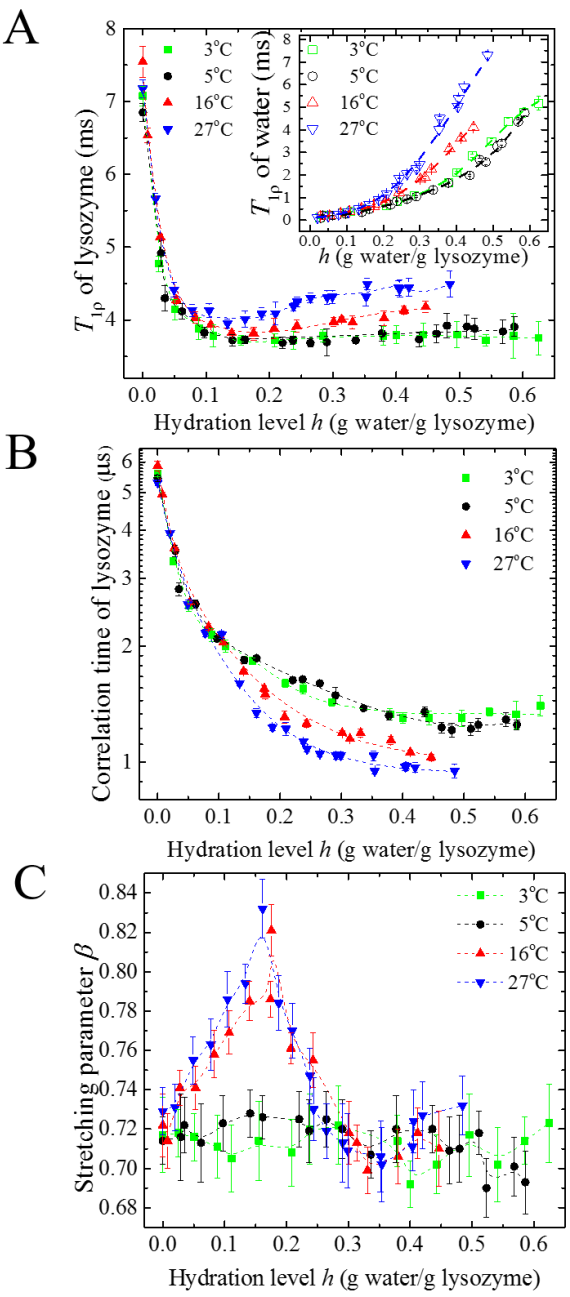

Figure A4: $T_{1\rho}$ measurement on lysozyme at the spin locking field B_1 ~50 kHz. (A) ^{1}H spin lattice relaxation in the rotating frame ($T_{1\rho}$) of lysozyme and its hydration water (inset), (B) the correlation times of lysozyme protons, and (C) stretching parameter β of lysozyme as a function of hydration level at 3 C, 5 C, 16 C, and 27 C.

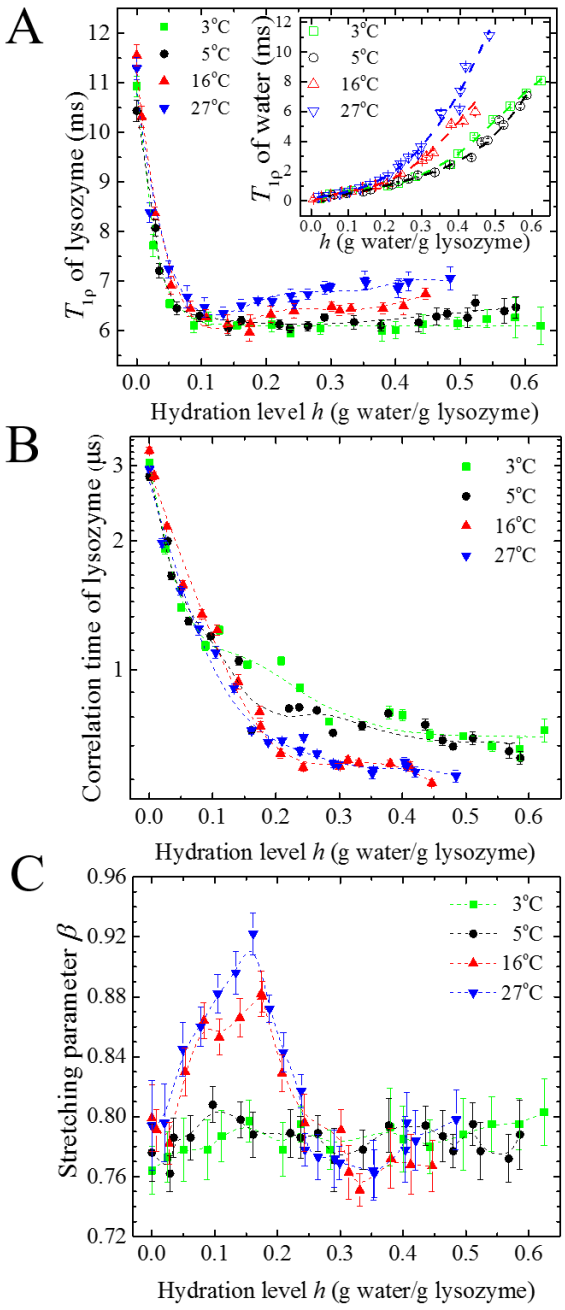

Figure A5: $T_{1\rho}$ measurement on lysozyme at the spin locking field B_1 ~90 kHz. (A) ^{1}H spin lattice relaxation in the rotating frame ($T_{1\rho}$) of lysozyme and its hydration water (inset), (B) the correlation times of lysozyme protons, and (C) stretching parameter β of lysozyme as a function of hydration level at 3 C, 5 C, 16 C, and 27 C.

To study the thermodynamics of lysozyme, changes in the Gibbs free energy ΔG, enthalpy ΔH, and entropy $T\Delta S$ associated with the hydration process of lysozyme are calculated and presented in Figure A6.

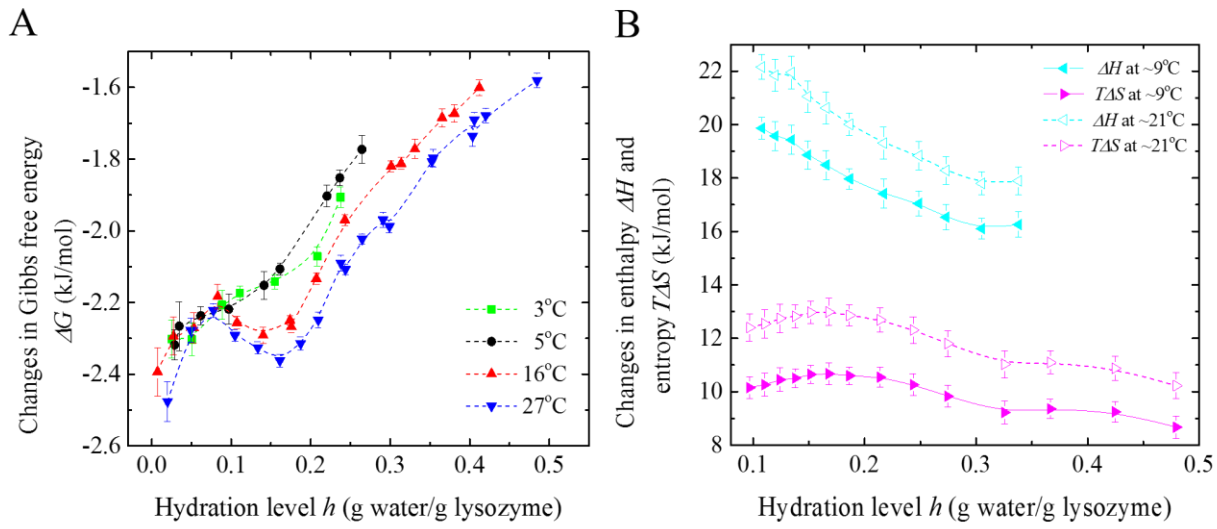

Figure A6: (A) Changes in the Gibbs free energy ΔG associated with the hydration process of lysozyme as a function of hydration level at 3 C, 5 C, 16 C, and 27 C. (B) Changes in enthalpy ΔH and entropy $T\Delta S$ associated with the hydration process of lysozyme at ~9 C and ~21 C.

It is seen that: (1) the effects of hydration on lysozyme and BSA are very similar (2) the crossover at 10 C in the dynamics and thermodynamics of lysozyme hydration are also revealed. These results indicate the similarity in the interaction between water and globular proteins.

APPENDIX B

Isotherms of TFE in hydrated BSA at 15 C and 25 C.

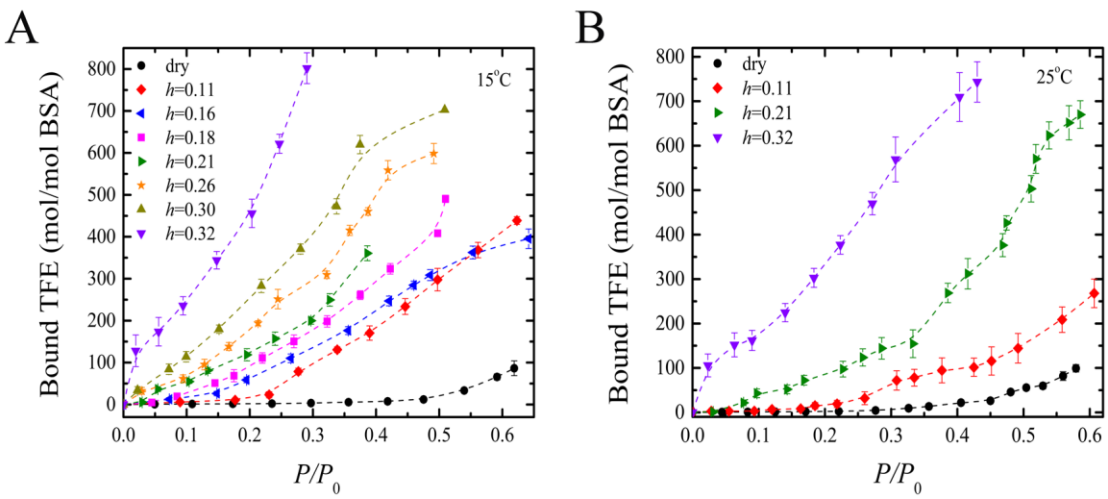

Figure B1. Isotherms of TFE in hydrated BSA at (A) 15 C and (B) 25 C at various hydration levels *h*. At both temperatures, hydration strongly enhances alcohol sorption. With increasing *h*, the threshold of alcohol vapor pressure decreases and is removed at *h*~0.2 (g water/g protein). The shape of isotherms also changes from sigmoidal to hyperbolic at *h*~0. 2 (g water/g protein). At each alcohol vapor pressure, NMR signal was measured five times when the interaction reached equilibrium, and then the standard deviations of NMR peak areas were used to calibrate the error bars in the isotherms.